NATURAL CONVECTION HEAT TRANSFER FROM FINNED TUBES

by

ROBERT BINLOUN PAN

A THESIS

submitted to

OREGON STATE UNIVERSITY

in partial fulfillment of
the requirements for the
degree of

MASTER OF SCIENCE

June 1962

APPROVED:

Redacted for privacy

Professor of Chemical Engineering

In Charge of Major

Redacted for privacy

Head of Department of Chemical Engineering

Redacted for privacy

Chairman of School Graduate Committee

Redacted for privacy

Dean or Graduate School

Date thesis is presented _February 28, 1962_

Typed by Elaine M. Anderson

ACKNOWLEDGMENTS

TABLE OF CONTENTS

LIST OF FIGURES

LIST OF TABLES

NATURAL CONVECTION HEAT TRANSFER FROM FINNED TUBES

Chapter I
Introduction

Natural convection heat transfer is that mode of heat transfer by which movement of portions of a fluid being heated or cooled by buoyancy force originates from density difference within the fluid. This manner of heat transfer is used extensively in space heating in which a heated surface is immersed in the medium to be heated.

Because of the small heat transfer coefficient characteristics of natural convection various means are employed to increase the rate of heat transfer. One way to increase heat transfer rate is to use extended surfaces, that is to increase the surface area per unit volume of the heater or cooler. Another method is to provide chimneys above the heat transfer surface so that buoyant forces are increased. Natural convection heat transfer from finned (extended surface) tubes has become an important method of space heating, and an understanding of the mechanism of natural convection from finned tubes is needed to aid in design of such systems.

Although, there has been extensive experimental work on forced convection from finned tubes, and on the application of finned tubes to baseboard heating and air

conditioning, little study has been devoted to natural convection from finned tubes. Theoretical investigations of natural convection have been restricted to some simple geometrical configurations, such as horizontal and vertical cylinders, vertical flat plates and vertical parallel plates. For more complex configurations most of the work done has been empirical because the non-linear nature and the complex form of the differential equations involved restrict satisfactory analytical solution. Even for theoretical work done on simple configurations results have usually been restricted to the dimensionless groups involved in the system and often constants must be evaluated empirically.

The purpose of the present work was to make an experimental study of natural convection heat transfer from finned tubes to air and to determine relationships between dimensionless groups derived from previous theoretical studies of simple geometric systems. Such variables as fin-shape, fin-spacing, fin-diameter and chimney height were studied to obtain optimum values of these parameters. Three different fin diameters and four different fin spacings of round fins, and four different fin spacings of square fins were investigated. The fins were mounted on a cylindrical horizontal tube and the systems heated by two immersion heaters and

immersed in still air. The natural convection heat transfer coefficients were correlated in terms of the various parameters of the system. A study on the effect of chimneys was also made using two different sizes of baffles mounted on the finned tubes.

Chapter II

Theoretical Considerations and Literature Survey

1. Natural convection heat transfer:

Natural convection heat is an important mode of
heat transfer brought about by buoyant forces. Gravita-
tional convection is a process which takes place in a
universal gravitational field; the different fluid
particles in a fluid medium possess different densities
and thereby cause motion of the fluid. The main reason
for the differences in density lie in the differences in
temperature or in composition; sometimes it is caused by
electrostriction, thermomagnetic, or thermoelectrostatic
effects. Density differences caused by temperature
variation in the fluid cause natural convection. The
boundaries of the fluid are stationary and the buoyancy
force causes the interior molecules to move.

It is necessary to distinguish between natural and
forced convection. In the case of forced convection,
the velocity field depends only slightly on the temper-
ature and is determined to a large extent by the rate of
flows. The temperature field depends on the velocity
field. The Reynolds ($\frac{LU\rho}{\mu}$) number and Prandtl ($\frac{c_p\mu}{k}$)
number are therefore two dominate parameters, and in most
cases the effect of the friction heat and compression work

are neglected unless the velocity reaches the speed of
the sound.

In the case of natural convection, the temperature
and velocity fields depend on each other, and the Grashof
($\frac{L^3 \rho^2 g \beta \theta}{\mu^2}$) and Prandtl numbers are dimensionless groups
by which the data may be correlated. The compression work
and friction heat are also neglected unless there is a
sufficiently high value of Grashof number. It was
reported by Brown and Marco (6, p. 111), that the Grashof
number may be transformed into a type of Reynolds number
by a force balance between the buoyancy force and the
kinetic force which is produced by the buoyancy force.
Therefore, the Grashof number in natural convection is
really equivalent to the Reynolds number in forced
convection.

It has been shown in fluid dynamics that, as a fluid
flows past a heated body, a momentum boundary layer, as
well as a thermal boundary layer forms. The thicknesses
of these boundary layers are very small as compared to
the linear dimension of the body. In the momentum
boundary layer, the velocity of the fluid changes from
that of the body to that of the main stream and likewise
in the thermal boundary layer the temperature changes
from that of the body to that of the main stream. In the
case of natural convection, since the fluid is stationary

outside the boundary layer, the fluid velocity is also equal to zero at the outer edge of the boundary layer.

Langmuir (21, p. 40) postulated that, in the case of natural convection heat transfer from a wire to a gas, most of the resistance to the heat transfer lies in a film which surrounds the wire. The thickness of the film is independent of the temperature of the wire, but probably increases with the temperature of the surrounding gas. The thickness of the film of the gas varies in a simple way with the diameter of the wire. Accordingly, the natural convection from any surface may be expressed in terms of the equivalent conduction through a fictitious stagnant film, i.e.

$$\frac{q}{A} = k \frac{t_s - t_a}{x_a}$$

where   q = total heat loss

k = thermal conductivity

t_s = temperature of the solid surface

t_a = temperature at the outer bound of the film
       which is equal to that of the fluid

x_a = thickness of a fictitious film

However, the real mechanism is not the case as mentioned above. Because of this and the difficulty in determining the thickness of the film, another expression has been derived instead of the film theory expression,

and is presently accepted.

It is

$$q = hA (t_s - t_a)$$

where the proportionality factor h is defined as the local heat transfer coefficient.

As long as the above mentioned assumptions for boundary layer hold, i.e. the thickness of boundary layer is very small as compared with the characteristic dimension of the solid body, the convection heat transfer may be determined from the following three boundary-layer differential equation:

Continuity equation $\quad \frac{\partial}{\partial x}(\rho U) + \frac{\partial}{\partial y}(\rho V) = 0 \qquad (1)$

Momentum equation $\quad \rho(U\frac{\partial U}{\partial x} + V\frac{\partial U}{\partial y}) = -\frac{\partial P}{\partial x} + \frac{\partial}{\partial y}(\mu\frac{\partial U}{\partial y}) + g_x\rho \quad (2)$

Energy equation $\quad \rho C_p(U\frac{\partial T}{\partial x} + V\frac{\partial T}{\partial y}) = \frac{\partial}{\partial y}(k\frac{\partial T}{\partial y}) \qquad (3)$

These equations are written in rectangular coordinates for the case of two dimensional flow; so far no attempt has been made to solve the three dimensional heat flow problem.

These equations may be solved theoretically either by exact or approximate methods. A complete solution of the boundary layer equations will be considered as an exact solution irrespective of whether it is obtained analytically, or by numerical methods. The approximate solutions are the solutions obtained from integral

relations, which are originally derived by von Karman.
In theory, the boundary layer equations are satisfied
both in the layer near the wall and in the immediate
region outside of the boundary layer. Details on the
comparison between the exact method and the approximate
method have been presented by Levy (23, p. 515)

Natural convection problems can be divided into
internal and external types. In the so called external
problems the heated (or cooled) surface being used is
much smaller than the body of the fluid in which it is
immersed. On the contrary, the internal problems are
those where the dimensions of the heater or the cooler
are comparable with the dimensions of the container of
the fluid. Since this thesis deals mainly with the case
of the external type, the discussion is restricted to
this type.

2. Combined natural and forced convection:

Natural convection occurs in conjunction with forced
convection heat transfer. The contribution of natural
convection to the total heat transfer depends on the
velocity of the main stream, and when its velocity
becomes small natural convection predominates and
ultimately accounts for all heat transfer when the main

stream velocity becomes zero.

Combined natural and forced convection is widely used in the after-shut-down cooling problems in nuclear reactors. Some earlier work dealing with the combined natural and forced convection with internal heat flux was done by Ostroumov (33). Hallman (15, p. 1830) also made a theoretical investigation in the combined convection problem inside a tube. Somers (40, p. 295) solved the problem of combined thermal and mass transfer from a vertical plate by a theoretical approach. In addition to the above mentioned continuity, momentum, and energy equations, an additional equation, the diffusion equation was needed in this case. A theoretical solution was obtained by means of the Pohlhausen-Karman approximate method. A theoretical analysis was also done by Ostrach on this topic.

Van Der Hegge Zijnen (44, p. 137) studied the problem of combined natural and forced convection heat transfer from horizontal cylinders and obtained the following relationship:

$$(Nu - 0.35)\sqrt{1 - \left[\frac{0.24Gr^{1/8} + 0.41Gr^{1/4}}{Nu - 0.35}\right]} = 0.5Re^{0.5} + 0.001Re$$

The main object of the above equation was to predict under what conditions the natural convection could be neglected.

3. Natural convection heat transfer from horizontal cylinders:

Natural convection from vertical plates (discussed in the next section) and natural convection from horizontal tubes are the simplest two dimensional cases in which the above mentioned three differential equations can be simplified and solved. Assuming constant fluid properties, the equations become

$$\frac{\partial U}{\partial x} + \frac{\partial V}{\partial y} = 0 \tag{4}$$

$$U \frac{\partial U}{\partial x} + V \frac{\partial U}{\partial y} = \nu \frac{\partial^2 U}{\partial y^2} + g\beta\theta \tag{5}$$

$$U \frac{\partial T}{\partial x} + V \frac{\partial T}{\partial y} = \alpha \frac{\partial^2 T}{\partial y^2} \tag{6}$$

where, $g\beta\theta$ is the buoyancy force term particularly appearing in the natural convection process, $(\nu = \frac{\mu}{\rho})$ is the kinematic viscosity, and $(\alpha = \frac{k}{c_p \rho})$ is the thermal diffusivity.

Nusselt (17, p. 2) solved the above differential equations by means of the uniquely determining boundary values, and reported that in the case of small temperature difference the Nusselt number (Nu) can be expressed as a function of Grashof number and Prandtl number. In this expression, the fluid properties have been assumed to be constant. This assumption is quite good for small temperature differences, however, for large temperature

differences this assumption no longer holds. Hence, in the case of large temperature drop, Nusselt suggested the following relationship:

$$Nu = f(Gr, Pr, Te)$$

Hermann (17, p. 3) made a study on the effect of this new parameter Te on the natural convection, and reported that the effect of Te will greatly exceed that of the Grashof number in the region $10^{-4} < Gr < 10$. On the other hand, the effect of Te will be negligible in the region $10^{4} < Gr < 10^{7}$. Therefore the factor Te appears as a third parameter for the variable-property problems. However, it was suggested later by Sparrow and Gregg (42, p. 879) that the addition of the factor Te is not necessary if a proper reference-temperature is chosen for evaluating the values of the fluid properties. They proved mathematically, that the constant-property problem is identical to that for the special variable-property fluid, and all the solutions obtained from the constant-property differential equations can be applied to the special-property fluid as well. Hence, by choosing a proper reference-temperature the results obtained for the constant-property conditions can be applied to the variable-property conditions, and it was obtained that for gases, the reference-temperature is

$$T_r = T_s - 0.38 (T_s - T_a)$$

It was further observed by them that the film temperature $T_f = \dfrac{T_s + T_a}{2}$, may be used as an adequate reference-temperature for most engineering purposes. All the above results obtained by Sparrow and Gregg were based on the boundary layer theory in which the thickness of the boundary layer is small compared to the linear dimension of the system.

As to the parameter Pr, it has been defined by the gas kinetic relation that for gases, $Pr = \dfrac{n + 2}{n + 4.5}$ where n is the number of degrees of freedom of the molecular motion. Therefore, Pr is solely dependent on the nature of the gas and independent on the temperature in the case of gas.

Hermann (17) made an extensive study of natural convection from a horizontal cylinder. He solved the differential equations under the assumptions that

1. The cylinder is infinitely long.

2. The flow in the boundary layer is laminar.

3. The assumption made for the boundary layer theory is satisfied, i.e. the thickness of the boundary layer is small as compared with the diameter of the cylinder.

He obtained the theoretical relationship $Nu = 0.37 Gr^{0.25}$ where the fluid properties in the Grashof and Prandtl number must be taken at the wall temperature. Experimentally, this relationship has been proved to be correct

from Schlieren photos obtained by Schmidt (44, p. 130).
It was also concluded by Hermann (17, p. 11) that the
above relationship changes to the form of Nu = constant
$(Gr^{1/3})$ for Gr > 3 x 10^8. He explained that this change
was caused by turbulence in the boundary layer. Experi-
ments of King also confirmed this one-third power law.
Hermann also observed the dependence of the Nusselt
number on the Prandtl number. He concluded that in the
region of very small Grashof numbers the Nusselt number
was almost independent of Pr, while in the region of
medium and large values of Gr, an increase of Nu with Pr
was observed.

It has been mentioned above that for Gr Pr < 10^4,
the fourth-power law is no longer valid. In light of
this, Langmuir (21, p. 401) proposed his "film theory".
He experimented with hot wires in air and reported that
as Gr decreases to 10^{-4}, Nu approaches a lower limit.
Ayrton and Kilgour, Bijlevelt and Kennelly (17, p. 6-7)
also tested wires of different materials in air in the
region of small Gr (10^{-4} to 10), their results are in
good agreement with Langmuir's. Koch and Walsmer
(17, p. 8-9) experimented with cylinders in the region of
large Gr (10^4 to 10^8), their results agree with the
theoretical fourth-power law. Elenbaas (14, p. 1148-1154)
obtained the following relationship with the aid of

Langmuir's film theory

$$Nu^3 e^{-6/Nu} = \frac{Gr\,Pr}{235\,f(Gr\,Pr)}$$

where the function f(GrPr) was found experimentally.
Nusselt and King (20, p. 350) experimented with horizontal
cylinders in air and obtained empirical correlations.
Their results are plotted in Figure (1). Jakob and Linke
(19, p. 529) combined Nusselt's and King's correlations
and obtained their following relationships:

$Nu = 0.555\,(GrPr)^{1/4}$ for $10^4 < GrPr < 10^8$

$Nu = 0.129\,(GrPr)^{1/3}$ for $10^8 < GrPr$

It was noted that the natural convection heat
transfer will be greatly increased if one were able
either to increase the values of the quantities in the
numerator or decrease the values of the quantity in the
denominator of the Grashof number, or do both. Based on
this concept, Doughty and Drake (9, p. 1843-1850)
proposed that for any substance in the gaseous phase, as
the critical point is approached, all the quantities in
the Gr will increase from their regular values in super-
heated region except viscosity, and for gases viscosity
will increase with temperature. Therefore, they suggested
that for any substance in the gaseous phase, there will
be a great increase in natural convection heat transfer
at its critical state. Through experimental test on
Freon 12, they reported that a tenfold increase in the
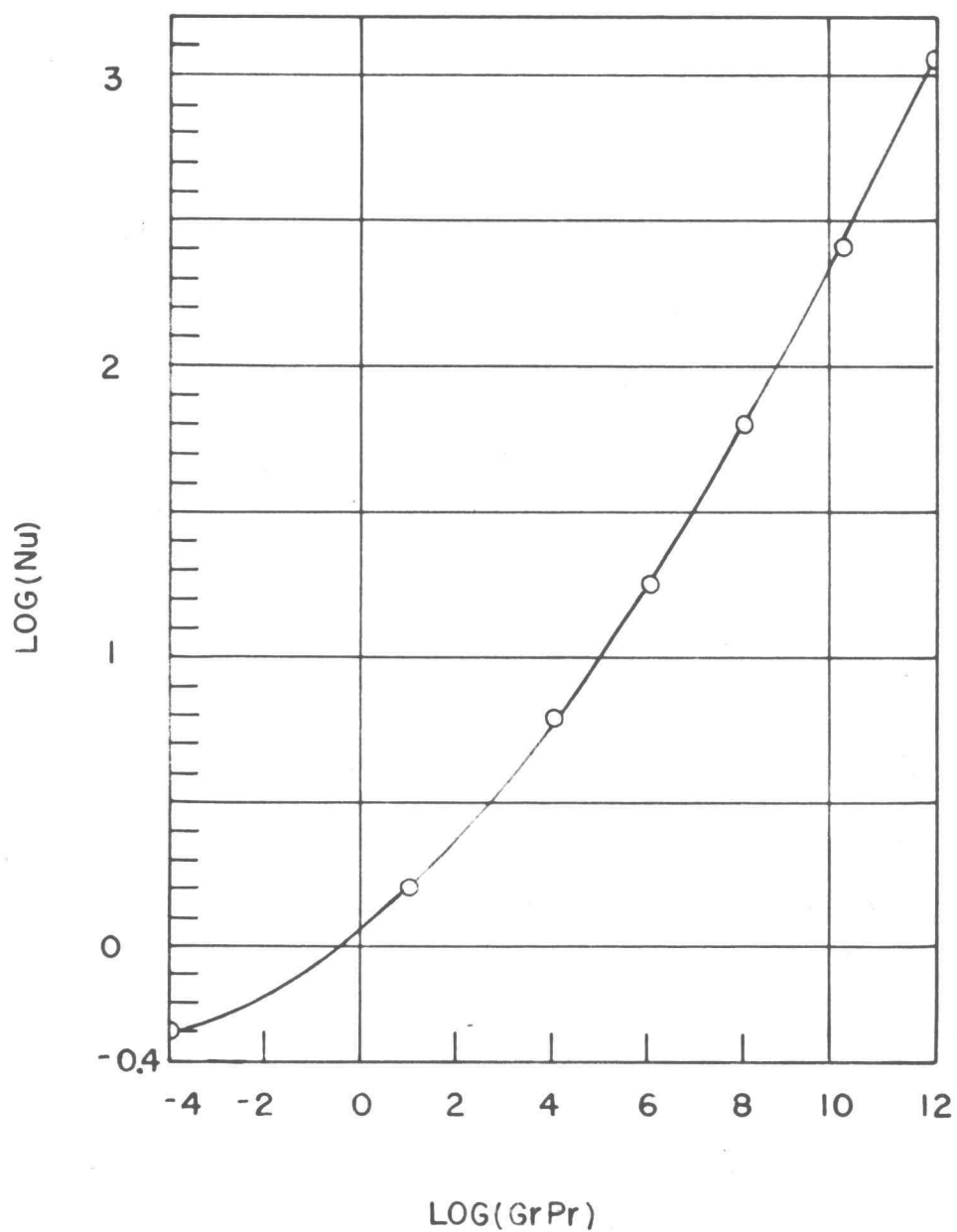
FIGURE 1   NATURAL CONVECTION FROM HORIZONTAL
CYLINDERS TO AIR

heat transfer coefficient was observed at the critical state. Dropkin and Carmi (10, p. 74) experimented with a horizontal cylinder rotating in air. They reported that for Re up to 1500 the following equation is applicable:

$$Nu = 0.095 \ (0.5 \ Re^2 + Gr)^{0.35}$$

For Re greater than 1500, the effect of rotation speed greatly overweighs that of the natural convection, and the following formula was proposed:

$$Nu = 0.073 \ (Re)^{0.7}$$

These relationships apply equally well to both film and bulk properties.

Y. P. Chang (8, p. 1501-9) proposed a new theoretical approach instead of the older conventional concept for heat transfer in natural convection and in boiling. He assumed that there is a boundary layer above a heating surface whose thickness depends on the heat flow. There is wave motion inside the layer which is stable in the lower part but unstable in the upper part. With the aid of his wave motion theory, Chang derived the following theoretical formula:

$$Nu = 0.146 \ (PrGr)^{1/3}$$

which agrees with the experimental results of other investigators. It is also suggested in his paper that this new concept applies not only to natural convection

but also to forced convection. However, since this new approach is idealized, further experiments and studies are needed for evaluating how close this concept is to reality.

There has been extensive study on the natural convection from heated bodies, however only little work has been done on the natural convection to cold bodies. Lemlich and Sharn (22, p. 1547) studied the natural convection to cold cylinders. Experimentally, they concluded that when the temperature difference is not too large, the equations obtained for natural convection from warm cylinders can be applied to the case of natural convection to cold cylinders as well.

A study was made by Boelter, Cherry, Johnson, and Martinelli (4, p. XII-38) of the effect of vibration on natural convection heat transfer. The following semi-empirical equation was recommended as within the range of laminar heat flow:

$$Re = Nu \sqrt{12,000 - 20 \frac{(GrPr)^2}{Nu^8}}$$

where

$$Re = \frac{a \omega d \rho}{\sqrt{2} \mu}$$

a = amplitude of displacement of the tube

d = diameter of the cylinder

ω = angular velocity of fluid

4. Natural convection from vertical flat plates:

Recently, with the increasing application of natural convection such as in the cooling of turbine blades or of helicopter ram jets, natural convection from vertical plates is becoming more important. There is considerable difference between the mechanism of natural convection from vertical plates and that of horizontal cylinders. In the case of a vertical plate the boundary layer starts with zero thickness which results in an infinitely large temperature gradient and an infinitely large local heat transfer coefficient at the lower edge. On the contrary, for horizontal cylinder the boundary layer starts with a finite thickness which gives the finite velocity and temperature gradients and hence a finite local heat transfer coefficient. For flat plates, the boundary layer thickness increases with the fourth root of the height above the lower stagnation edge. However, for the horizontal cylinder, the boundary layer thickness increases from the lower stagnation edge according to a complex law and at the upper stagnation point it reaches a theoretically infinite thickness with diminishing velocity and with diminishing heat transfer coefficient. Hence, for natural convection from a vertical plate, since the boundary layer thickness increases with the height above the lower edge, the capacity of heat transfer

decreases along the surface, which results in more heat
transfer per unit area for plates with shorter height.
For tall surfaces, the heat transfer coefficient has a
high value at the lower part and it decreases to a
minimum at somewhere near 17 per cent of the total height.
At this point, flow in the boundary layer becomes
turbulent and an increase in heat transfer coefficient
will be observed for a short distance, after which it
reaches a constant value for the remaining distance. In
spite of the difference in flow mechanisms, the equation
Nu = constant$(Gr)^{1/4}$ is applicable to all the two
dimensional cases of natural convection heat flow within
the range of the validity of the boundary layer theory.

In 1881, Lorenz proposed his assumption which leads
to a possible solution of the problem of natural convec-
tion from the vertical plate. He assumed that the temp-
erature isotherm and the constant velocity lines were
parallel to the plate. By experimental investigation it
was found that this was not the case. Pohlhausen solved
the differential equations using the temperature and
velocity gradients measured by Schmidt and Beckmann for air
as the medium. However, his solution was only valid for
air, and could not be applied to other fluids. Saunders
(35, p. 62) investigated the same problem and obtained the
following series-type solution which was entirely

theoretical and hence could be applied to any fluid:

$$\frac{\bar{Nu}}{(GrPr)^{1/4}} = 0.524 \left[\frac{Pr}{Pr + 0.167} \right]^{1/4}$$

where $\bar{Nu}$ is the mean Nusselt number. Saunder's experimental data were correlated by McAdams into the following empirical relationships:

$$Nu = 0.13 \left[GrPr \right]^{1/3} \quad \text{for } 10^9 < GrPr < 10^{12}$$
$$Nu = 0.59 \left[GrPr \right]^{1/4} \quad \text{for } 10^4 < GrPr < 10^9$$

where all the fluid properties were measured at film temperature.

Schuh also solved the differential equations numerically by successive approximation for the case of heated vertical plate. Later, Ostrach (31) solved the differential equations numerically on an electronic computer.

Squire and Eckert (11, p. 312) studied the problem of natural convection and proposed an approximate formulae for the velocity and temperature profiles based on the assumption that, in the region of laminar heat flow, the temperature profile may be expressed by a parabolic equation and the velocity profile may be expressed by a third power equation similar to that of the profiles shown in the following sketch.
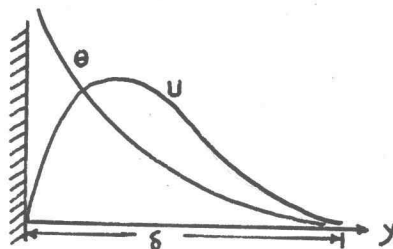
The proposed formula are

$$\theta = \theta_s \left(1 - \frac{y}{\delta}\right)^2 \tag{7}$$

$$U = U_1 \frac{y}{\delta} \left(1 - \frac{y}{\delta}\right)^2 \tag{8}$$

With the aid of their proposed formulae they solved the differential equations by means of Karman's integral relations, and obtained

$$Nu_x = 0.508 Pr^{1/2}(0.952 + Pr)^{-1/4}(Gr_x)^{1/4}$$

where Nu_x and Gr_x are respectively the local Nusselt number and Grashof number for a vertical distance x measured from the lower edge of the plate. The above equation obtained by the approximate method agrees very well with the solutions obtained by the exact method. The exact method is far more cumbersome.

Merk and Prins (27, p. 11) introduced a refined Squire-Eckert approximation by assuming not only the first derivatives of U and θ but also their second derivatives equal to zero at $y = \delta$. A more accurate solution was obtained.

For the problem of natural convection in the region of turbulent heat flow, Eckert ($_{12}$, p. 256) suggested the

following equations for the temperature and velocity
profiles:

$$\theta = \theta_s \left[1 - \left(\frac{y}{\delta}\right)^{1/7} \right] \qquad (9)$$

$$U = U_1 \left(\frac{y}{\delta}\right)^{1/7} \left(1 - \frac{y}{\delta}\right)^4 \qquad (10)$$

Where the velocity profile equation was intentionally
chosen such that, when the layer is very close to the
surface, i.e., y becomes small compared to δ , it will be
similar to the velocity profile equation for turbulent
forced flow $U = U_1 \left(\frac{y}{\delta}\right)^{1/7}$. Eckert then suggested that the
last terms in the Karman's integral equations which were
originally derived from the continuity, momentum, and
energy equations, may be replaced by the shearing stress
and heat flow that are used in forced-convection flow,
under the assumption that, in the layer very close to
the wall, the conditions are similar for natural and
forced convection flow:

$$\frac{d}{dx} \int_0^\delta U^2 \, dy = \int_0^\delta g\beta\theta \, dy - \nu \left(\frac{\partial U}{\partial y}\right)_s \qquad (11)$$

$$\frac{d}{dx} \int_0^\delta U\theta \, dy = -\alpha \left(\frac{\partial T}{\partial y}\right)_s \qquad (12)$$

where the subscript s stands for the layer at the plate
surface; x stands for the distance measured vertically
from the lower edge; y is the distance measured normal
to the plate surface, and U and V are respectively the

velocities parallel and normal to the surface. He obtained the following solution:

$$Nu_x = 0.0295(Gr_x)^{2/5}(Pr)^{7/5}\left[1+0.494(Pr)^{2/3}\right]^{-2/5}$$

which is in good agreement with experiment for values of Gr between 10^{10} and 10^{12}.

Hougen and Colburn (4, p. XII-38) derived the equation for natural convection from vertical plates in turbulent region under the assumption that the resistance to heat flow exists in the laminar sublayer only and none exists in the turbulent region, and the thickness of the laminar sublayer is the same as that in forced convection heat flow. Their equation is

$$Nu = \frac{hL}{k} = 0.108 \left(\frac{L^3\rho^2 g\beta\theta}{\mu^2}\right)^{1/3}$$

Based on Langmuir's film theory, Rutkowski (34) suggested that for natural convection from vertical plates the temperature profile may be expressed by an error function since conduction alone takes place, and the velocity profile was also expressed by an error function which was calculated from the temperature profile. By von Karman's integral relations, he calculated the temperature and velocity profiles. The results are in good agreement with the results of other investigators. It was suggested by Rutkowski that this method may also be applied to the case of parallel vertical plates,

spheres, and cylinders.

In all the above mentioned approaches, the terms for compression work and friction heat have been neglected in the energy equation because of their small magnitudes as compared to the other terms. However, it was pointed out by Ostrach (29, p. 1287) that these two terms depend on a new parameter, which he obtained theoretically. This new parameter is

$$\bar{K} = Gr \frac{\beta f_x L}{c_p}$$

It was observed that in the case of the cooling of turbine blades and helicopter ram jets, there was a high body force being generated parallel to the plates, and hence a high value of $\bar{K}$. Therefore, it was not always safe to neglect the compression work and friction heat in the energy equation.

The approaches discussed above are all for vertical plates with uniform temperature. The problem of natural convection from non-isothermal vertical plates was studied by Sparrow and Gregg (42, p. 879). They studied this for the following two families of surface temperatures

$$T_s - T_a = NX^n$$
$$T_s - T_a = Me^{mX}$$

and obtained a numerical solution by solving the differential equations for gases. The problem of natural convection from vertical plates with uniform surface

heat fluxes was also studied by Sparrow and Gregg, and the problem of non-uniform wall heat fluxes and non-uniform wall temperature has also been studied by Sparrow.

Since the fuel rods in a nuclear reactor may have to be cooled solely by natural convection in case of a coolant-pump failure, a knowledge of how the boundary layer changes during a process of transient natural convection is necessary for designing the nuclear-reactor fuel elements. This problem was studied by Siegel (38, p. 347) by employing the Pohlhausen-Karman approximate method and the temperature and velocity profiles proposed by Eckert (11, p. 312). It was observed that, for a time during the thermal transient, the thickness of boundary layer exceeds that for a steady-state, hence the heat transfer coefficient would pass through a minimum before the steady state was achieved. The equations for the time required to reach a steady state for a plate suddenly raised to a certain uniform temperature and for a plate suddenly subjected to a certain heat flux were obtained as follows:

For uniform temperature

$$\tau = \left[\frac{0.524(0.952 + Pr)^{1/2} + 7.10(0.377 + Pr)^{1/2}}{2} \right]$$

$$(Gr_L)^{-1/2}(Pr)^{-1}x^{1/2}$$

For uniform heat flux

$$\tau = 4.78(0.8 + Pr)^{2/5}(Gr_L^*)^{-2/5}(Pr)^{-4/5}x^{2/5}$$

There are some other special problems of natural convection from vertical plates which have been studied by different investigators. The natural convection heat transfer in regions of maximum fluid density was studied by Schechter and Isbin (18, p. 81-89) and the natural convection from a vertical plate with an obstruction placed above the point of initiation of the heated section was studied by Bevans (1, p. 114-119).

5. Natural convection from vertical cylinders

Vertical cylinders are classified as the bodies with rotational symmetry. To date, there has been little study done on the natural convection from the outer surface of a vertical cylinder. However, it has been observed that as the boundary layer is sufficiently thin, the results of the natural convection from vertical cylinders will be similar to those of vertical plates. As the boundary layer thickness increases, behavior deviates more and more from that of a vertical plate. It was also observed (5, p. 101) that for short cylinders having ratio of length to diameter less than 40, natural convection heat transfer from vertical cylinders will be less than that from horizontal ones. Hence, there is an additional

variable appearing in the case of vertical cylinders, i.e.
the length, which may be eliminated in the case of a
horizontal cylinder by choosing it sufficiently long.

In 1932, King (20, p. 347) experimented with vertical
cylinders, horizontal cylinders, vertical planes and
spheres, and obtained his correlation. In 1948,
Touloukian, Hawkins, and Jakob tested vertical cylinders
in water and ethylene glycol (43, p. 530). The results
obtained by them were quite close to those for vertical
plates. Their results can be shown by the following
relationships:

For the value of GrPr between 0.2 (10^9) and 40 (10^9)
$$Nu = 0.726 \ (GrPr)^{1/4}$$
For the value of GrPr between 40 (10^9) and 900 (10^9)
$$Nu = 0.0674 \left[Gr(Pr)^{1.29} \right]^{1/3}$$

Elenbaas (14, p. 1152) studied the natrual convection
from vertical cylinders based on Langmuir's film theory,
and obtained the following theoretical equation:

$$Nu_{d,s} \ exp \left(\frac{-2}{Nu_{d,m}} \right) = 0.6 \ \frac{(GrPr)_{d,s}^{1/3}}{(GrPr)_{L,s}^{1/2}}$$

where the subscript s indicates that the value must be
taken at the wall temperature, subscript m indicates that
the mean of the quantity in the interval $T_s - T_a$ must be
taken, for instance

$$\lambda_m = \frac{1}{T_s - T_a} \int_{T_a}^{T_s} \lambda(T)\, dT$$

Sparrow and Gregg (41, p. 1823) solved the differential equations for natural convection from the outer surface of a vertical cylinder, and obtained the following quantitative criterion under which the results of vertical plates can be applied to the case of vertical cylinders:

For local Nusselt number

$$\frac{2^{3/2}}{Gr_x^{1/4}} \left(\frac{x}{r_o} \right) \ll 0.11 \qquad\qquad \text{for Pr} = 0.72$$

$$\frac{2^{3/2}}{Gr_x^{1/4}} \left(\frac{x}{r_o} \right) \ll 0.13 \qquad\qquad \text{for Pr} = 1$$

For average Nusselt number

$$\frac{2^{3/2}}{Gr_x^{1/4}} \left(\frac{x}{r_o} \right) \ll 0.15 \qquad\qquad \text{for Pr} = 0.72$$

$$\frac{2^{3/2}}{Gr_x^{1/4}} \left(\frac{x}{r_o} \right) \ll 0.17 \qquad\qquad \text{for Pr} = 1$$

6. Natural convection from parallel plates:

Natural convection in a space between two vertical parallel plates is of particular importance in the problem of cooling of turbine blades and the helicopter ram jet. An extensive study on this problem was made by Elenbaas (13, p. 1). He experimented with the square plates having different spaces and sizes in air, and observed that for high values of plate spacing the heat

dissipation (watt/cm^{2}°C) becomes independent of plate
space, b, increases with the temperature difference
between the plates and the air, Θ, and decreases slowly
with the length of plates. For small values of b, the
heat dissipation increases rapidly with b, increases with
Θ in the region of small values of Θ, and decreases
slightly with Θ in the region of large values of Θ.
Theoretically, Elenbaas analyzed the differential equations
of the case that the plates are infinitely long in the
horizontal direction, and obtained an empirical equation
in which an additional variable L appears. His equation
is

$$Nu = \frac{1}{24} \cdot \frac{b}{L} GrPr \left[1 - e^{\frac{-35L}{bGrPr}} \right]^{3/4}$$

Siegel and Norris (39, p. 603) did some experimental
study on two vertical plates. The top of the rectangular
space between the plates was left open, and the bottom
and sides were closed for most of the tests. It was
observed that the local Nusselt number decreases when
the space was reduced. It was also found that when the
duct was open at the bottom, the local heat transfer
coefficients were slightly affected by the space between
the heated plates, the presence or absence of side-
inclosing walls, and the clearance between the lower
edges and the floor. When the duct was closed at the
bottom and at the sides, the local heat transfer

coefficient was considerably affected by both the duct width and the space between the heated plates.

Ostrach (30, p. 1-55) solved the differential equations of natural convection heat transfer in channels with constant wall temperature by numerical methods. It was found that the parameter $\bar{K} = Gr\dfrac{\beta f_x d}{c_p}$ determines the contribution of the compression work and friction heat. Those are neglected in most cases of natural convection. The velocity and temperature profiles for different configurations were also calculated in his paper.

Lietzke (24, p. 1-23) analyzed the problem of natural convection between two parallel plates one of which was heated uniformly and the other cooled uniformly. An exact solution was obtained from the differential equations, and presented in the form of velocity and temperature profiles. Good agreement with the experiment results was observed. It was observed that when the value of GrPr increases the point of maximum velocity shifts closer to the wall.

As a case of simulating the cooling of turbine blades, Ostrach and Thornton (32, p. 363) studied the problem of the laminar natural convection in a closed-end tube with a linear wall temperature and large length-radius ratio. In this process, the group $GrPr\dfrac{r}{L}$ is the determining parameter, where L is the length of the tube,

and r its inner diameter. The velocity and temperature profiles were calculated by Karman's integral relations.

7. Natural convection heat transfer from finned tubes:

The purpose of adding fins to a surface such as a cylinder is to increase the available area for heat transfer. However, the adding of fins to a surface will result in a decrease of surface temperature unless the fin material has a very high thermal conductivity. If the increase of surface area is greater than the decrease of surface temperature, then the adding of fins will cause an increase in heat transfer rate. In general, the fin effectiveness is used as a criterion for estimating the fin-efficiency, and which is defined as the ratio of heat transfer rate from a fin to the heat transfer rate that would be obtained if the entire fin surface area were to be maintained at the same temperature as the primary surface (i.e. the cylinder). Finned tubes are widely used in industry, but there has been little work done on the subject of natural convection from finned tubes. To date, most of the work done on the finned tubes has been concentrated in the field of forced convection, and heating and air-conditioning, and is solely experimental.

The heat transfer between the finned tubes and the

fluid may be divided into two steps taking place simultaneously. The first step is concerning the conduction of heat through fins. The temperature distribution along the fins has been solved from the differential equation obtained by a heat balance. The second step is the convection of heat from the finned tube to the heating medium. The problem of heat transfer by convection from a finned tube in forced air current has been studied by several investigators. Biermann and Pinkel (3) tested the finned tubes by various fin shapes, widths, thicknesses and spaces under different air speeds in a wind tunnel. It was observed that the value of heat transfer coefficient varies mainly with the air speed and the fin space, and is affected slightly by the other fin dimensions. An equation was derived for designing the optimum fins which will give the maximum amount of heat dissipation for a given weight of material.

Biermann and Ellerbrock, Jr. (2, p. 401-424) reported that for a given fin weight, the magnesium alloy gives the highest heat dissipation; pure copper and aluminum alloy are only slightly inferior to magnesium alloy. For a given fin height, copper, which has a high thermal conductivity, will give the highest heat dissipation. In the problem of cooling, it is rather important

to know how much heat is dissipated through the plain cylinder. For this purpose, a term of so-called cooling effect was derived in reference (3, p. 263) and (25, p. 111). It gives the rate of heat removed from the area of the plain cylindrical surface.

Schey and Rollin (36, p. 111-124) tested the effect of different types of baffles on the heat transfer of finned tubes. Four kinds of baffles, streamline baffle, plate baffle, shell baffle, and integral baffle were tested, and it was found that the shell baffles gave the best cooling effect when they were mounted as closely to the tube as possible.

Finned tubes are also widely used in heating and air-conditioning. An extensive study has been carried out by the Institute of Boiler and Radiator Manufacturers. It was concluded that the fin thickness used in the investigation should be sufficiently consistent, and the fin to tube bond can affect the output.

Murray (28, p. A-78-80) made a mathematical investigation on the heat flow in an annular disk of uniform thickness.

Carrier and Anderson (7, p. 304-318) studied the temperature distribution on the finned tubes.

Seigel and Bryon (37, p. 129) studied the problem

of natural convection cooling and dehumidifying on a
bare horizontal tube, and on other tubes with extended
surfaces. One horizontal bare tube, one horizontal finned
tube, and one complete gravity cooling coil were used.
Their results will be discussed in Chapter VI.

Chapter III
Experimental Apparatus

The experimental apparatus consisted of the finned tubes, power source, temperature measuring system, and other miscellaneous components. These will be discussed in detail.

1. Finned tubes

Each of the finned tubes consisted of a 1.375 inch OD by 1.261 inch ID bare copper tube with a length of one foot, on which fin plates were mounted. The fin-plates were made from 23 gauge copper (0.0239 inch thick) and they were fitted on the copper tube by thermal-shrinking. The inside diameter of the fin-plates was made 0.006 inch smaller than the outside diameter of the tube. By heating to $1600^{O}F$ in an oven for three minutes, the fin-plates expanded to the extent that the inside diameter was bigger than the outside diameter of the tube. After being mounted on the tube and cooling, the fin-plates were fitted very well on the tube. Two kinds of fin-plates were made, round fins and square fins. Of the round fins, three different sizes were made, i.e. 2 3/8 inches, 2 7/8 inches, and 3 3/8 inches fin diameter. Only one size of square fin was made with an area equal to that of the round fin-plates of 2 7/8 inches diameter.

The finned tubes were heated by two quartz immersion heaters with an overall length of 11 inches and a heated length of 6 inches. These were obtained from the Glo-Quartz Electric Heater Co., Inc. They were inserted into the tube from either end through rubber stoppers and placed in such a way that they were completely immersed when the horizontal tube was half filled with water. A glass tube passed through one of the stoppers, and connected to a water manometer by a rubber tube so that the vapor pressure inside the tube could be observed. The finned tube was mounted on a stand so that it was two feet from the floor, and it was enclosed on the sides by an open top enclosure 40 by 40 by 40 inches.

Six iron-constantan thermocouple junctions were soldered on the finned tube, three on the upper part and three on the lower part. Of the three thermocouples on each part, one was soldered on the copper tube, one on the mid-point between the fin-base and fin-tip, and one on the fin-tip. Only one fin-plate was chosen for temperature measuring purposes. However, the calibration curves of the temperature distributions on different fins have been plotted so the average temperature of the fins can be obtained by the measurement on one fin. The general set-up of the finned tube and its accessories are shown in the sketch of Fig (2), and all the finned tubes tested

U — POWERSTAT
P — POTENTIAL METER
T — THERMOMETER
C — COLD JUNCTION OF
      THERMOCOUPLE
H — HOT JUNCTION OF
      THERMOCOUPLE
R — RUBBER TUBE
B — THERMOS BOTTLE

S — KNIFE SWITCH
M — IMMERSION HEATER
F — FINNED TUBE
J — WATER BAROMETER
E — ENCLOSURE BOX
A — AMMETER
V — VOLTMETER
L — VOLTAGE STABILIZER
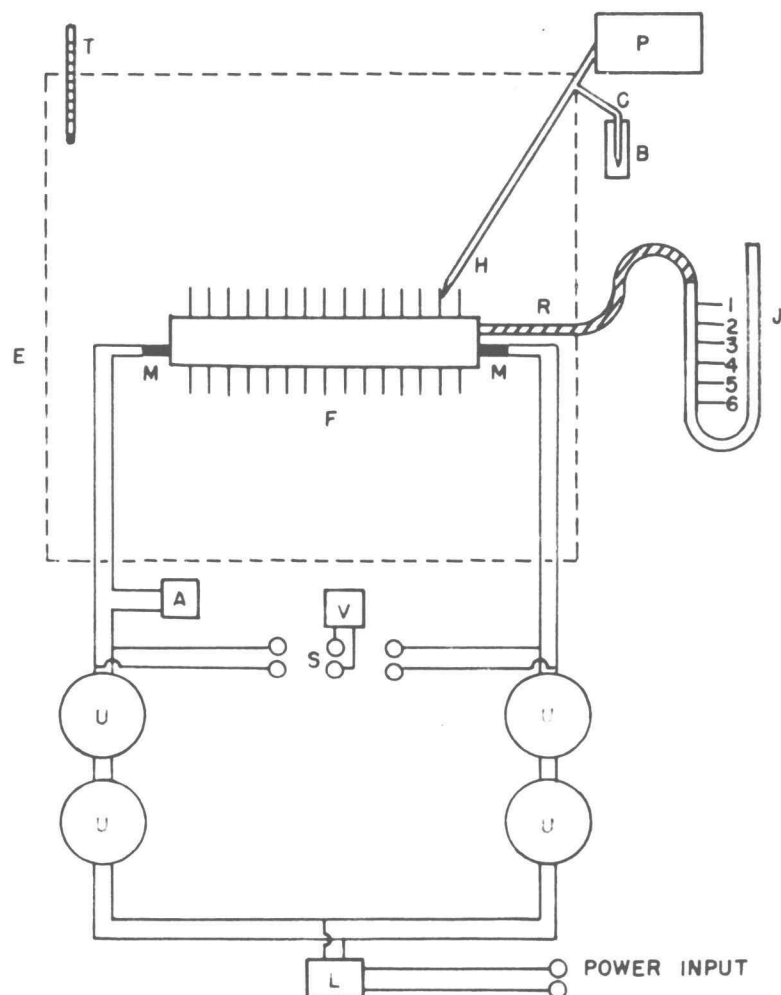
FIGURE 2   FINNED TUBE AND ASSOCIATED EQUIPMENT

are shown separately in the photograph of Fig (3).

2. Power source

The power source consisted of a Raytheon voltage stabilizer, and four powerstats made by the General Radio Co. The powerstats were used for adjusting the power supply to the immersion heaters. Each pair formed one group, and they were arranged in series for the purpose of achieving better adjustment of the 60 cycle AC voltage. A Simpson voltmeter with a range from zero to fifty volts and a Triplett ammeter with a range from zero to two amp were used to measure the power supply. Accuracy of the voltmeter was $\pm$ 0.2 volt, while that of the ammeter was $\pm$ 0.01 amp. A wiring diagram of the power system is shown in Fig (4).

3. Temperature measuring system

Temperatures on the surface of finned tubes were measured with thermocouples and a potentiometer. The e.m.f. readings from the potentiometer were converted to temperature units by means of a calibration curve. The e.m.f. measuring system consisted of No. 30 iron-constanten thermocouples, a rotary selector switch, a cold junction, and a Leeds and Northrup potentiometer (No. 737621). The cold junction was immersed in a thermos bottle filled with cracked ice in water to keep

FIGURE 3 FINNED TUBES

L — VOLTAGE STABILIZER
U — POWERSTAT
S — KNIFE SWITCH

POWER INPUT
110 VOLT
60 CYCLE

L

U   U

U   U

VOLTMETER

S

AMMETER
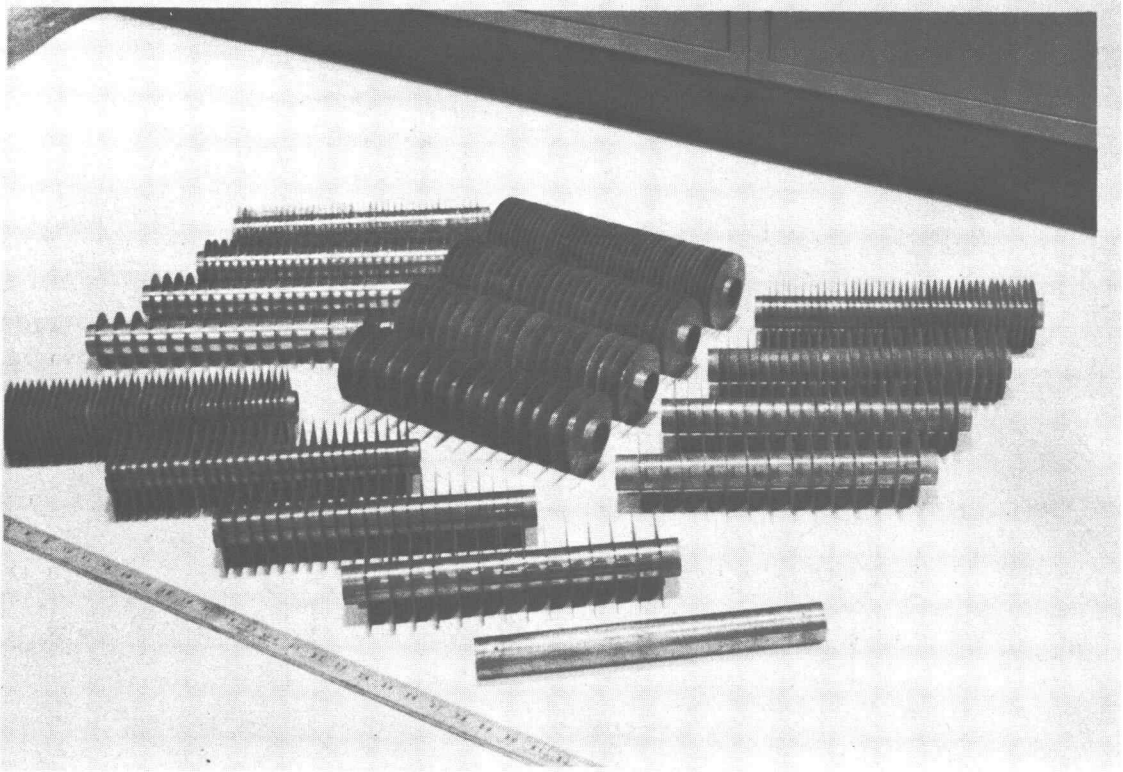
POWER INTO
IMMERSION
HEATERS
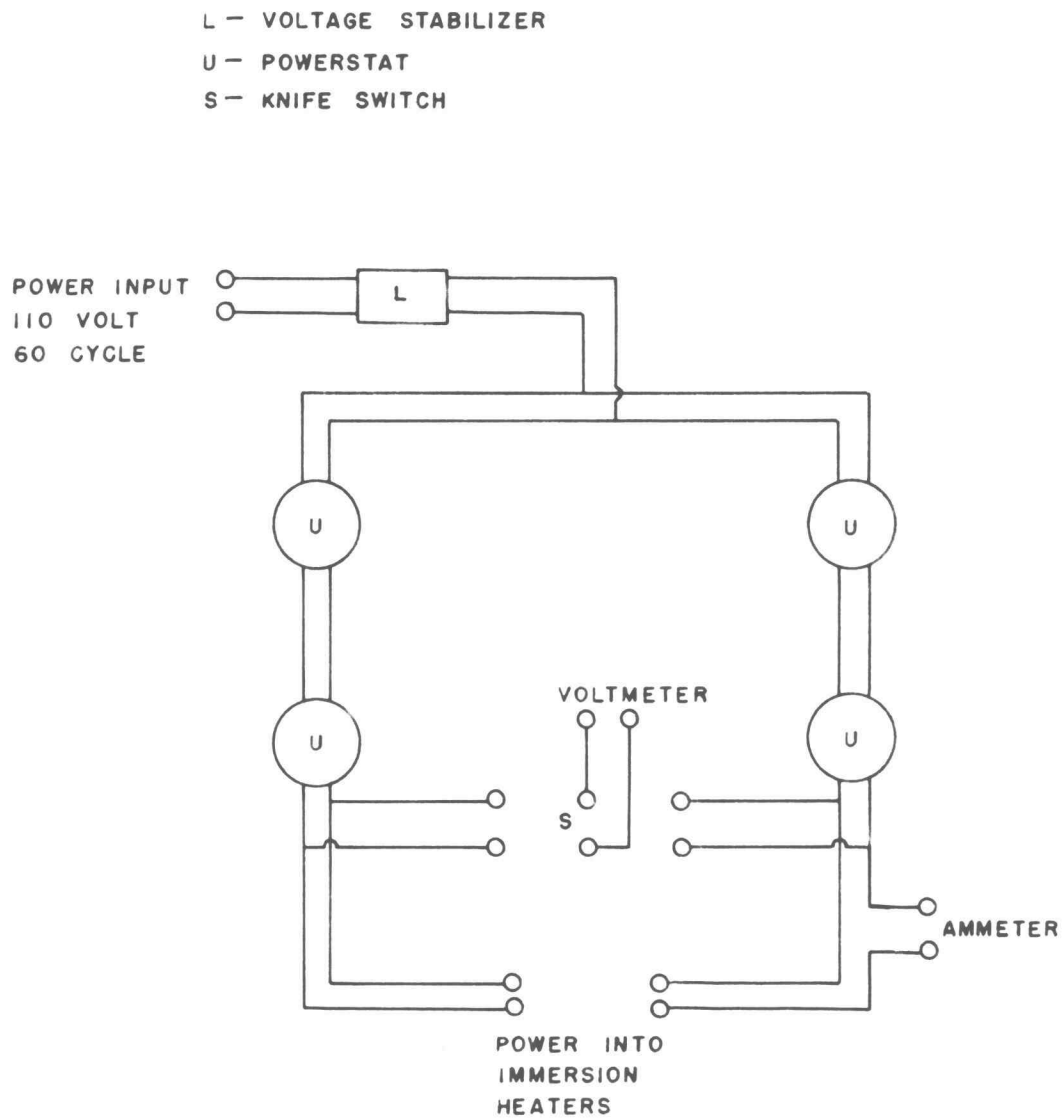
FIGURE 4   WIRING   DIAGRAM   FOR   POWER   SYSTEM

the temperature of the cold junction at $32^{\circ}F$. A Fischer
vibradamp support was placed underneath the potentiometer
for the purpose of absorbing any ambient vibration, because
the accuracy of the reading of the potentiometer was
unfavorably affected by any vibration.

The temperature of the air was measured by a
thermometer made by the Standard Calorimeter Co. with an
accuracy of $0.01^{\circ}F$.

4. Miscellaneous component parts

During the study of chimney effect, baffle-plates
were mounted on the sides of the tubes by means of four
sets of wood rods which could be fitted on the finned-
tube stand. Two sizes of baffle-plate having heights
of 2.548 inches and 3.78 inches were used. They were
rectangular in shape, and had the same length as that of
the finned tube. They were placed 1/8 inch from the fin
tip, in a vertical position on either side of the fin as
shown in Fig (5).
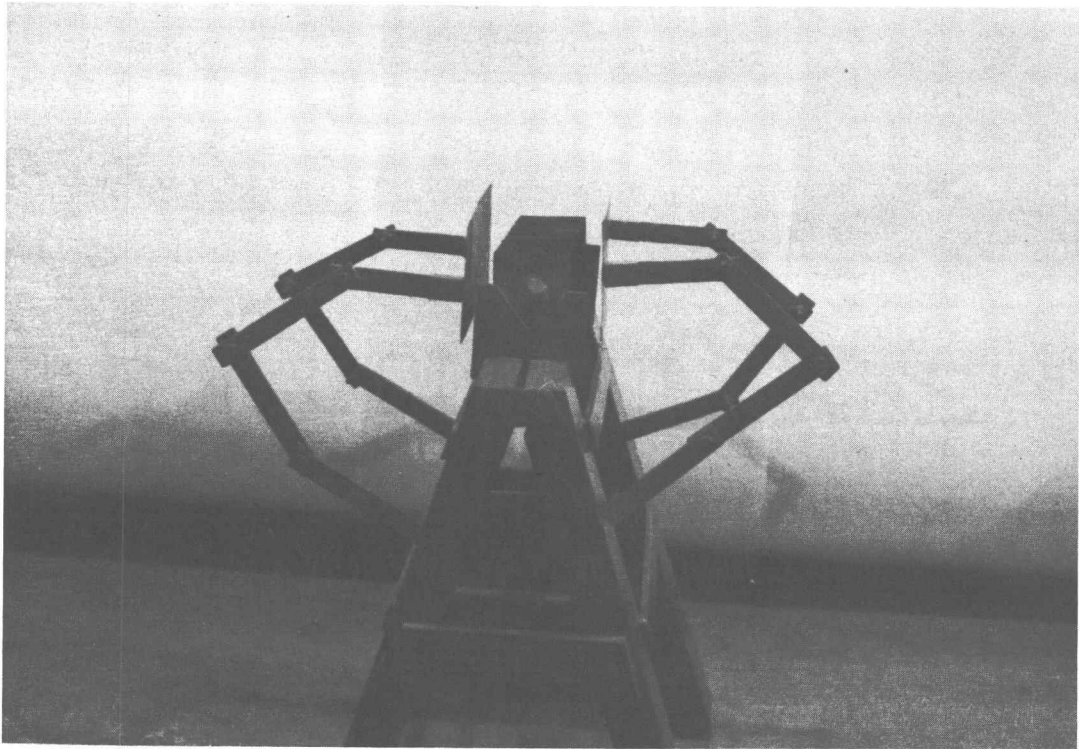
FIGURE 5 ASSEMBLY OF CHIMNEY BAFFLES AND FINNED TUBES

Chapter IV

Experimental Program and Experimental Procedure

I. Experimental program

This thesis is an investigation of natural convection heat transfer from finned tubes. Air was used as the ambient fluid. The primary purpose of this investigation is to correlate the experimental data in terms of the parameters of the system. The variables involved in the correlation were the temperature difference between the surface of finned tube and the air, fin spacing, and fin diameter. Arithmetic mean heat transfer coefficients were used in the correlation, and the necessary data for calculating the arithmetic mean heat transfer coefficients were the average temperature of finned tube, the time-average temperature of the air, the area available for heat transfer, and the power input to the two heaters.

1. Round finned tubes

Three different fin diameters (2 3/8, 2 7/8 and 3 3/8 inches) and four spacings (1/4, 3/8, 1/2, and 3/4) were studied during the course of investigation. However, due to the difficulty of making an exact fin spacing the real fin spacings of the tubes deviated somewhat from above nominal values. By adjusting the power input, temperature differences ranging from 20°F to 100°F could

be obtained. Each finned tube was studied at six
temperature differences in this range. Duplicate runs
were made at each temperature difference. During the
progress of the experiments, the enclosure-box was
raised 2 1/2 inches from the table top so that sufficient
air circulation could be obtained. However, for the
purpose of determining effect of air circulation, two
other values (0 and 3 1/2 in.) of clearance between the
lower edge of the enclosure-box and the table top were
studied for the finned tube of 2 7/8 inches fin diameter
and 6/8 inch fin spacing.

2. Square finned tube

Since the results of the square finned tubes were very
similar to those of the round finned tubes with the same
fin area, only one fin height and four fin spacings were
studied. The fin-plates were made 2.548 x 2.548 inches
in size; so the fin area was equal to that of the 2 7/8
inches diameter round fins. The same fin spacing as those
for the round finned tube were studied.

Study of chimney effect was made on the tube of 6/8
inch fin spacing.

3. Temperature measurement on finned tubes

Average temperature of finned tubes was needed for
calculating mean heat transfer coefficients. Since only

the temperature of one arbitrarily-chosen fin-plate was measured during the progress of the experiment, experimental data for evaluating the average temperature of the finned tube from that of the arbitrarily-chosen fin were needed. For this reason preliminary experiments for each finned tube were carried out before the main experiments were made. The purpose of carrying out these preliminary experiments was to obtain sufficient experimental data for plotting the calibration curves relating the average temperature of the finned tube to the temperature of the arbitrarily-chosen fin-plate. With the aid of these calibration curves, evaluation of the average temperature from the temperature of chosen fin was possible. Temperatures of fifteen fin-plates were measured for the average temperature determination of the 1/4 inch-spacing tubes, temperatures of seven fin-plates were measured for the 3/8 inch-spacing tubes; and temperatures of seven and four fin-plates were recorded respectively for the 1/2 inch- and 6/8 inch-spacing tubes. Temperatures of the middle points of the upper and lower portions of the fin-plate were taken for representing the average temperatures of these two portions. Therefore, only two thermocouples were needed for each plate. These two thermocouples were respectively soldered on the middle points of the upper and lower

portions of the fin-plate. It is seen in the main experimental data that it was a good approximation for taking the temperature of the middle point as the average of the temperature of the base, middle and tip of the fin-plate.

4. Thermocouple numbering system

Thermocouple numberings are presented in Fig (6). Three thermocouple junctions were soldered on the upper part of the fin-plate, and the other three were soldered on the lower part.

5. Bare copper tube

For the purpose of testing the reliability of the apparatus, a bare copper tube was also tested. Thermocouple numberings system of bare tube is also presented in Fig (7).

II. Experimental procedure

The procedure in operating the equipment and recording the data are listed as follows:

1. Set the voltage of the powerstats so that two heaters would have the same power input.

2. Closed all the doors and windows of the laboratory, in which the equipment was set up, so that the air inside the laboratory would

ARRANGEMENT OF
THERMOCOUPLE WIRES

SWITCH

POTENTIOMETER

COLD JUNCTION

THERMOCOUPLES

I = IRON THERMOCOUPLE WIRE

C = CONSTANTAN THERMOCOUPLE WIRE
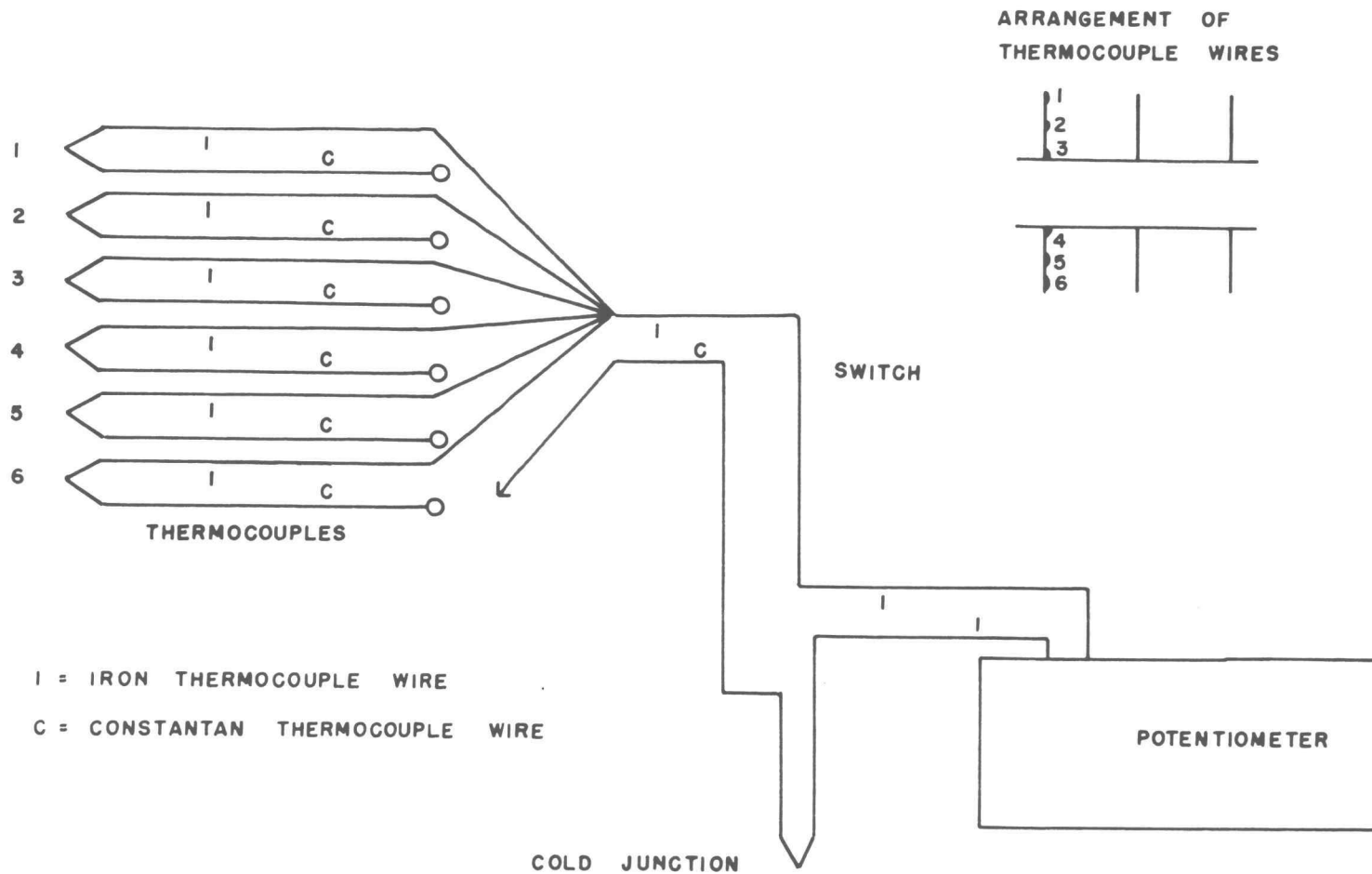
FIGURE 6   DIAGRAM OF EMF METERING SYSTEM

ARRANGEMENT OF
THERMOCOUPLE WIRES

1   2   3

4   5   6

1

2

3

4

5

6

I   C

I   C

I   C

I   C

I   C

I   C

THERMOCOUPLES

I   C

SWITCH

I   I

I = IRON THERMOCOUPLE WIRE

C = CONSTANTAN THERMOCOUPLE WIRE

POTENTIOMETER

COLD JUNCTION
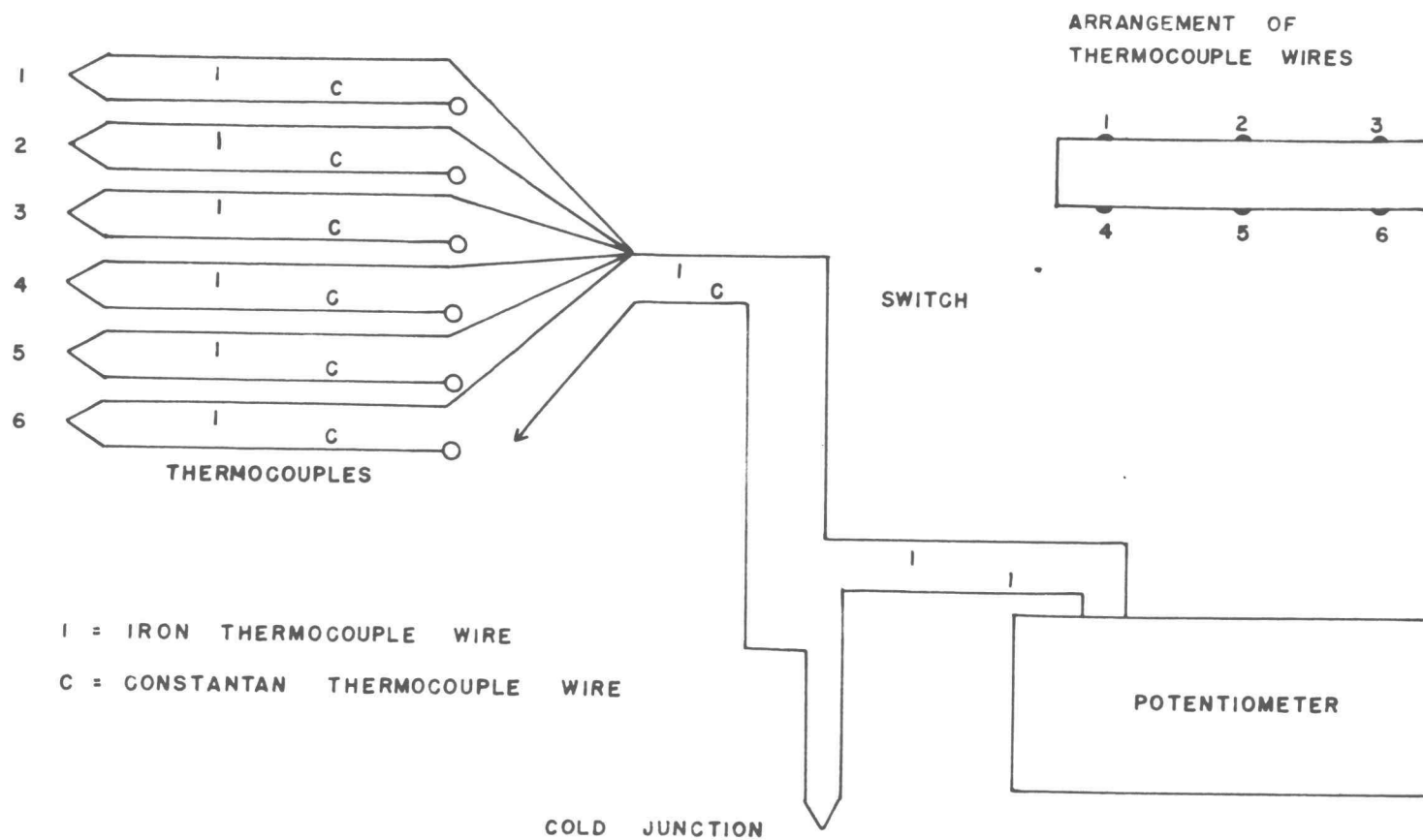
FIGURE 7   DIAGRAM OF EMF METERING SYSTEM OF BARE TUBE

remain undisturbed.

3. Allow two hours for the experiment to reach steady state. Under the condition of steady state, amount of water vapor evaporated by the heaters was balanced by that condensed down from losing heat to the air through the finned tube.

4. After two hours, the rubber tube was connected to the water manometer. Constant reading on the manometer indicated the constant pressure inside the finned tube and so the arrival of steady state. Usually, the steady state could be maintained for 10 or 20 minutes.

5. Thermocouple readings were recorded. After the last thermocouple reading was taken, a check was made on the first thermocouple reading in order to assure the achieving of steady state.

6. Air temperature was recorded; before the thermocouple readings were taken, and after the thermocouple readings were taken.

7. Readings of the electric current of the two heaters were recorded.

8. Voltage readings of the heaters were recorded.

Chapter V

Calculation of Experimental Data And Estimation of Error

I. Calculation of experimental data

Since the main objective of this thesis was to evaluate the mean heat transfer coefficient for natural convection from finned tubes, an energy balance is required. It was mentioned in the preceding chapter that all the experimental data were recorded under the steady state. At steady state, the energy input should be equal to the energy output. The energy input was equal to the amount of power supplied to the immersion heaters, while the energy output was equal to the heat loss from the finned tube to the air by both natural convection and radiation. Hence, an energy balance could be established in the following manner:

$$q_{input} = q_{conv} + q_{rad} \qquad (13)$$

where

q_{conv} = rate of heat loss by natural convection

q_{rad} = rate of heat loss by radiation

q_{input} = rate of energy input

In order to calculate q_{conv} from the above, calculation of radiation loss was necessary by means of the following formula:

$$q_{n=1} = A_n \mathcal{F}_{n1} B(T_n^4 - T_1^4) \qquad (14)$$

where

q_{n-1} = heat transfer rate by radiation between
surfaces 1 and n

For calculating $\mathcal{F}_{nr}$, it was assumed that each section
between two adjacent fin-plates might be represented by
one of the configurations discussed in reference (16,
p. 29), and which is presented in Fig (8) where A_3 and
A_4 are the surfaces of the fin-plates, A_2 is the cylinder
surface, and A_1 is a fictitious surface. All the surfaces
were assumed to be gray bodies except surface A_1.
Surface A_1 was assumed to have the same emissivity as
that of surrounding enclosure and the room walls. These
were assumed to be black bodies. Thus surface A_1 was
assumed to have an emissivity of unity. Details for the
calculation of $\mathcal{F}_{nl}$ are presented in Appendix (A). The
over-all interchange factors of the square finned tubes
were evaluated under the assumption that the configura-
tion in Fig (8) might be applied to square finned tubes
as well.

With the aid of radiation loss calculation heat
transfer coefficients for natural convection can be
calculated from the following equations:

$$q_{conv} = q_{input} - q_{rad} = KIE - \frac{A}{A_2 + A_3 + A_4} \sum_{n=2}^{4} A_n \mathcal{F}_{nl} B (T_n^4 - T_1^4) \quad (15)$$

$$h_{a.m.} A (T_w - T_a) = KIE - \frac{A}{A_2 + A_3 + A_4} \sum_{n=2}^{4} A_n \mathcal{F}_{nl} B (T_n^4 - T_1^4) \quad (16)$$

$$h_{a.m.} = \frac{KIE - \frac{A}{A_2+A_3+A_4} \sum_{n=2}^{4} A_n \mathfrak{J}_{n1} B(T_n^4 - T_1^4)}{A(T_w - T_a)} \tag{17}$$

The whole finned tube (primary and secondary surface) was assumed to have uniform temperature T_w, then

$$h_{a.m.} = \frac{KIE - \frac{AB(T_w^4 - T_a^4)}{A_2+A_3+A_4} \sum_{n=2}^{4} A_n \mathfrak{J}_{n1}}{A(T_w - T_a)} \tag{18}$$

where T_w was the arithmetic mean temperature of the whole finned tube. As mentioned in Chapter IV, during the progress of the experiment only the temperature of one arbitrarily-chosen fin-plate was measured. Therefore, charts of calibration curves, in which the arithmetic average temperature of fins versus the temperature of the arbitrarily-chosen fin-plate where the temperature measurement was taken, was needed for evaluating T_w. These plots are presented in Figs (9) through (24). Maximum deviation of the data points from the curves is ±3%. However, it is observed that the maximum deviation of the data of the individual fins from the average is ±6%.

As to the temperature distribution across a single fin-plate, it was observed that, for the finned tubes of 3 3/8 inches fin diameter, the temperature difference between the tip and base of the lower part of fin-plates was about $2.5^{\circ}F$ when the average surface temperature of finned tube was $167^{\circ}F$, i.e. 1.5% of the average fin

temperature. The temperature difference across the upper part of fin-plates was 2.5°F at the same average surface temperature, while the temperature difference between the middle points of upper and lower parts was 2.5°F, i.e. both of them were also equal to 1.5% of the average fin temperature. Since lower temperature differences occurred at lower average surface temperatures, and lower temperature difference also occurred for smaller fin-plates, it is reasonable to assume that the finned tube possesses a uniform temperature.

The arithmetic mean temperature T_w of the finned tube could be obtained from the temperature of the arbitrarily-chosen fin-plate by using the calibration curves mentioned above. From T_w, the arithmetic heat transfer coefficient $h_{a.m.}$ was calculated. For evaluating T_w a conversion chart was needed to convert the millivolts of e.m.f. into degrees Farenheit. This conversion chart was made by calibrating the thermocouples against a National Bureau Standard thermometer which is presented in Fig (25).

Also the thermometer used in measuring the air temperature was calibrated against the above-mentioned standard thermometer and its calibration curve is presented in Fig (26).

Since the immersion heaters were the coil-type
heaters, knowledge of how much power loss by self-
inductance was necessary for evaluating the accurate
power input. The following equation was used for
calculating the self-inductance of the heaters:

$$H = \frac{r^2 n^2}{9r + 10L'} \tag{19}$$

where

L' = length of wire, inch

r = radius of wire in the heaters, inch

In the present work,

r $\cong$ 1/8 inch

n $\cong$ 170

L $\cong$ 6 inches

Hence,

$$H = \frac{(1/8)^2 (170)^2}{(9)(1/8) + (10)(6)} \cong 7 \; \mu H$$

This was negligible compared to the total power input.

The total surface area of the finned tube was
calculated from the following equation:

$$A = 2NA_f + A_c + NM(P_f - P_c)$$

A Nusselt number and a Rayleigh number (Ra) were
calculated from the data obtained

$$Nu = \frac{h_{a.m.} L}{k}$$

$$Ra = Gr\, Pr = \left(\frac{L^3 \rho^2 \beta \, \partial \theta}{\mu^2}\right)\left(\frac{c_p \mu}{k}\right) = \left(\frac{\rho^2 \beta g c_p}{\mu k}\right)(L^3)(\theta)$$

The quantity ($\frac{\rho^2 \beta g c_p}{\mu k}$) which includes only air properties was given the symbol Y is plotted in Fig (27) on a function of temperature. Fig (27) was developed from the data on page 483 of reference (26). Thermal conductivity k in the Nusselt number was obtained from the plot in Fig (28) which was developed also from the thermal conductivity data of reference (26, p. 483).

L was any characteristic length of the finned tube. All the air-properties were taken at the film temperature because the film temperature has been shown to be an adequate reference temperature for gases as mentioned in Chapter II.

II. Estimation of experimental errors

The errors involved in the evaluation of mean heat transfer coefficients consist of the errors in reading the e.m.f. values of the various thermocouples, voltage and current values of the power supply, and the estimation of radiation loss.

The values of e.m.f. on the potentiometer were read to $\pm$ 0.002 which was equivalent to $\pm 0.07^{\circ}F$ from the conversion chart. However, there was also some amount of error involved in the preparing of conversion chart. The error in temperature measurement by thermocouple is, therefore, estimated to be $\pm 0.1^{\circ}F$. Besides, the maximum

error involved in averaging procedure for temperature was ±3% as mentioned before.

The current was read to ±0.01 amp, and the voltage was read to ±0.2 volts. The air temperature was read to ±0.01°F.

The greatest radiation loss was provided by the finned tube with smallest fin diameter and largest fin spacing, i.e. the round finned tube of 2 3/8 inches fin diameter and 6/8 inch fin spacing in the present work. By taking the emissivities of the fin-plates and copper tube as listed below, the error involved in the estimation of radiation loss is shown by the following calculation.

Since the possible values of ϵ_3 and ϵ_4 range from 0.7 to 0.57, while those of ϵ_2 range from 0.2 to 0.072, by assuming $\epsilon_3 = \epsilon_4 = 0.7$

$$\epsilon_2 = 0.2$$

it was obtained that

$$\sum_{n=2}^{4} A_n \mathcal{J}_{n1} = 0.254$$

but the value of $\sum_{n=2}^{4} A_n \mathcal{J}_{n1}$ used in this work was equal to 0.0208 as taking

$$\epsilon_3 = \epsilon_4 = 0.57$$

$$\epsilon_2 = 0.072$$

The maximum possible error involved in the evaluation of

$\sum_{n=2}^{4} A_n \mathcal{J}_{n1}$ is therefore

        $0.0254 - 0.0208 = 0.0048$

where ϵ_2, ϵ_3, and ϵ_4 are respectively the emissivities of surfaces A_2, A_3 and A_4. Details of the above calculations are presented in Appendix (A).

The range of error in the mean heat transfer coefficients caused by above errors is shown by the following calculation which was the run 1 of the experiment of round finned tube of 2 3/8 inches fin diameter and 6/3 inch fin spacing:

$$KIE = (3.413)(2)(2.5 \pm 0.2)(0.68 \pm 0.01) = 116.04 \pm 2.63$$

$$T_w - T_a = 153.4(1 \pm 0.03) \pm 0.1 \ -(73.715 \pm 0.01) = 79.685 \pm 4.712$$

$$T_w^4 - T_a^4 = (604.321 \pm 6.791) \times 10^8$$

Substituting the above terms into equation (17), gives

$$h_{a.m.} = \frac{(116.04 \pm 2.63) - \frac{(0.981)(0.1713)}{0.0635}(0.0208 + 0.0048)(604.321 \pm 6.791)}{(0.981)(79.685 \pm 4.712)}$$

$$= \frac{(116.04 \pm 2.63) - (33.238 + 7.679 \pm 0.373)}{78.171 \pm 4.622}$$

$$= \frac{82.802 + 7.679 + 3.003}{78.171 \pm 4.622} = 1.059 + 0.0982 \pm 0.101$$

The percentage error is

$$+ \frac{(0.1992)(100)}{1.059} = +18.8\%$$

$$- \frac{(0.101)(100)}{1.059} = -9.54\%$$

The above value of percentage error appears quite large,

because there is a large amount of error involved in the
over-all interchange factor calculation. However, the
error on the over-all interchange factor shown above has
been estimated for the worst case. It is believed that
there would be less amount of error involved in the
present experiment.

Chapter VI
Analysis of Data

I. Bare tube data

The experimental results of the bare tube are
presented in Fig (29) in which the Rayleigh number
$\left(\frac{d^3\rho^2 g\beta\theta}{\mu^2}\right)_f \left(\frac{c_p\mu}{k}\right)_f$ is plotted versus the Nusselt number $\left(\frac{h_{a.m.}d}{k}\right)_f$
on a logarithmic scale, where the subscript f indicates
that all the fluid properties are taken at the film
temperature. Evaluation of the arithmetic mean heat
transfer coefficient, $h_{a.m.}$, is based on the arithmetic
temperature of the upper and lower parts of the tube. At
an average surface temperature of $200^\circ F$, the difference
in temperature between the upper part and lower part of
the tube was $0.2^\circ F$. Smaller temperature differences would
be obtained for smaller average surface temperatures.
Hence, it was satisfactory to assume a uniform surface
temperature over the tube. Also plotted is the curve
recommended by McAdams for horizontal cylinders. By a
least square analysis of the present data, the following
empirical relationship was obtained with $\pm 2\%$ deviation
of the data:

$$Nu_f = 0.558 \ (GrPr)_f^{1/4} \qquad (20)$$

As compared with McAdams' equation $Nu = 0.53(GrPr)^{1/4}$,
it is seen that the present data for the bare tube are

5.3% higher than those of McAdams'. This may have
resulted from the different length-diameter ratio of the
tubes and the error involved in estimating the radiation
loss in the present work. Since there is a smaller value
of length-diameter ratio used in the present work, it is
possible that the length of the tube may appear as an
additional parameter and affect the heat transfer
coefficient. Also estimation of radiation loss was based
on the assumption that the emissivity of the shiny copper
tube was equal to 0.072. A higher value of emissivity
would provide better agreement with McAdams. Reasonably
good agreement of the present results of the bare tube
with McAdams' results of horizontal cylinder indicates
the reliability of the experimental equipment.

II.   Effect of the clearance between the lower edge of
      the enclosure-box and the table top

It was the object of the study to obtain natural
convection heat transfer coefficients for the tubes
immersed in a large body of still air. Therefore, it was
first determined if the 40 by 40 inches open top
enclosure around the apparatus affected the rate of heat
transfer. It was of particular interest to determine if
the clearance between the lower edge of the enclosure and
table top affected air circulation, and therefore
influenced the heat transfer coefficient. The round

finned tube of 2 7/8 inches fin diameter and 6/8 inch fin
spacing was employed to determine the effect of clearance.
Experiments were conducted with three different values of
clearance between the enclosure and the table top, i.e.
0, 2.5, and 3.5 inches. Results are presented in Fig
(30) where the mean heat transfer coefficient $h_{a.m.}$ is
plotted versus temperature difference. All the data for
the three clearances fall on a single line. Each group
of data deviated from the line a minimum of 1.8% and a
maximum of 18%. It was thought that the heat transfer
coefficient obtained in the case of zero clearance might
be different from that of the other two cases. However,
it is shown in Fig (30) that this is not the case. The
independence of heat transfer coefficient with the
clearance may be explained by examining the flow pattern
of the air circulation. It is thought that, when there
is no clearance between the box and the table top, the
flow pattern of air circulation may be represented by
the sketch in Fig (31). The warm air moved up in the
central portion of the cross section of the box, while
the cold fresh air is sucked in from the sides. This
type of flow pattern keeps the air as well circulated as
in the case with a clearance between the box and the
table top and hence gave the same value of heat transfer
coefficient. All succeeding experiments were made with

a clearance of 2.5 inches.

III. Analysis of heat transfer data of finned tubes

The heat transfer data of all the finned tubes, including that for the two sizes of chimneys, are presented in Figs (32) through (35) in which the Rayleigh number $\left(\frac{d_e^3 \rho^2 g \beta \theta}{\mu^2}\right)_f \left(\frac{c_p \mu}{k}\right)_f$ is plotted versus Nusselt number $\left(\frac{h_{a.m.} d_e}{k}\right)_f$. The equivalent diameter d_e is the arithmetic average of the fin diameter and tube diameter, and the temperature difference is the arithmetic average of the temperature difference between different parts of the finned tube and the air. Each curve is for a constant fin spacing.

The present correlation may be applied to bare tube as well, because in the case of bare tube, fin height is zero. Therefore according to $d_e = \frac{d + d_f}{2}$, it is adequate to use tube diameter to replace the equivalent diameter in the dimensionless quantities and plot the data of bare tubes as well. In the case of single vertical plates d_e reduces to $\frac{d_f}{2}$, because d diminishes to zero. The two dimensionless quantities, then reduce to $\left(\frac{h_{a.m.} d_e}{2k}\right)_f$ and $\left(\frac{d_f^3 \rho^2 g \beta \theta}{8 \mu^2}\right)_f \left(\frac{c_p \mu}{k}\right)_f$, and they can be plotted in Figs (32) through (35) by transformation of axis. With the aid of the plots of horizontal tubes, a comparison of the results of finned tubes with those of

simpler configurations is possible. For square finned
tubes, same value of d_e is used as that for the 2 7/8
inches round finned tubes.

The following empirical equations result from a
least square analysis of the experimental data:

(a) round finned tubes

2 3/8 inches fin diameter:

1/4 inch fin spacing $\quad Nu_f = 0.00854(GrPr)_f^{0.543} \quad$ (21)

3/8 inch fin spacing $\quad Nu_f = 0.0224(GrPr)_f^{0.47} \quad$ (22)

1/2 inch fin spacing $\quad Nu_f = 0.0585(GrPr)_f^{0.402} \quad$ (23)

6/8 inch fin spacing $\quad Nu_f = 0.186(GrPr)_f^{0.312} \quad$ (24)

2 7/8 inches fin diameter:

1/4 inch fin spacing $\quad Nu_f = 0.0132(GrPr)_f^{0.513} \quad$ (25)

3/8 inch fin spacing $\quad Nu_f = 0.18(GrPr)_f^{0.447} \quad$ (26)

1/2 inch fin spacing $\quad Nu_f = 0.119(GrPr)_f^{0.356} \quad$ (27)

6/8 inch fin spacing $\quad Nu_f = 0.304(GrPr)_f^{0.278} \quad$ (28)

3 3/8 inches fin diameter:

1/4 inch fin spacing $\quad Nu_f = 0.01(GrPr)_f^{0.521} \quad$ (29)

3/8 inch fin spacing $\quad Nu_f = 0.0636(GrPr)_f^{0.396} \quad$ (30)

1/2 inch fin spacing $\quad Nu_f = 0.154(GrPr)_f^{0.338} \quad$ (31)

6/8 inch fin spacing $\quad Nu_f = 0.134(GrPr)_f^{0.340} \quad$ (32)

(b) square finned tubes

1/4 inch fin spacing $\quad Nu_f = 0.015(GrPr)_f^{0.502} \quad$ (33)

3/8 inch fin spacing $\quad Nu_f = 0.131(GrPr)_f^{0.345} \quad$ (34)

1/2 inch fin spacing $\quad Nu_f=0.049(GrPr)_f^{0.428}$ (35)

6/8 inch fin spacing $\quad Nu_f=0.131(GrPr)_f^{0.345}$ (36)

6/8 inch fin spacing
with 2.548 inch $\quad Nu_f=0.216(GrPr)_f^{0.317}$ (37)
chimney

6/8 inch fin spacing
with 3.78 inch $\quad Nu_f=0.184(GrPr)_f^{0.336}$ (38)
chimney

It is seen that the characteristic slopes in the
above equations decrease with the fin spacing, but appear
to be nearly independent of the fin diameter and the
addition of chimneys although there are some individual
exceptions. It is believed that the dependence of charac-
teristic slope on fin spacing is brought about by the
overlapping of boundary layers. When the fin spacing
becomes smaller, not only the boundary layers of the two
adjacent fin-plates overlap with the boundary layer of
the cylinder, but also they overlap with each other. This
causes the values of characteristic slope different from
that of horizontal cylinders or vertical single plates,
i.e. slope = 1/4. When fin spacing becomes larger, i.e.
more characteristics of horizontal cylinder or vertical
plate appears, this results in a slope closer to 1/4.
For small fin spacings, more resistance is offered to
natural convection flow which could account for the
smaller $(Nu)_f$ for finned tubes with smaller fin spacing.

In addition, turbulence caused by the irregular geometrical shape could also influence the slope in a way not yet understood for this system. However, the highest Nusselt number is obtained with the finned tubes of 1/2 inch fin spacing, hence there is apparently an optimum fin spacing existing which gives the highest heat transfer coefficient. This will be discussed in the next section.

It is noted that the data for the chimneys lie higher than those of the other tubes. Data of the finned tube installed with the taller chimney lie above those of the tube with shorter chimney. This is expected because the chimneys confine the air and provide greater buoyant force, and thus the higher heat transfer rate. However, since only two different dimensions of chimney have been investigated, a quantitative conclusion of the chimney effect on heat transfer rate is not possible.

In general, data of horizontal bare tubes obtained in McAdams' correlation and obtained in the present work lie above those of finned tubes for Grashof numbers smaller than a certain value dependent upon the fin spacing. The reason for the relatively higher heat transfer coefficient of bare tubes is probably due to the fact that the boundary layer flow is not interferred with; so more free flow is allowed and a higher heat transfer coefficient is obtained. However, the data of horizontal

bare tubes are in a region of laminar flow, while those
of finned tubes apparently are in a region of turbulent
flow. Details of the different regions in which these
data lie are presented in section V.

The correlation presented in Figs (32) through (35)
is satisfactory for each individual finned tubes but
further analysis of the data is needed in order to obtain
a more general correlation involving all the parameters
of the system.

IV. Analysis of heat transfer coefficients

Since air is the only ambient fluid used in the
present work, one may assume that, for constant values of
fin diameter and fin spacing, heat transfer coefficient
varies solely with the temperature difference. Plots of
mean heat transfer coefficient versus temperature
difference are shown in Figs (36) through (39). Apparent-
ly the largest fin spacing, 6/8 inch, in the present work,
does not give the highest heat transfer coefficient.
There is an intermediate value of fin spacing which gives
the highest heat transfer coefficient. By interpolating
the data in Figs (36) through (39), sufficient information
is obtained to show the variation of $h_{a.m.}$ with fin
spacing at constant diameter. This is presented in Figs
(40) through (43). It is seen that maximum heat transfer

coefficient lies generally on the fin spacing between 1/2 inch and 6/8 inch except some curves of the 2 3/8 inches fin-diameter finned tubes. The existing of an optimum fin spacing may be explained by the following qualitative sketch:

$$C$$

$$h_{a.m.}$$

$$A \qquad B$$

$$1/b$$
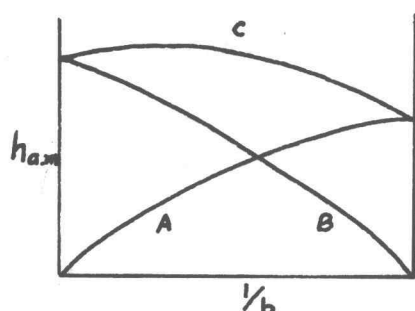
Line A indicates the influence of fin spacing on $h_{a.m.}$ by the chimney effect caused by two adjacent fins; line B indicates the influence of the interference of the boundary layer; and line C represents the total effect of A and B. It is assumed that fin spacing may affect the mean heat transfer coefficient by two means, i.e. the chimney effect of two adjacent fins, and the interference of boundary layers. As seen in the above sketch, $h_{a.m.}$ increases with 1/b by chimney effect, but decreases with 1/b by interference of fin spacing. As a result of these two effects, line C shows a maximum in $h_{a.m.}$ at a certain value of b, i.e. the optimum fin spacing.

However, the data obtained are not sufficient to give an accurate prediction on the optimum fin spacing. Approximately, 1/2 inch fin spacing is recommended for

the tubes studied in this work.

The optimum heat transfer coefficient, however, does not necessarily correspond to the highest heat transfer rate per unit of length. It is observed in Fig (44), in which $h_{a.m.}A$ is plotted versus fin spacing, that the total heat dissipation decreases with fin spacing even though there is a maximum heat transfer coefficient. Hence, for the purpose of obtaining higher heat dissipation, finned tubes with small fin spacing are preferred. Although data are not obtained in the region of fin spacing below 1/4 inch, the broken lines shown in Fig (44) indicate a possible optimum fin spacing for maximum value of $h_{a.m.}A$ would be preferred in actual operation.

Results of the chimney effect are also plotted in Fig (45). The chimney has the effect of giving higher heat transfer coefficients. The results indicate a slight increase in heat transfer coefficient with the height of chimney. Approximately, two per cent increase in heat transfer coefficient was obtained with the addition of 2.548-in. chimney, and three per cent increase in heat transfer coefficient was obtained with the addition of 3.78-in. chimney.

Plots of mean heat transfer coefficient versus fin diameter are made with the aid of Figs (36) through (39). These are shown in Figs (46) through (47) in which fin

spacing is kept constant. Results show that the value of heat transfer coefficient is somewhat higher at 2 7/8 inches fin diameter than that at 3 3/8 inches fin diameter. This is expected because, referring to the case of a single vertical plate, heat transfer coefficient decreases with the plate height, measured from the lower edge, until a certain value of height. A smaller chimney effect also prevails with the smaller fin diameter. There is an optimum fin diameter which gives the highest heat transfer coefficient. It is seen that, in the present work, this optimum fin diameter lies somewhere near the value of 2 7/8 inches. However, for the purpose of obtaining higher heat dissipation, finned tubes with large fin diameter are preferred.

V. Correlation and comparison of heat transfer data

Heat transfer data are correlated by using the quantities $\left(\frac{d_e^3 \rho^2 g \beta \theta}{\mu^2}\right)_f \left(\frac{c_p \mu}{k}\right)_f \left(\frac{b}{d}\right)\left(\frac{d_f}{d}\right)$ and $\left(\frac{h_{a.m.} d_e}{k}\right)_f$, where the two length ratios account for the geometry of the system. These are plotted in Fig (48). By a least square analysis, the data of the round finned tubes can be represented by the following equation with a deviation of $\pm 7.5\%$:

$$\text{Nu}_f = (0.184) \left[(\text{GrPr})_f \left(\frac{b}{d}\right)\left(\frac{d_f}{d}\right) \right]^{0.321} \qquad (39)$$

where

$$Nu_f = \left(\frac{h_{a.m.} d_e}{k}\right)_f$$

$$(Gr\, Pr)_f = \left(\frac{d_e^3 \rho^2 g \beta \theta}{\mu^2}\right)_f \left(\frac{c_p \mu}{k}\right)_f$$

It is observed that the data for finned tubes of 6/8 inch
fin spacing lie lower than those of the other three fin
spacings. This is expected because, for 6/8 inch spacing
finned tubes, values of $h_{a.m.}$ are only little higher, but
values of b are much higher than those of the other fin
spacings. In other words, the quantity $(GrPr)_f (\frac{b}{d}) (\frac{d_f}{d})$
increases faster than the quantity $(Nu)_f$ for 6/8 inch
spacing finned tubes, and this causes the data of 6/8
inch fin spacing lying lower.

Another simpler type of correlation is obtained in
which quantity $(GrPr)_f (\frac{b}{d})$ is plotted versus $(Nu)_f$ on a
logarithmic scale, where

$$(Gr)_f = \left(\frac{d_e^3 \rho^2 g \beta \theta}{\mu^2}\right)_f$$

$$(Nu)_f = \left(\frac{h_{a.m.} d_e}{k}\right)_f$$

For round finned tubes results are presented in Fig (49)
in which all the experimental data fall around a straight
line, line A, which can be represented by the following
equation:

$$(Nu)_f = 0.201 (GrPr \frac{b}{d})_f^{1/3} \tag{40}$$

The average deviation of the data is $\pm 7.5\%$. As in Fig
(48), the data of the finned tubes of 6/8 inch fin dia-
meter lie lower than those of the others. In this
correlation, scattering of data is somewhat identical to
that in the previous correlation, however, the equation

obtained in this correlation is simpler, and there is no duplication in using the fin diameter d_f. Therefore, this correlation is preferred. However, for fin spacing larger than 6/8 inch more deviation of data will likely be obtained.

Line B in Fig (49) is replotted from the results obtained by Siegel and Bryan (37). In their experiment, a finned tube with the following dimensions was used:

outside diameter of copper tube = 0.638 inch

fin spacing = 0.32 inch

fin thickness = 0.0095 inch

fin plate = 2x2 inches square, aluminum

Air was used as the ambient fluid and the following equation was obtained which is similar to that of vertical plates:

$$h_m = 0.29 \left(\frac{\Delta t}{L} \right)^{1/4}$$

where, h_m is the mean heat transfer coefficient, and L is the width of fin plates. It is seen that line B lies above line A and has a slope of 1/4 as compared to the slope of 1/3 obtained in the present correlation. The difference in slope and in intercept of line A and line B may be attributed to the following two factors:

1. The finned tube used by Siegel and Bryan is of smaller fin diameter and tube diameter. According to the results obtained for horizontal cylinders and vertical

plates as mentioned in Chapter II, the heat transfer coefficient is inversely proportional to the plate height and cylinder diameter respectively for the cases of vertical plates and horizontal cylinders. Therefore, higher heat transfer coefficient are expected in Siegel and Bryan's experiment.

2. The range of temperature difference used in their experiment is approximately from $10^{O}F$ to $30^{O}F$. The corresponding values of $Log(Gr\,Pr\frac{b}{d})_f$ are 3.992 and 4.431. It can be seen in Fig (49) that their experimental data lie in the region of lower $(GrPr)_f(\frac{b}{d})$ values than those covered in the present work. There is good reason to believe that their data lie in the laminar region while the present data lie in the turbulent region and transition region. This accounts for the value of slope obtained in the present correlation, i.e. slope = 1/3.

In general, it appears that Siegel and Bryan's results when extrapolated will be reasonably close to the present results.

Using the same type of correlation, results of square finned tubes are presented in Fig (50). A least square analysis of the data gives the following equation:

$$(Nu)_f = 0.217 \left[(GrPr)_f(\frac{b}{d}) \right]^{0.333} \qquad (41)$$

Again the data for the 6/8 inch square fin are lower so the correlation applies best to spacings less than this.

Also plotted is the equation for 2 7/8 inches round
finned tube, which has the same fin-area as that of the
square finned tubes, so that a direct comparison between
the equal-area round and square finned tubes is possible.
The empirical equation for 2 7/8 inches round finned tube
is

$$(Nu)_f = 0.212 \left[(GrPr)_f (\tfrac{b}{d}) \right]^{0.333} \tag{42}$$

Equations (41) and (42), are nearly equivalent so it is
concluded that similar results will be obtained for
other equal-area round and square finned tubes, at least
in the range of dimensions studied.

The effect of chimneys on the 6/8 inch square finned
tube is presented in Fig (51) in which the same dimension-
less quantities are used as in Fig (49). The least
analysis of the data gave exponents between 0.28 and 0.3,
so an average of 0.3 was used and the intercepts adjusted
accordingly giving the following:

2.548 inches chimney, $(Nu)_f = 0.317 \left[(GrPr)_f (\tfrac{b}{d}) \right]^{0.3}$ (43)

3.78 inches chimney, $(Nu)_f = 0.378 \left[(GrPr)_f (\tfrac{b}{d}) \right]^{0.3}$ (44)

An increase in heat transfer rate with chimney height
is again observed. It would be possible to obtain a
correlation with present data to include chimney height.
However, this would be based only on the two heights
studied and further work would be needed to obtain a more
reliable correlation.

The comparisons of the results obtained in the present work with those obtained by other investigators on other geometric configurations are shown respectively in Fig (52) for round finned tubes and in Fig (53) for square finned tubes. In these figures quantity $(Gr_b Pr)_f (\frac{b+d}{d_f+d})$ is plotted versus $(Nu_b)_f$ on a logarithmic scale, where

$$(Gr_b)_f = \left[\frac{(b+d)^3 \rho^2 g \beta \theta}{\mu^2} \right]_f$$

$$(Nu_b)_f = \left[\frac{h a.m. (b+d)}{k} \right]_f$$

A least square analysis of the experimental data results in the following equations:

for round finned tubes,

$$(Nu_b)_f = 0.113 \quad (Gr_b Pr)(\frac{b+d}{d_f+d})^{0.375} \qquad (45)$$

for round finned tubes with 2 7/8 inches fin diameter only,

$$(Nu_b)_f = 0.12 \left[(Gr_b Pr)(\frac{b+d}{d_f+d}) \right]^{0.375} \qquad (46)$$

for square finned tubes,

$$(Nu_b)_f = 0.118 \left[(Gr_b Pr)(\frac{b+d}{s+d}) \right]^{0.375} \qquad (47)$$

for 6/8 inch square finned tube with 2.548 inches chimney,

$$(Nu_b)_f = 0.252 \left[(Gr_b Pr)_f (\frac{b+d}{s+d}) \right]^{0.32} \qquad (48)$$

for 6/8 inch square finned tube with 3.78 inches chimney,

$$(Nu_b)_f = 0.394 \left[(Gr_b Pr)_f (\frac{b+d}{s+d}) \right]^{0.29} \qquad (49)$$

where, s = width of the square fin-plate.

It is seen from the above equations that again identical results are obtained for square finned tubes and the round finned tubes of 2 7/8 inches fin diameter. Average deviation of the data from equation (45) is $\pm 10\%$, while the deviation from equation (47) is $\pm 7\%$. Elenbaas' theoretical and experimental equations for vertical parallel plates are also plotted. For the finned tubes as d becomes zero the quantities used in the present correlation become

$$Nu_b = \frac{hb}{k}$$

$$Gr_b = \frac{b^3 \rho^2 g \beta \theta}{\mu^2}$$

These are the exact dimensionless groups used by Elenbaas in his correlation for parallel plates. Hence, the quantities used in the present correlation for finned tubes are equivalent to the quantities used by Elenbaas in his correlation for parallel plates as the diameter approaches zero.

Also McAdams' equation for horizontal cylinders is plotted. For bare tube b diminshes to zero and d_f reduces to d. This causes quantity $\frac{h(b+d)}{k}$ to become $\frac{hd}{k}$, and

quantity $\left[\frac{(b+d)^3\rho^2 g\beta\theta}{\mu^2}\right]\left(\frac{c_p\mu}{k}\right)\left(\frac{b+d}{d_f+d}\right)$ to become to $\left(\frac{d^3\rho^2 g\beta\theta}{\mu^2}\right)\left(\frac{c_p\mu}{k}\right)\left(\frac{1}{2}\right)$. Hence, McAdams' equation can be plotted in Figs (52) and (53) by transformation of axis.

It is seen that Elenbaas' and McAdams' data lie above those of the present work. Their curves also have the smaller slope, i.e. 1/4. In reference (13), Elenbaas' curves show two different slopes at different values of $(GrPr)_f(\frac{b}{d_f})$. For $(GrPr)_f(\frac{b}{d_f}) < 50$ the slope of his curves is equal to one; for $(GrPr)_f(\frac{b}{d_f}) > 50$ the slope is equal to 1/4. However, $(GrPr)_f(\frac{b}{d_f}) = 10^5$ is the upper limit of his experimental data. It is believed that Elenbaas' data are in the conduction and laminar convection region. For the values of $(GrPr)_f(\frac{b}{d_f}) < 50$, his experimental data are undoubtedly in the region where heat conduction dominates. In the case of parallel plates, the transition point from laminar heat flow to turbulent heat flow is doubtessly at a value of $(GrPr)_f(\frac{b}{d_f}) > 10^5$ from results obtained with single vertical plates and vertical enclosed air spaces. Therefore, his data is in the laminar convection region when $(GrPr)_f b/d_f > 50$.

For horizontal cylinders, the laminar region extends from $(GrPr)_f = 10^4$ to $(GrPr)_f = 10^8$. Therefore, in Figs (52) and (53) McAdams' data are also in the laminar region.

The present results would indicate that flow was
turbulent probably because of the complicated geometrical
shape of the finned tube. This could shift the upper
limit of laminar flow to a lower value of $(GrPr)_f(\frac{b + d}{d_f + d})$
and account for the different slope obtained. The present
data, however, are reasonably close to those obtained by
Elenbaas considering the different geometrical systems
studied in each case.

73

Chapter VII

Conclusion

The following conclusions are drawn for this investigation.

I. Results for the horizontal bare tube

The following empirical equation was obtained:

$$\left(\frac{h_{a.m.}d}{k}\right)_f = 0.558\left[\left(\frac{d^3\rho^2 g\beta\theta}{\mu^2}\right)\left(\frac{c_p\mu}{k}\right)_f\right]^{1/4} \tag{20}$$

where, the subscript f indicates that all the fluid properties are taken at the film temperature, i.e. arithmetic average of the surface temperature and air temperature. This equation gives coefficients which are 5.3% higher than those predicted by the relation recommended by McAdams. This may be due to the relatively smaller length-diameter ratio used in the present experiment and to errors involved in the estimation of radiation losses, although it is also possible that the correlation of McAdams gives low values.

II. Effect of the clearance between the lower edge of the enclosure-box and table top

Experiments at clearances of 0, 2.5 and 3.5 inches between the lower edge of the enclosure and table top were conducted on the round finned tube of 2 7/8 inches fin diameter and 6/8 inch fin spacing. Similar results

were obtained for all three cases. The independence of
heat transfer coefficients with the clearance values can
be explained by the flow pattern of air circulation. When
the bottom is closed, warm air moves up in the central
portion while cold air is sucked in from the sides of the
enclosure-box. This provides as good air circulation as
in the cases of 2.5 and 3.5 inches clearance when the
cold air comes in through the clearance area.

III. Analysis of heat transfer data

The quantity $\left(\frac{d_e^3 \rho^2 g \beta \theta}{\mu^2}\right)_f \left(\frac{c_p \mu}{k}\right)_f$ was plotted versus
$\left(\frac{h_{a.m.} d_e}{k}\right)_f$ with fin spacing as the parameter. Where
the equivalent diameter d_e is the arithmetic average of
the tube diameter and fin diameter. For square finned
tubes, the same value of d_e as that of the 2 7/8 inches
round finned tubes was used. A family of straight lines
were obtained. It was found that their characteristic
slopes decreased with fin spacing, but appears to be
nearly independent of fin diameter and chimney baffles.
On the contrary, their intercepts increased with fin
spacing.

The results for finned tubes were compared with those
for horizontal cylinders, and higher coefficients are
observed on the latter shape.

Higher heat transfer coefficients were obtained on

the finned tubes installed with chimney baffles.

IV. Analysis of heat transfer coefficients

With the aid of the plots of $h_{a.m.}$ versus b, it is found that there is an optimum fin spacing approximately between the 1/2 inch and 6/8 inch fin spacings which gives the maximum heat transfer coefficient. The reason for the optimum fin spacing is believed to be due to the combined influence of chimney effect caused by the adjacent fin-plates and overlapping of boundary of the boundary layers. When fin spacing becomes small, interference of the boundary layers decreases the heat transfer rate. When fin spacing becomes larger than the optimum value, the chimney effect caused by the adjacent fin-plates decreases, and so a lower heat transfer rate is obtained.

In addition, there is also an optimum fin diameter. Lower heat transfer coefficients are obtained for finned tubes with large fin diameters, because heat transfer coefficient decreases with fin diameter as in the case of single vertical plates. Since smaller fin-plates possess less chimney effect, lower heat transfer coefficients are also obtained at an fin diameter smaller than the optimum value. The approximate value of the optimum fin diameter is found to be around 2 7/8 inches.

From a plot of $h_{a.m.}A$ versus b, Fig (43), it is observed that, in the present work, the total heat dissipation per unit length of finned tube per degree of temperature difference decreases with fin spacing, even though there is an optimum fin spacing existing which gives the maximum heat transfer coefficients. The optimum spacing for maximum $h_{a.m.}A$ may be estimated from Fig (43). It is believed that same results will be obtained with the fin diameter, i.e. total heat dissipation increases with fin diameter.

V. General correlation of heat transfer data

The experimental data were correlated by the following empirical equation with an average deviation of $\pm 7.5\%$:

$$\left(\frac{h_{a.m.}d_e}{k}\right)_f = 0.201 \left[\left(\frac{d_e^3 \rho^2 g \beta \theta}{\mu^2}\right)_f \left(\frac{c_p \mu}{k}\right)_f \left(\frac{b}{d}\right)\right]^{1/3} \quad (40)$$

where, the slope 1/3 indicates that the present data lie in the turbulent region. Good agreement of the present data with that of Siegel and Bryan's extrapolated results is obtained. However, the experimental data of these two workers fall in the laminar region, because of the lower values of temperature difference they used.

Another form of correlation was also obtained with the same deviation of experimental data:

$$\left(\frac{h_{a.m.}d_e}{k}\right)_f = (0.184) \left[\left(\frac{d_e^3 \rho^2 g \beta \theta}{\mu^2}\right)_f \left(\frac{c_p \mu}{k}\right)_f \left(\frac{b}{d}\right)\left(\frac{d_f}{d}\right)\right]^{0.321} \quad (39)$$

Equation (40) is recommended because of its simpler form.

Results of data from the square finned tubes resulted a similar empirical equation as that of the 2 7/8 inches round finned tubes which has the same fin-area as that of square finned tubes. Hence, it is concluded that similar results will be obtained on round finned tubes and square finned tubes if they have the same surface area, at least within the dimensions studied in the present investigation.

Third type of correlation was carried out for the purpose of comparing the results of finned tubes with those of horizontal cylinders and parallel plates, in which the quantity $\left[\frac{(b+d)^3 \rho^2 g \beta \theta}{\mu^2}\right]_f \left(\frac{c_p \mu}{k}\right)_f \left(\frac{b+d}{d_f+d}\right)$ is plotted versus the $\left[\frac{h_{a \cdot m} \cdot (b+d)}{k}\right]_f$. By use of this correlation, it is possible to plot the present data on finned tubes, Elenbaas' parallel plates data, and McAdams' horizontal cylinder correlation for direct comparison. Elenbaas and McAdams obtained a different slope value as compared to that of the present work. This is expected because their data are in the laminar natural convection and conduction regions while the present data are in the turbulent region. It is believed that in the present experiment the turbulence was caused by the base tube rather than the fin-plates because the height of fin-plates is not sufficient to produce turbulence. Based

on this, the conclusion is drawn that, geometrically, the finned tube is a combination of parallel plates and horizontal cylinder. However, transition to turbulent natural convection at a lower value of $(GrPr)_f(\frac{b + d}{d_f + d})$ occurs because of the disturbing effect of the base tube.

Chapter VIII

Recommendations

This thesis describes one of the first investigations of the effect of fin spacing and fin diameter on the heat transfer by natural convection from finned tubes. This work has indicated a need for further investigations as follows:

I. The main objective of this work was to obtain a quantitative relationship between the mean heat transfer coefficients and different dimensions of finned tubes. It is believed that the base tube caused turbulence in the flow. Since higher heat transfer coefficients can be obtained for turbulent flow, it would be useful to determine the value of $(GrPr)_f (\frac{b}{d})$, at which turbulence starts. For this, it is proposed that different tube diameter should be studied so that the value of an optimum base tube diameter would also be obtained.

II. It would be desirable to find an optimum combination of fin diameter, fin spacing, and base tube diameter, which would give the highest heat transfer coefficient.

III. In order to eliminate the errors involved in estimation of radiation loss, it is desirable to have the finned tubes plated with shiny metal, such as nickel, so

that the emissivity of finned tubes will be reduced to a lower value.

IV. Since the addition of chimney baffles is a satisfactory way of increasing heat transfer coefficient, more detailed study on the chimney effect is desired.

Chapter IX

Nomenclature

A   Area of a surface, square feet; A, total surface area of finned tube; A_f, area of the fin-plate; A_c, area of the tube; A_n, area of surface n.

B   Stefan-Boltzmann constant, 0.171×10^{-8} Btu/(sq ft)(hr)(deg R)^4.

b   Fin spacing or plate spacing, feet.

C_p Heat capacity, Btu/(lb)(deg. F).

d   Diameter of tube, feet; d_f, fin diameter.

E   Electric voltage, volt.

f_x Negative of the body force in X direction, lbs/(sec)^2.

g_x Body force in X direction, lbs/(sec)^2.

Gr   Grashof number $= \dfrac{L^3 \rho^2 g \beta \theta}{\mu^2}$, dimensionless; Gr_L, local Grashof number; Gr_L^*, modified local Grashof number.

h   Heat transfer coefficient by natural convection, Btu/(hr)(sq ft)(deg.F), $h_{a.m.}$, arithmetic mean heat transfer coefficient.

H   Self-inductance, microhenry.

I   Electric current, amp.

K   Conversion constant = 3.413 Btu/watt-hr.

k   Thermal conductivity, Btu/(hr)(sq ft)(deg. F)/ft.

L   Characteristic length, feet.

M   Thickness of fin-plate, feet.

N   Number of fin-plate on the tube.

Nu   Nusselt number = hd/k, dimensionless.

n   Winding number of the heating wire.

P   Perimeter of a surface, square feet; P_f, perimeter of fin-plate; P_e, perimeter of the tube.

Pr   Prandtl number $= \dfrac{c_p \mu}{k}$, dimensionless.

q   Total heat transferred, Btu.

r   Radius of the cylinder, feet.

T   Temperature, deg. R; T_s, temperature of the solid surface or the finned tube; T_a, temperature of the ambient fluid; T_n, temperature of the surface n; T_f, film temperature $= \dfrac{T_s + T_a}{2}$; T_r, reference temperature; T_w, temperature of the finned tube.

T_e Θ / T_a, dimensionless.

U   Velocity, ft/sec; U_1, an arbitrary function with the dimension of velocity; U, velocity in X direction.

V   Velocity in Y direction, ft/sec.

X   Length, feet.

β Volumetric expansion coefficient, reciprocal degrees Fahrenheit.

β_n Reflectivity of surface n $= 1 - \epsilon_n$, dimensionless.

ϵ_n Emissivity of surface n, dimensionless.

Θ Temperature difference between the solid surface and the ambient fluid, deg. F; Θ_s, temperature difference at the surface wall.

μ Viscosity, lb/(sq ft)(hr); μ_s , viscosity at the wall.

ρ Density, lb/cu ft.

δ Thickness of the boundary layer, feet.

τ Dimensionless time.

Chapter X

Bibliography

1. Bevans, J. T. Vertical free convection from isothermal surface. Industrial and Engineering Chemistry 49 (1):114-119. 1957.

2. Biermann, Arnold E. and Hermann H. Ellerbrock, Jr. The design of fins for air-cooled cylinders. Washington, 1941. 24 p. (National Advisory Committee for Aeronautics. Report No. 726)

3. Biermann, A. E. and B. Pinkel. Heat transfer from finned metal cylinders in an air stream. Washington, 1934. 19 p. (National Advisory Committee for Aeronautics. Report No. 488)

4. Boelter, L. M. K. et al. Heat transfer notes. Berkeley, University of California Press, 1948. 601 p.

5. Bosworth, R. C. L. Heat transfer phenomena. New York, Wiley, 1952. 211 p.

6. Brown, Aubrey I. and Salvatore M. Marco. Introduction to heat transfer. New York, McGraw-Hill, 1942. 232 p.

7. Carrier, W. H. and S. W. Anderson. Resistance to heat flow through finned tubing. Heating, Piping & Air Conditioning 16:304-318. 1944.

8. Chang, Y. P. Theoretical analysis of heat transfer in natural convection and in boiling. Transactions of the American Society of Mechanical Engineers 79:1501-1509. 1957.

9. Daughty, D. L. and R. M. Drake, Jr. Free convection heat transfer from horizontal right circular cylinder to freon 12 near critical state. Transactions of the American Society of Mechanical Engineers 78:1843-1850. 1956.

10. Dropkin, David and Arieh Carmi. Natural convection heat transfer from a horizontal cylinder rotating in air. Transactions of the American Society of Mechanical Engineers 79:741-749. 1957.

11. Eckert, E. R. G. and R. M. Drake, Jr. Heat and mass transfer. 2d ed. New York, McGraw-Hill, 1959. 530 p.

12. Eckert, E. R. G. and Thomas W. Jackson. Analysis of turbulent free-convection boundary layer on flat plate. Washington, 1951. 7 p. (National Advisory Committee for Aeronautics. Report No. 1015. Formerly Technical Notes No. 2207)

13. Elenbaas, W. Heat dissipation of parallel plates. Physica 9:1-28. 1942.

14. Elenbaas, W. The dissipation of heat by free convection from vertical and horizontal cylinders. Journal of Applied Physics 19:1148-1154. 1948.

15. Hallman, T. M. Combined forced and free-laminar heat transfer in vertical tubes with uniform internal heat generation. Transactions of the American Society of Mechanical Engineers 78:1830-1849. 1956.

16. Hamilton, D. C. and W. R. Morgan. Radiant-interchange configuration factor. Washington, 1952. 110 p. (National Advisory Committee for Aeronautics. Technical Notes No. 2836)

17. Hermann, R. Heat transfer by free convection from horizontal cylinders in diatomic gases. Washington, 1954. 73 p. (National Advisory Committee for Aeronautics. Technical Memorandum No. 1366. Tr. from VDT Forschungsheff: No. 379. 1936)

18. Isbin, H. S. Natural convection heat transfer in regions of maximum fluid density. American Institute of Chemical Engineering Journal 4 (1):81-89. 1958.

19. Jakob, Max. Heat transfer. 2 vol. New York, Wiley, 1949-1957. 1410 p.

20. King, W. J., III. Free convection. Mechanical Engineering 54:347-353. 1932.

21. Langmuir, I. Convection and conduction of heat in gases. Physical Review 34:401-422. 1912.

22. Lemlich, Robert and Charles Sharn. Natural convection to cold cylinder. Industrial and Engineering Chemistry 47 (8):1547-1549. 1955.

23. Levy, Salomon. Integral methods in natural convection flow. Journal of Applied Mechanics 22 (4): 515-522. Dec 1955.

24. Lietzke, A. F. Theoretical and experimental investigation of heat transfer by laminar natural convection between parallel plates. Washington, 1954. 23 p. (National Advisory Committee for Aeronautics. Technical Notes No. 3328)

25. Lohner, K. and G. Chone. Heat transmission through fins and finned cylinders. Engineers' Digest 19 (3):111-114. 1958.

26. McAdams, William H. Heat transmission. 3d ed. New York, McGraw-Hill, 1954. 532 p.

27. Merk, H. J. and J. A. Prins. Thermal convection in laminar boundary layers. Applied Science Research, Section A, 4 (1):11-24. 1954.

28. Murray, W. M. Heat dissipation through annula disk or fin of uniform thickness. Journal of Applied Mechanics 5 (2):A78-A80. June, 1938.

29. Ostrach, Simon. New aspects of natural convection heat transfer. Transactions of the American Society of Mechanical Engineers 75:1287-1289. 1953.

30. Ostrach, Simon. Laminar natural-convection flow and heat transfer of fluids with and without heat sources in channels with constant wall temperature. Washington, 1952. 55 p. (National Advisory Committee for Aeronautics. Technical Notes No. 2863)

31. Ostrach, Simon. An analysis of laminar free-convection flow and heat transfer about a flat plate parallel to the direction of the generation body force. Washington, 1953. 17 p. (National Advisory Committee for Aeronautics. Report No. 1111)

32. Ostrach, Simon and P. R. Thornton. On the stagnation of natural-convection flows in closed-end tubes. Transactions of the American Society of Mechanical Engineers 80:363-366. 1958.

33. Ostroumov, G. A. Free convection under conditions of internal problem. Washington, 1958. 233 p. (National Advisory Committee for Aeronautics. Technical Memorandum No. 1407)

34. Rutkowski, J. Free convection from heated surfaces-laminar boundary layers. New York, 1957. 22 p. (The American Society of Mechanical Engineers. Paper No. 57-S-59)

35. Saunders, O. A. Natural convection in liquid. Proceedings of the Royal Society, Series A, 172 (948):55-71. 1939.

36. Schey, O. W. and V. G. Rollin. The effect of baffles on the temperature distributing and heat-transfer coefficients of finned cylinders. Washington, 1935. 14 p. (National Advisory Committee for Aeronautics. Report No. 511)

37. Siegel, L. G. and W. L. Bryan. Natural convection cooling dehumidifying. Heating, Piping and Air Conditioning 29 (12):129-134. 1957.

38. Siegel, Robert. Transient free convection from a vertical flat plate. Transactions of the American Society of Mechanical Engineers 80:347-357. 1958.

39. Siegel, Robert and R. H. Norris. Tests of free convection in a partially enclosed space between two heated vertical plates. New York, 1957. 8 p. (The American Society of Mechanical Engineers. Paper No. 56-SA-5)

40. Somers, E. V. Theoretical consideration of combined thermal and mass transfer from a vertical flat plate. Journal of Applied Mechanics 78:295-301. 1956.

41. Sparrow, E. M. and T. L. Gregg. Laminar-free-convection heat transfer from the outer surface of a vertical circular cylinder. Transactions of the American Society of Mechanical Engineers 78:1823-1828. 1956.

42. Sparrow, E. M. and J. L. Gregg. The variable fluid-property problem in free convection. Transactions of the American Society of Mechanical Engineers 80:879-886. 1958.

43. Touloukian, Y. S., G. A. Hawkins, and M. Jakob. Heat transfer by free convection from heated vertical surfaces to liquids. Transactions of the American Society of Mechanical Engineers 70:13-17. 1948.

44. Van Der Hegge Zijnen, B. G. Modified correlation formulae for the heat transfer by natural and by forced convection from horizontal cylinders. Applied Science Research, Section A, 6 (2-3):129-140. 1956.

APPENDIXES

APPENDIX A

CALCULATION OF RADIATION LOSS

In equation (18) $A_n \mathcal{I}_{n1}$ was calculated by the following equation:

$$A_n \mathcal{I}_{n1} = \frac{\epsilon_1 A_1}{\beta_1} \cdot \frac{{}_n D_1}{D} \tag{50}$$

In the present work,

$$
{}_n D_1 = \epsilon_n
\begin{vmatrix}
-\overline{n1} & \overline{12} & \overline{13} & \overline{14} \\
-\overline{n2} & -\frac{A_2}{\beta_2} & \overline{23} & \overline{24} \\
-\overline{n3} & \overline{23} & -\frac{A_3}{\beta_3} & \overline{34} \\
-\overline{n4} & \overline{24} & \overline{34} & -\frac{A_4}{\rho_4}
\end{vmatrix}
$$

Where n = 2, 3, 4, and ${}_2 D_1$, ${}_3 D_1$, and ${}_4 D_1$ could be simplified to the following forms:

$$
{}_2 D_1 = \frac{\epsilon_2 A_2}{\beta_2}
\begin{vmatrix}
\overline{12} & \overline{13} & \overline{14} \\
\overline{23} & -\frac{A_3}{\beta_3} & \overline{34} \\
\overline{24} & \overline{34} & -\frac{A_4}{\beta_4}
\end{vmatrix} \tag{51}
$$

$$
{}_3 D_1 = -\frac{\epsilon_3 A_3}{\beta_3}
\begin{vmatrix}
\overline{12} & \overline{13} & \overline{14} \\
-\frac{A_2}{\beta_2} & \overline{23} & \overline{24} \\
\overline{24} & \overline{34} & -\frac{A_4}{\beta_4}
\end{vmatrix} \tag{52}
$$

$$
{}_4 D_1 = \frac{\epsilon_4 A_4}{\beta_4}
\begin{vmatrix}
\overline{12} & \overline{13} & \overline{14} \\
-\frac{A_2}{\beta_2} & \overline{23} & \overline{24} \\
\overline{23} & -\frac{A_3}{\beta_3} & \overline{34}
\end{vmatrix} \tag{53}
$$

D could be also simplified to

$$
D = \begin{vmatrix} \overline{11} - \dfrac{A_1}{\beta_1} & \overline{12} & \overline{13} & \overline{14} \\ \overline{12} & -\dfrac{A_2}{\beta_2} & \overline{23} & \overline{24} \\ \overline{13} & \overline{23} & -\dfrac{A_3}{\beta_3} & \overline{34} \\ \overline{14} & \overline{24} & \overline{34} & -\dfrac{A_4}{\beta_4} \end{vmatrix} = -\dfrac{A_1}{\beta_1} \begin{vmatrix} -\dfrac{A_2}{\beta_2} & \overline{23} & \overline{24} \\ \overline{23} & -\dfrac{A_3}{\beta_3} & \overline{34} \\ \overline{24} & \overline{34} & -\dfrac{A_4}{\beta_4} \end{vmatrix} \quad (54)
$$

In equation (51), through (54), $\overline{mn} = A_m F_{mn} = A_n F_{nm}$.
Various values of F_{mn} could be calculated from the factors
F_{12} and F_{11} which were obtained from the figures 21 and
22 in reference (16) with D = d/r and L' = b/r as
parameters. With the aid of various $\overline{mn}$ values, calcula-
tion of the various $A_n \mathcal{F}_{n1}$ values for different fin
spaces and fin diameters was done on a digit computer.
For the finned tubes with chimney baffles, emissivity of
the surface A_1 was taken as the arithmetic average of
the emissivities of the copper baffles and the black-body
surroundings, i.e. $\epsilon_1 = (1 + 0.5)/2 = 0.75$. Results of
calculations are tabulated in Table (I).

APPENDIX B

CALCULATED DATA

TABLE I

CALCULATED RADIATION LOSS

1 Fin Diameter	2 Fin Space	3 Nominal Fin Space	4 ϵ_1	5 ϵ_2	6 ϵ_3', ϵ_4	7 $L'=\frac{b}{r}$	8 $D=\frac{d}{r}$	9 F_{12}	10 F_{11}	11 $A_2 \mathcal{J}_{21}$ x 10^4	12 $A_3 \mathcal{J}_{31}$, $A_4 \mathcal{J}_{41}$	13 $\Sigma A_n \mathcal{J}_{n1}$
$\frac{3}{28}$	0.271	1/4	1	0.072	0.57	1.971	1.727	0.089	0.033	1.87	0.0053	0.0108
	0.385	3/8				0.28		0.125	0.046	3.44	0.00736	0.0150
	0.508	1/2				0.369		0.16	0.057	5.38	0.00809	0.0167
	0.753	6/8				0.548		0.22	0.089	9.85	0.0099	0.0208
$\frac{7}{28}$	0.266	1/4	1	0.072	0.57	0.193	2.091	0.052	0.031	1.35	0.00675	0.0136
	0.375	3/8				0.279		0.074	0.043	2.65	0.00897	0.0182
	0.52	1/2				0.378		0.099	0.0575	4.5	0.0112	0.0229
	0.771	6/8				0.56		0.136	0.083	8.46	0.0143	0.0295
$\frac{3}{38}$	0.273	1/4	1	0.072	0.57	1.971	1.727	0.089	0.033	1.17	0.00858	0.0173
	0.393	3/8				0.28		0.125	0.046	2.26	0.0115	0.0232
	0.528	1/2				0.369		0.16	0.057	3.5	0.0143	0.0290
	0.759	6/8				0.548		0.22	0.089	6.52	0.018	0.0367
Square	0.273	1/4	1	0.072	0.57	0.198	2.091	0.055	0.031	1.61	0.00766	0.0155
	0.39	3/8				0.283		0.075	0.043	2.99	0.0101	0.0204
	0.508	1/2				0.508		0.095	0.054	4.68	0.0121	0.0247
	0.774	6/8				0.774		0.138	0.082	9.24	0.0156	0.0320
Chimney Effect			0.75	0.072	0.57	0.774	2.091	0.138	0.082	6.93	0.0121	0.0249

95

TABLE II

CALCULATED HEAT TRANSFER COEFFICIENTS

1	2	3	4				5						6	7	8
Fin Diameter	Nominal Fin Space	Air Temp. °F	Power Input				Thermocouple Reading						Θ	$q_{rad.}$	$h_{a.m.}$
			Volt	Amp	Volt	Amp	I	II	III	IV	V	VI			
Bare Tube		75.56	11.36	0.308	11.36	0.308	2.702	2.694	2.672	2.698	2.687	2.695	49.64	4.317	1.287
		76.10	11.38	0.311	11.38	0.311	2.735	2.726	2.722	2.733	2.718	2.73	49.5	4.316	1.306
		75.6	14.6	0.395	14.6	0.395	3.48	3.466	3.446	3.475	3.462	3.47	75.98	7.109	1.377
		76.33	14.59	0.392	14.59	0.392	3.486	3.474	3.453	3.482	3.48	3.478	75.42	7.067	1.375
		73.9	20	0.528	20	0.528	4.882	4.875	4.884	4.88	4.874	4.879	125	13.22	1.62
		75.3	20	0.518	20	0.518	4.805	4.8	4.808	4.804	4.8	4.806	121.2	12.78	1.63
$3\frac{3}{8}$	$1\frac{1}{4}$	74.88	14	0.39	14	0.39	1.926	1.93	1.93	1.928	1.923	1.92	24.38	12.15	0.511
		75.15	14	0.39	14	0.39	1.936	1.937	1.937	1.933	1.93	1.927	24.25	12.1	0.515
		75.72	20	0.539	20	0.539	2.417	2.417	2.417	2.413	2.407	2.403	40.03	20.93	0.652
		74.04	21	0.553	20	0.542	2.4	2.4	2.4	2.4	2.39	2.93	41	21.28	0.67
		75.4	25	0.676	25	0.676	2.88	2.884	2.884	2.876	2.862	2.858	55.78	30.4	0.755
		75.12	25	0.678	25	0.678	2.877	2.88	2.88	2.871	2.858	2.855	55.98	30.49	0.755
		75.54	29	0.785	25	0.785	3.29	3.292	3.292	3.28	3.265	3.261	69.36	39.27	0.829
		75.18	29	0.785	25	0.785	3.268	3.722	3.272	3.261	3.242	3.24	69.03	38.98	0.836
		75.6	31.1	0.842	31.1	0.842	3.522	3.524	3.524	3.507	3.497	3.493	77.2	44.66	0.861
		75.22	31.1	0.846	31.1	0.846	3.511	3.512	3.512	3.497	3.484	3.478	76.39	44.01	0.88
		74.64	35	0.955	35	0.955	3.95	3.952	3.952	3.93	3.915	3.909	92.26	55.33	0.929
		75.66	35	0.954	35	0.954	3.982	3.987	3.986	3.969	3.952	3.949	92.54	0.911	0.911

TABLE II

1	2	3	4			5 I	5 II	5 III	5 IV	5 V	5 VI	6	7	8
	74.18	14	0.388	14	0.388	1.964	1.964	1.964	1.963	1.96	1.957	26.33	13.25	0.557
	74.11	14	0.378	14	0.378	1.946	1.946	1.946	1.944	1.942	1.94	25.79	12.96	0.576
	74.1	18.05	0.492	18	0.49	2.3	2.297	2.297	2.294	2.292	2.287	37.7	19.58	0.694
	73.9	18.05	0.49	18.1	0.492	2.312	2.312	2.312	2.307	2.301	2.299	38.39	19.95	0.658
$2\frac{3}{8}$ $\frac{3}{8}$	74.14	22.1	0.602	22.1	0.602	2.725	2.723	2.723	2.718	2.713	2.713	52.11	28.17	0.771
	73.9	22	0.592	22	0.592	2.688	2.687	2.687	2.682	2.678	2.673	51.1	27.53	0.772
	73.68	28.1	0.76	28.1	0.76	3.396	3.396	3.396	3.388	3.378	3.373	72.1	43.01	0.914
	75.07	28	0.785	28.2	0.787	3.424	3.421	3.421	3.416	3.406	3.401	74.73	43.19	0.922
	75.3	31.1	0.846	31	0.845	3.714	3.7	3.704	3.707	3.697	3.583	83.6	49.56	0.994
	77.1	31	0.838	31	0.838	3.859	3.852	3.848	3.842	3.837	3.802	86.7	52.3	0.924
	73.59	33.2	0.9	33.1	0.9	4.032	4.028	4.028	4.014	4.005	4.005	96.16	58.46	0.968
	73.63	32.9	0.893	33.1	0.897	4.015	4.008	4.008	3.996	3.987	3.983	95.48	57.94	0.965
	74.49	10	0.292	10	0.292	1.72	1.718	1.718	1.714	1.711	1.706	17.42	7.24	0.573
	73.96	10	0.289	10	0.289	1.71	1.707	1.707	1.705	1.701	1.701	17.64	7.32	0.553
	74.57	14	0.39	14	0.39	2.036	2.033	2.032	2.025	2.02	2.012	28.18	12.08	0.703
	73.95	14	0.39	14	0.39	2.008	2.005	2.005	2.00	1.995	1.99	27.8	11.87	0.719
	74.98	20	0.54	20	0.54	2.619	2.614	2.598	2.609	2.594	2.575	47.53	21.54	0.864
$2\frac{3}{8}$ $\frac{1}{2}$	74.65	20	0.549	20	0.549	2.622	2.614	2.609	2.6	2.593	2.58	47.6	21.54	0.883
	74.68	25	0.686	25	0.686	3.253	3.242	3.238	3.223	3.212	3.197	68.83	33.02	0.96
	74.61	25.03	0.688	25.03	0.688	3.242	3.234	3.228	3.22	3.209	3.19	68.49	32.83	0.973
	74.78	29	0.792	29	0.792	3.775	3.775	3.75	3.733	3.718	3.697	85.82	43.15	1.042
	74.18	29.05	0.794	29	0.792	3.774	3.755	3.748	3.736	3.724	3.702	86.38	43.36	1.036
	74.58	32.9	0.901	33	0.905	4.31	4.294	4.275	4.265	4.25	4.22	103.78	54.72	1.125
	74.64	33	0.907	33	0.907	4.6	4.343	4.34	4.312	4.292	4.266	105.36	55.82	1.109
	72.62	9	0.26	9	0.26	1.627	1.627	1.625	1.62	1.623	1.416	15.78	5.482	0.678
$2\frac{3}{8}$ $\frac{6}{8}$	72.08	9	0.26	9	0.26	1.635	1.635	1.634	1.628	1.632	1.622	16.67	5.79	0.623
	71.87	13	0.362	13	0.362	1.99	1.99	1.986	1.976	1.983	1.967	29.24	10.5	0.754
	73.43	13	0.362	13	0.362	2.054	2.059	2.05	2.042	2.05	2.032	29.87	10.84	0.726

TABLE II

1	2	3	4			5						6	7	8
						I	II	III	IV	V	VI			
	74.02	17	0.468	17	0.468	2.522	2.522	2.517	2.502	2.513	2.485	44.68	16.95	0.852
	74.12	17.25	0.47	17	0.469	2.539	2.538	2.532	2.526	2.526	2.502	45.18	17.18	0.851
3/28 6/8	74.19	21.1	0.572	21.25	0.575	3.068	3.067	3.062	3.051	3.052	3.012	62.72	25.04	0.94
	73.9	21.05	0.572	21.05	0.572	3.028	3.028	3.02	3.002	3.017	2.975	61.7	24.52	0.953
	73.72	25	0.68	25	0.68	3.593	3.588	3.578	3.572	3.56	3.527	79.69	33.24	1.059
	73.09	25.1	0.687	25	0.68	3.578	3.574	3.564	3.554	3.551	3.517	80.72	33.65	1.051
	73.62	29.2	0.792	29.04	0.791	4.24	4.236	4.222	4.215	4.216	4.165	102.12	45.25	1.12
	73.93	29.2	0.792	29.2	0.792	4.277	4.263	4.253	4.242	4.242	4.197	103.02	45.83	1.11
	77.6	20	0.549	20	0.549	2.177	2.168	2.164	2.171	2.155	2.108	29.01	18.70	0.814
	77.49	20	0.549	20	0.549	2.174	2.164	2.16	2.167	2.151	2.105	28.91	18.62	0.614
	75	25	0.687	25	0.687	2.482	2.378	2.374	2.471	2.362	2.306	39.23	25.65	0.736
	74.7	25	0.687	25	0.687	2.4	2.385	2.382	2.392	2.37	2.358	38.8	25.3	0.746
	74.63	30	0.812	30	0.812	2.835	2.693	2.689	2.82	2.67	2.594	50.27	33.82	0.83
7/28 1/4	75.32	30	0.813	30	0.813	2.882	2.741	2.733	2.867	2.717	2.635	51.08	34.57	0.814
	73.56	35	0.977	35	0.977	3.249	3.063	3.052	3.229	3.031	2.936	62.59	43.31	0.957
	74.53	35	0.977	35	0.977	3.283	3.1	3.091	3.262	3.065	2.973	63.74	44.47	0.934
	72.89	40	1.101	40	1.101	3.713	3.471	3.46	3.685	3.43	3.312	77.86	55.98	0.96
	72.93	40	1.101	39.8	1.092	3.694	3.457	3.448	3.667	3.417	3.301	77.34	55.54	0.99
	89.08	44.05	1.202	44	1.202	4.1	3.82	3.806	4.07	3.768	3.632	89.08	66.13	1.04
	73.33	44	1.201	43.9	1.198	4.083	3.79	3.777	4.05	3.745	3.61	88.63	65.76	1.05
	77.28	20	0.505	20	0.505	2.17	2.17	2.168	2.166	2.62	2.143	30.18	18.79	0.693
	75.87	20.1	0.505	20	0.505	2.138	2.136	2.134	2.134	2.13	2.112	30.38	18.78	0.69
	77.3	25.1	0.684	25	0.684	2.533	2.527	2.525	2.522	2.515	2.486	42.1	27.09	0.889
7/28 3/8	77.62	25	0.68	25	0.68	2.544	2.539	2.538	2.533	2.524	2.508	42.0	27.06	0.883
	77.86	30.2	0.82	30.1	0.82	2.97	2.96	2.96	2.955	2.948	2.912	55.84	37.43	0.99
	78.34	30	0.824	30	0.824	2.979	2.976	2.965	2.964	2.957	2.92	55.52	37.28	0.987
	78.2	34.1	0.925	34	0.925	3.328	3.318	3.312	3.312	3.2	3.253	67.0	46.38	1.05
	77.65	34	0.923	33.8	0.92	3.298	3.295	3.278	3.28	3.271	3.228	67.05	46.29	1.037
	77.48	38.03	1.032	38.03	1.032	3.67	3.658	3.647	3.65	3.637	3.581	79.33	56.57	1.11

TABLE II

1	2	3	4				5						6	7	8
							I	II	III	IV	V	VI			
7/8	3/8	77.4	38.03	1.032	38.03	1.032	3.66	3.649	3.642	3.638	3.627	3.574	80.9	57.91	1.08
2	8	77.6	42	1.14	41.9	1.136	4.06	4.045	4.039	4.033	4.021	3.952	92.1	68.03	1.17
		77.51	43	1.17	42.8	1.17	4.173	4.16	4.144	4.146	4.125	4.063	95.69	71.34	1.18
		75.86	15	0.403	15	0.403	1.873	1.87	1.868	1.871	1.865	1.845	21.4	11.8	0.75
		75.36	15	0.403	15	0.403	1.848	1.842	1.842	1.847	1.84	1.818	20.89	11.47	0.776
		75.88	19	0.412	19	0.512	2.169	2.162	2.16	2.163	2.156	2.123	31.23	17.7	0.849
		75.7	19	0.512	19	0.512	2.145	2.137	2.132	2.138	2.13	2.1	30.55	17.26	0.876
7/8	1/2	75.85	24	0.649	24	0.649	2.578	2.566	2.563	2.57	2.558	2.513	44.95	26.46	0.967
2 8		75.19	23.95	0.643	23.8	0.642	2.556	2.545	2.538	2.552	2.537	2.492	44.92	26.34	0.95
		76.03	29	0.787	29	0.787	3.038	3.024	3.019	3.027	3.008	2.948	60.27	37.03	1.073
		76.78	29.1	0.79	29.03	0.789	3.048	3.033	3.022	3.038	3.03	2.955	60.81	37.37	1.068
		76.35	34.04	0.924	34.04	0.924	3.553	3.535	3.515	3.524	3.513	3.434	76.85	49.49	1.17
		76.1	34.04	0.924	34.04	0.924	3.55	3.53	3.52	3.532	3.509	3.43	77.1	49.62	1.17
		76.81	39.1	1.056	39.1	1.056	4.139	4.116	4.095	4.115	4.093	3.981	96.84	65.98	1.212
		75.63	39.2	1.057	39.2	1.057	4.13	4.097	4.083	4.105	4.078	3.973	97.39	66.05	1.212
		75.77	11	0.312	11	0.312	1.743	1.737	1.735	1.745	1.732	1.728	16.33	7.70	0.716
		75.6	11.1	0.32	11	0.312	1.748	1.739	1.736	1.746	1.732	1.728	16.49	7.77	0.725
		76.7	16.1	0.445	16	0.44	2.198	2.174	2.168	2.191	2.163	2.159	31.04	15.32	0.794
7/8	6/8	75.32	16.03	0.445	16.03	0.445	2.158	2.136	2.132	2.155	2.126	2.12	31.19	15.28	0.797
2 8		76.8	21	0.568	21	0.568	2.685	2.645	2.642	2.674	2.628	2.622	46.8	24.14	0.91
		77.3	21.1	0.574	21.05	0.57	2.718	2.682	2.675	2.703	2.666	2.65	47.7	24.73	0.897
		77.5	26	0.702	26	0.702	3.268	3.22	3.212	3.255	3.198	3.186	65.7	35.8	1.005
		76.57	26	0.703	26	0.703	3.246	3.199	3.185	3.232	3.172	3.162	65.58	35.57	1.01
		76.27	31	0.846	30.9	0.84	3.836	3.77	3.755	3.815	3.755	3.722	85.68	49.0	1.12
		77.6	31.0	0.846	31.03	0.85	3.888	3.87	3.819	3.869	3.791	3.781	87.1	50.36	1.10
		76.65	35.9	0.975	36.03	0.98	4.56	4.475	4.45	4.422	4.422	4.41	108.6	66.16	1.19
		77.59	36.03	0.98	36.03	0.98	4.623	4.536	4.518	4.585	4.498	4.478	109.9	67.56	1.17
3/8	1/4	75.15	21.2	0.575	21.2	0.575	1.98	1.977	1.977	1.972	1.969	1.956	26	20.64	0.542
3 8		75.53	21.1	0.574	21.1	0.574	2.005	2.002	2.002	1.996	1.993	1.982	26.56	21.16	0.522

TABLE II

1	2	3	4			5						6	7	8
						I	II	III	IV	V	VI			
	75.53	27.05	0.724	27.05	0.724	2.316	2.314	2.314	2.303	2.299	2.278	36.78	30.14	0.641
	75.13	27	0.725	27	0.725	2.32	2.314	2.314	2.305	2.299	2.282	37.175	30.43	0.632
	74.6	35.2	0.94	35.2	0.94	2.809	2.8	2.798	2.782	2.774	2.75	53.25	45.43	0.785
	74.96	35.2	0.94	35.2	0.94	2.826	2.817	2.815	2.8	2.795	2.77	53.57	45.84	0.779
$3\frac{3}{8}$ $\frac{1}{4}$	74.62	40.2	1.07	40.1	1.066	3.163	3.152	3.152	3.129	3.122	3.09	64.83	57.11	0.819
	76	40.08	1.062	40.08	1.062	3.184	3.172	3.17	3.15	3.145	3.108	64.15	56.82	0.839
	75.2	45	1.196	45.1	1.198	3.535	3.522	3.52	3.495	3.484	3.448	77.18	70.53	0.884
	74.44	44.9	1.185	44.9	1.185	3.49	3.478	3.475	3.449	3.444	3.408	76.06	69.02	0.887
	74.66	49	1.3	49	1.3	3.859	3.844	3.842	3.813	3.803	3.76	88.04	82.65	0.915
	75.3	49.5	1.3	49.5	1.3	3.865	3.85	3.849	3.805	3.795	3.758	87.31	87.06	0.936
	75.17	20	0.555	20	0.555	1.952	1.948	1.948	1.95	1.94	1.935	24.83	18.51	0.701
	73.48	20	0.558	20	0.558	1.907	1.902	1.902	1.903	1.893	1.888	24.88	18.37	0.706
	76.85	27	0.73	26.9	0.725	2.426	2.409	2.407	2.415	2.397	2.387	38.85	30.38	0.809
	74.8	27	0.744	27	0.744	2.373	2.367	2.363	2.372	2.348	2.346	39.41	30.51	0.822
$3\frac{3}{8}$ $\frac{3}{8}$	74.74	33	0.928	33	0.928	2.802	2.787	2.776	2.792	2.758	2.758	53.46	43.02	0.944
	74.86	33.2	0.932	33	0.928	3.795	2.78	2.774	2.783	2.75	2.75	53.14	42.75	0.957
	75.2	39	1.075	39	1.075	3.237	3.217	3.214	3.225	3.185	3.182	67.6	56.69	1.032
	74.64	39	1.074	39	39	3.256	3.236	3.225	3.225	3.195	3.193	68.67	57.58	1.011
	75.54	45.1	1.195	45.1	1.195	3.784	3.757	3.748	3.757	3.706	3.712	84.71	74.56	1.076
	75.3	44.9	1.232	45	1.232	3.748	3.72	3.707	3.728	3.676	3.673	83.7	73.37	1.106
	75.55	49	1.333	49	1.333	4.105	4.068	4.052	4.07	4.008	4.002	94.85	85.81	1.154
	75.58	49	1.33	49	1.33	4.134	4.096	4.078	4.095	4.038	4.034	95.73	86.82	1.137
	76.26	20	0.54	20	0.54	2.022	2.015	2.014	2.017	2.007	1.985	25.94	18.27	0.836
	76.25	20	0.54	20	0.54	2.031	2.024	2.023	2.025	2.018	1.991	26.25	18.24	0.827
$3\frac{3}{8}$ $\frac{1}{2}$	76.43	25	0.677	25	0.677	2.366	2.358	2.354	2.358	2.346	2.312	37.82	27.11	0.928
	76.75	25	0.675	25	0.675	2.378	2.37	2.367	2.37	2.355	2.317	37.3	27.18	0.923
	76.19	30	0.814	30	0.814	2.738	2.724	2.727	2.728	2.708	2.66	48.91	37.64	1.032
	76.23	30.03	0.82	30.03	0.82	2.733	2.72	2.715	2.718	2.7	2.655	49.53	37.21	1.033
	76.5	35.05	0.952	35.05	0.952	3.162	3.14	3.135	3.136	3.112	3.053	63.05	49.24	1.107

TABLE II

1	2	3	4			5 I	II	III	IV	V	VI	6	7	8
3 3/8 1/2 **3 3/8**	76.42	35.02	0.953	35	0.95	3.142	3.122	3.115	3.125	3.105	3.047	62.69	49.54	1.11
	77.56	40	1.092	40	1.092	3.63	3.605	3.596	3.604	3.58	3.513	77.7	63.49	1.18
	76.36	40	1.09	40	1.09	3.58	3.555	3.552	3.563	3.542	3.459	77.25	62.66	1.189
	77.6	44	1.19	44.1	1.194	4.01	3.978	3.976	3.988	3.957	3.87	90.2	76.26	1.22
	76.09	43.9	1.188	43.8	1.186	3.961	3.928	3.915	3.93	3.896	3.812	89.96	75.41	1.22
3 3/8 6/8	75.76	38.98	1.05	38.98	1.05	4.1	4.08	4.038	4.083	4.063	4.026	31.05	20.08	0.788
	76.79	19	0.52	18.9	0.514	2.80	2.75	2.63	2.77	2.68	2.62	30.86	19.94	0.88
	76.73	24.2	0.65	24	0.647	2.598	2.591	2.575	2.587	2.578	2.572	45.03	30.24	0.88
	76.91	23.9	0.645	23.8	0.643	2.587	2.582	2.565	2.585	2.574	2.563	44.49	29.85	0.874
	76.02	30.1	0.818	30.0	0.813	3.13	3.122	3.091	3.12	3.098	3.084	63.98	45.09	0.99
	76.01	30.1	0.818	30.0	0.816	3.135	3.22	3.093	3.13	3.107	3.098	64.19	45.26	0.988
	76.12	34	0.922	34	0.922	3.538	3.523	3.485	3.531	3.508	3.488	76.98	56.24	1.062
	76.11	34	0.922	34	0.922	3.542	3.522	3.491	3.531	3.502	3.488	76.99	56.25	1.062
	75.5	37	1.0	37	1.0	3.847	3.825	3.788	3.832	3.8	3.788	87.75	65.8	1.103
	76.35	37	1.0	37	1.0	3.871	3.875	3.814	3.861	3.832	3.812	87.87	66.2	1.099
	75.76	38.98	1.05	38.93	1.05	4.1	4.08	4.038	4.083	4.063	4.026	95.84	75.54	1.113
	75.59	38.98	1.05	38.98	1.05	4.07	4.052	4.003	4.055	4.012	3.992	94.41	72.11	1.138
2 7/8 6/8 (2.5 inches clearance)	79.3	10.66	0.285	10.66	0.288	1.8	1.789	1.788	1.8	1.785	1.783	14.7	7.035	0.693
	79.02	10.7	0.286	10.7	0.286	1.758	1.749	1.748	1.76	1.746	1.744	13.29	6.323	0.815
	79.04	16.04	0.396	16.04	0.396	2.155	2.136	2.133	2.154	2.125	2.122	27.465	13.6	0.806
	79.33	16.04	0.395	16.04	0.395	2.162	2.144	2.14	2.162	2.134	2.132	27.37	13.57	0.806
	78.84	20.7	0.527	20.9	0.529	2.646	2.613	2.606	2.644	2.597	2.592	43.76	22.63	0.889
	79.35	21.2	0.533	21.06	0.532	2.69	2.658	2.652	2.687	2.687	2.635	44.76	23.27	0.889
	79.17	26.4	0.674	26.3	0.673	3.287	3.241	3.232	3.282	3.223	3.211	64.84	35.58	0.981
	80.39	26.37	0.673	26.37	0.673	3.317	3.27	3.259	3.31	3.246	3.236	64.4	35.53	0.987
	78.77	31.5	0.798	31.5	0.798	3.846	3.805	3.786	3.855	3.772	3.76	84.03	48.47	1.089
	81.36	31.1	0.787	31.15	0.788	3.71	3.915	3.908	3.972	3.887	3.875	85.24	49.99	1.023
	80.23	37	0.968	37	0.968	4.746	4.662	4.645	4.73	4.625	4.606	111.47	69.72	1.166
	78.98	38	0.972	37.8	0.956	4.724	4.638	4.619	4.702	4.598	4.585	111.9	69.65	1.194

TABLE II

1	2	3	4				5						6	7	8
							I	II	III	IV	V	VI			
7/8	6	79.41	15.95	0.394	16.05	0.396	2.157	2.137	2.134	2.156	2.132	2.126	27.1	13.43	0.185
2 5/8		80.83	16	0.396	16	0.396	2.197	2.178	2.174	2.197	2.74	2.169	27.12	39.54	0.814
		81.16	21	0.522	21	0.529	2.705	2.673	2.666	2.703	2.662	2.655	43.54	22.79	0.905
3.5 inches o.d. (clearance)		79.3	20.85	0.522	20.86	0.525	2.632	2.598	2.59	2.63	2.586	2.58	42.91	22.19	0.872
		80.25	26.4	0.668	26.44	0.672	3.268	3.223	3.213	3.263	3.202	3.95	63.05	34.63	1.017
		78.99	26.37	0.674	26.27	0.674	3.273	3.225	3.215	3.266	3.205	3.197	64.42	35.28	0.993
		81.44	31.15	0.785	31.15	0.785	3.852	3.793	3.776	3.848	3.765	3.754	81.07	47.03	1.101
		84.05	31.15	0.789	31.15	0.789	3.933	3.876	3.855	3.925	3.846	3.831	81.05	47.66	1.102
		76.15	37.04	0.971	37.04	0.971	4.571	4.508	4.501	4.501	4.481	4.298	109.16	66.47	1.219
		76.15	37.35	0.976	37.35	0.976	4.58	4.636	4.567	4.578	4.55	4.362	111.56	68.31	1.203
		74.4	26.74	0.674	26.74	0.674	2.374	2.367	2.367	2.358	2.353	2.346	39.81	29.45	0.739
		74.02	26.74	0.678	26.75	0.678	2.364	2.358	2.358	2.307	2.348	2.348	39.68	29.3	0.748
Square Finned Tube 1/4		74.63	32	0.81	32	0.81	2.766	2.755	2.756	2.75	2.74	2.73	52.77	40.53	0.812
		72.72	32	0.81	32	0.81	2.708	2.703	2.701	2.687	2.68	2.675	53.89	41.09	0.792
		73.55	36.54	0.937	36	0.926	3.105	3.095	3.095	3.082	3.07	3.056	65.26	51.57	0.862
		74.33	36.67	0.935	37.07	0.94	3.142	3.138	3.138	3.121	3.105	3.100	65.88	52.36	0.876
		75.22	41.5	1.051	41.35	1.04	3.43	3.416	3.416	3.406	3.391	3.37	74.28	60.7	0.994
		76.86	41.8	1.078	42.1	1.08	3.563	3.543	3.543	3.524	3.508	3.503	77.15	64.08	0.998
1 1/4		72.03	46.65	1.2	4.665	1.2	3.787	3.775	3.77	3.745	3.739	3.689	89.48	74.95	1.079
		73.44	46.35	1.18	45.88	1.175	3.835	3.817	3.817	3.794	3.773	3.72	89.32	75.33	1.04
		76.45	15.42	0.395	15.52	0.397	1.804	1.795	1.794	1.799	1.787	1.787	18.66	12.55	0.652
		75.96	15.47	0.393	15.35	0.393	1.784	1.775	1.775	1.787	1.769	1.768	18.54	12.43	0.648
		75.43	21.55	0.53	22	0.536	2.088	2.082	2.082	2.086	2.066	2.064	29.58	20.42	0.826
Square Finned Tube 3/8		81.17	21.4	0.548	21.2	0.534	2.228	2.215	2.214	2.226	2.205	2.2	28.43	20.16	0.853
		79.54	26.5	0.676	26.5	0.676	2.608	2.583	2.583	2.599	2.568	2.568	43.07	31.51	0.876
		78.89	26.5	0.675	26.5	0.675	2.582	2.556	2.556	2.577	2.545	2.544	42.88	31.24	0.88
		81.7	32	0.811	31.5	0.811	3.088	3.061	3.051	3.082	3.038	3.03	57.8	44.53	0.944
		83.35	32	0.805	32	0.805	3.124	3.09	3.09	3.114	3.066	3.06	57.4	44.55	0.95
		84.26	39.44	1.008	39.6	1.008	3.812	3.766	3.766	3.807	3.726	3.707	80.04	66.34	1.068

TABLE II

1	2	3			4		5 I	II	III	IV	V	VI	6	7	8
Sq. F. Tube	3/8	83.72	39.6	1.01	39.6	1.01	3.808	3.752	3.752	3.789	3.711	3.668	79.89	66	1.077
		81.46	46.8	1.18	46.8	1.18	4.408	4.348	4.345	4.413	4.298	4.27	103.05	89.53	1.16
		78.45	46.8	1.18	46.8	1.18	46.8	4.316	4.257	4.295	4.207	4.2	103.45	88.63	1.159
Square Finned Tube	1/2	77.83	15.85	0.406	15.86	0.406	1.923	1.918	1.911	1.918	1.905	1.896	21.48	13.5	0.741
		77.24	15.76	0.403	15.76	0.403	1.897	1.909	1.891	1.894	1.884	1.882	21.52	13.49	0.726
		76.73	21.1	0.526	21.1	0.526	2.221	2.211	2.196	2.213	2.194	2.181	32.07	20.64	0.899
		75.95	21.1	0.531	21.1	0.531	2.194	2.184	2.174	2.185	2.166	2.16	33.55	21.59	0.839
		76.62	26.5	0.67	26.5	0.67	2.645	2.63	2.619	2.634	2.604	2.592	46.48	31.11	1.01
		75.26	26.5	0.662	26.5	0.662	2.585	2.572	2.555	2.572	2.552	2.54	45.84	30.41	1.019
		76.38	32	0.806	32	0.806	3.111	3.086	3.071	3.094	3.06	3.048	61.92	43.19	1.122
		75.75	32	0.808	32	0.808	3.092	3.071	3.052	3.082	3.048	3.025	62.05	43.15	1.124
		76.39	37.33	0.963	36.33	0.963	3.691	3.668	3.645	3.682	3.625	3.607	81.36	59.83	1.193
		75.09	37.33	0.96	37.33	0.96	3.632	3.311	3.592	3.622	3.56	3.558	80.72	58.86	1.204
		77.25	42.9	1.1	42.63	1.1	4.17	4.12	4.095	4.14	4.09	4.071	96.25	74.02	1.343
		76.08	43.1	1.073	42.9	1.071	4.033	3.998	3.976	4.014	3.973	3.946	93.43	70.87	1.365
Square Finned Tube	6/8	76.44	15.95	0.41	15.95	0.41	2.095	2.085	2.084	2.09	2.075	2.086	27.76	14.76	0.799
		76.47	15.83	0.405	15.85	0.409	2.095	2.082	2.081	2.088	2.074	2.085	27.73	14.75	0.783
		79.55	21.1	0.535	21.1	0.535	2.624	2.605	2.605	2.612	2.595	2.595	42.26	23.79	0.936
		78.89	21.65	0.538	21.1	0.531	2.618	2.599	2.599	2.608	2.59	2.59	42.86	24.08	0.933
		79.62	26.5	0.664	26.5	0.664	3.181	3.16	3.155	3.168	3.145	3.145	61.14	36.25	1.018
		79.5	26.7	0.674	26.5	0.665	3.208	3.183	3.183	3.194	3.168	3.168	62.11	36.9	1.01
		78.6	32	0.811	32	0.811	3.844	3.806	3.806	3.82	3.79	3.79	83.7	52.48	1.105
		79.73	32	0.805	32	0.805	3.872	3.825	3.825	3.845	3.815	3.815	83.87	52.91	1.088
		78.26	37.33	0.937	37.33	0.937	4.534	4.485	4.485	4.517	4.567	4.465	107.04	71.33	1.116
		77.52	37.45	0.947	37.36	0.947	4.51	4.466	4.466	4.496	4.442	4.446	106.99	71.01	1.185
Sq. F. Tube	6/8	74.76	15.05	0.389	15.05	0.389	1.922	1.914	1.91	1.915	1.907	1.867	23.45	12.31	0.875
		74.8	14.93	0.388	14.99	0.389	1.917	1.905	1.902	1.91	1.901	1.861	23.11	12.02	0.887
		78.09	21.1	0.537	21.1	0.537	2.152	2.495	2.495	2.5	2.494	2.418	39.91	22.15	1.026
		76.82	21.1	0.548	21.1	0.548	2.50	2.483	2.477	2.485	2.478	2.140	40.79	22.53	1.026

TABLE II

1	2	3	4	5 I	II	III	IV	V	VI	6	7	8
Sq. Finned Tube	βq 6 (2.548") chim.	76.15 26.5	0.688 26.5 0.688	3.031	2.992	2.99	2.999	2.987	2.87	58.66	33.92	1.133
		77.08 26.5	0.678 26.5 0.678	3.045	3.017	3.0	3.026	3.002	3.886	58.23	33.79	1.132
		77.18 32	0.827 32 0.827	3.695	3.652	3.624	3.677	3.64	3.579	79.93	49.24	1.22
		76 32	0.82 32 0.82	3.606	3.558	3.557	3.566	3.551	3.393	77.6	47.21	1.261
		77.33 37.35	0.975 36.9 0.97	4.252	4.126	4.105	4.192	4.166	3.98	96.28	62.03	1.142
		78.51 37.35	0.972 37.35 0.972	4.373	4.303	4.302	4.307	4.304	4.15	100.1	65.55	1.135
Square Finned Tube	βq 6 (with 3.78 in) chimney	75.63 14.94	0.383 14.94 0.383	1.905	1.895	1.895	1.896	1.89	1.829	21.87	11.39	0.939
		76.49 14.98	0.385 14.9 0.383	1.93	1.917	1.916	1.92	1.915	1.852	21.91	11.47	0.938
		76.89 21.1	0.542 21.1 0.542	2.452	2.428	2.427	2.427	2.42	2.302	38.61	21.21	1.093
		74.11 21.1	0.533 21.1 0.533	2.344	2.324	2.32	2.323	2.317	2.203	37.69	20.35	1.111
		74.45 27.1	0.686 27.1 0.686	2.905	2.873	2.87	2.873	2.863	2.684	55.85	31.76	1.264
		72.94 27.1	0.674 26.5 0.672	2.846	2.811	2.81	2.815	2.803	2.622	55.56	31.32	1.229
		76.59 32	0.794 32 0.794	3.437	3.397	3.397	3.4	3.385	3.15	71.31	42.78	1.36
		76.88 32	0.812 32 0.812	3.55	3.508	3.505	3.492	3.494	3.249	74.73	45.32	1.31
		74.82 36.23	0.952 36.23 0.952	4.078	4.019	4.019	4.022	4.005	3.727	93.78	59.26	1.394
		77.1 36.23	0.955 36.23 0.955	4.177	4.114	4.114	4.118	4.101	3.81	92.4	58.85	1.424

TABLE III

CALCULATED DIMENSIONLESS GROUPS

1	2	3	4	5	6	7	8	9
Fin Diameter	Nominal Fin Space	θ	$\left(\dfrac{h.a.m.\,d_e}{k}\right)_f$	$\left[\dfrac{h.a.m.(b+d)}{k}\right]_f$	$\left(\dfrac{d_e^3\rho^2 g\beta\theta}{\mu^2}\times\dfrac{c_p\mu}{k}\right)_f\times10^{-4}$	$\left(\dfrac{d_e^3\rho^2 g\beta\theta}{\mu^2}\times\left(\dfrac{b}{d}\right)\times\left(\dfrac{c_p\mu}{k}\right)_f\right)\times10^{-4}$	$\left(\dfrac{d_e^3\rho^2 g\beta\theta}{\mu^2}\times\dfrac{c_p\mu}{k}\times\dfrac{f}{k}\right)_f\times10^{-4}$	$\left[\dfrac{(b+d)^3\rho^2 g\beta\theta}{\mu^2}\times\left(\dfrac{c_p\mu}{k}\right)\times\dfrac{b+d}{d}\right]_f\times10^{-4}$
Bare Tube		49.64	9.17		7.13			
		49.5	9.3		7.08			
		75.98	9.59		9.96			
		75.42	9.57		9.98			
		125	10.91		14			
		121.2	11.01		13.6			
$2\frac{3}{8}$	$\frac{1}{4}$	24.38	5.086	4.47	12.32	4.194	2.43	3.23
		24.25	5.089	4.47	12.29	4.182	2.42	3.65
		40.03	6.392	5.613	19.01	6.47	3.75	5.64
		41	6.575	5.277	19.6	6.67	3.86	5.82
		55.78	7.29	6.402	25.0	8.51	4.93	7.42
		55.98	7.293	6.404	25.1	8.54	4.95	7.45
		69.36	7.92	6.956	29.74	10.12	5.86	8.83
		69.03	7.985	7.011	29.6	10.08	5.84	8.79
		77.2	8.17	7.174	32.1	10.93	6.33	9.53
		76.39	8.36	7.34	31.91	10.86	6.29	9.47
		92.26	8.721	7.658	36.78	12.52	7.25	10.91
		92.54	8.544	7.502	36.54	12.44	7.20	10.84
$2\frac{3}{8}$	$\frac{3}{8}$	26.33	5.539	5.2	13.34	6.45	3.73	5.18
		25.79	5.73	5.38	13.09	6.33	3.66	5.08
		37.7	6.836	6.36	18.32	8.86	5.13	7.11

TABLE III

1	2	3	4	5	6	7	8	9
$2\frac{3}{8}$	$\frac{3}{8}$	38.39	6.472	6.077	18.66	9.02	5.23	7.24
		52.11	7.488	7.03	23.86	11.54	6.68	9.26
		51.1	7.509	7.05	23.63	11.43	6.62	9.17
		72.1	8.711	8.18	30.67	14.83	8.59	11.91
		74.73	8.711	8.24	31.65	15.30	8.86	12.28
		83.6	9.381	9.37	34.29	16.58	9.6	13.31
		86.7	8.684	8.15	34.73	16.8	9.72	13.48
		96.16	9.078	8.52	38.03	18.4	10.65	14.77
		95.48	9.052	8.499	37.88	18.32	10.61	14.71
$2\frac{3}{8}$	$\frac{1}{2}$	17.42	5.739	5.763	9.14	5.83	3.38	4.65
		17.64	5.546	5.57	9.29	5.93	3.43	4.72
		28.18	6.974	7.003	14.19	9.05	5.24	7.22
		27.8	7.142	7.172	14.05	8.97	5.19	7.15
		47.53	8.416	8.452	22.19	14.16	8.20	11.29
		47.6	8.607	8.643	22.21	14.17	8.21	11.29
		68.83	9.184	9.222	29.57	18.86	10.92	15.03
		68.49	9.316	9.354	29.42	18.77	10.87	14.96
		85.82	9.832	9.873	35.03	22.35	12.94	17.81
		86.38	9.775	9.816	35.26	22.5	13.03	17.93
		103.78	10.49	10.53	39.97	25.51	14.77	20.33
		105.36	10.33	10.37	40.20	25.65	14.85	20.44
$2\frac{3}{8}$	$\frac{6}{8}$	15.78	6.83	7.75	8.49	8.03	4.65	7.04
		16.67	6.28	7.122	8.97	8.48	4.91	7.44
		29.24	7.51	8.52	14.91	14.1	8.17	12.37
		29.87	7.21	8.178	15.08	14.26	8.26	12.5
		44.68	8.33	9.453	21.07	19.93	11.45	17.47
		45.18	8.32	9.442	21.30	20.15	11.67	17.67
		62.72	9.05	10.27	27.75	26.25	15.2	23.02
		61.7	9.19	10.42	27.38	25.89	14.99	22.7

TABLE III

1	2	3	4	5	6	7	8	9
$2\frac{3}{8}$	$\frac{6}{8}$	79.69	10.06	11.41	33.29	31.48	18.23	27.61
		80.72	9.98	11.33	33.72	31.89	18.47	27.96
		102.02	10.45	11.86	39.82	37.66	21.8	33.02
		103.02	10.35	11.75	39.77	37.62	21.78	32.99
$2\frac{7}{8}$	$\frac{1}{4}$	29.01	6.826	5.27	20.48	8.26	3.95	3.64
		28.91	6.863	5.30	20.47	8.26	3.95	3.64
		39.23	8.182	6.32	27.43	11.07	5.296	4.87
		38.8	8.315	6.42	27.18	10.97	5.25	4.83
		50.27	9.15	7.06	33.76	13.63	6.52	5.99
		51.08	8.95	6.91	33.88	13.67	6.54	6.02
		62.59	10.45	8.07	40.47	16.33	7.81	7.19
		63.74	10.18	7.86	40.68	16.42	7.85	7.23
		77.86	10.69	8.25	47.97	19.36	9.26	8.52
		77.34	10.69	8.25	47.64	19.23	9.20	8.46
		89.08	11.16	8.61	52.90	21.35	10.21	9.4
		88.63	11.17	8.63	52.36	21.24	10.16	9.35
$2\frac{7}{8}$	$\frac{3}{8}$	30.18	7.732	6.401	21.37	12.48	5.97	5.02
		30.38	7.727	6.4	21.67	12.65	6.605	5.09
		42.1	9.757	8.077	28.43	16.59	7.94	6.67
		42.0	9.831	8.14	28.51	16.64	7.96	6.69
		55.84	10.79	8.94	35.73	20.86	9.98	8.39
		55.52	10.75	8.902	35.43	20.69	9.90	8.32
		67.0	11.33	9.4	40.98	23.92	11.44	9.62
		67.05	11.2	9.28	41.68	24.33	11.64	9.79
		79.33	11.88	9.83	47.33	27.63	13.22	11.11
		80.9	11.56	9.57	48.04	28.05	13.42	11.28
		92.1	12.36	10.24	52.39	30.59	14.63	12.3
		95.69	12.45	10.31	53.80	31.41	15.02	12.63

TABLE III

1	2	3	4	5	6	7	8	9
$2\frac{7}{8}$	$\frac{1}{2}$	21.4	8.461	7.545	15.88	12.54	6.0	5.02
		20.89	8.232	7.34	15.65	12.36	5.91	4.95
		31.23	9.50	8.47	22.3	17.62	8.43	2.05
		30.55	9.801	8.74	21.87	17.28	8.26	6.91
		44.95	10.69	9.53	30.54	24.12	11.54	9.65
		44.92	10.51	9.37	30.54	24.12	11.54	9.65
		60.27	11.69	10.43	38.47	30.39	14.53	12.15
		60.81	11.64	10.38	38.81	30.66	14.66	12.27
		26.85	12.57	11.21	46.06	36.39	17.4	14.56
		77.1	12.53	11.17	46.21	36.51	17.46	14.61
		96.84	12.83	11.44	54.39	42.96	20.55	17.19
		97.39	12.84	11.45	55.35	43.72	20.91	17.49
$2\frac{7}{8}$	$\frac{6}{8}$	16.33	8.12	8.2	12.45	14.59	6.98	6.47
		16.49	8.22	8.3	12.58	14.74	7.05	6.54
		31.04	8.88	8.96	21.98	25.75	12.32	11.42
		31.19	8.92	9.01	22.33	26.16	12.51	11.61
		46.8	10.03	10.03	31.17	36.52	17.47	16.2
		47.7	9.861	9.96	31.50	36.91	17.65	16.38
		65.7	10.87	10.98	40.98	48.02	22.96	21.30
		65.58	10.96	11.06	40.98	48.02	22.96	21.30
		85.68	11.95	12.06	50.41	59.06	28.25	26.20
		87.1	11.73	11.67	52.21	61.17	29.26	27.14
		108.6	12.51	12.63	58.74	68.82	32.92	30.53
		109.9	12.29	12.41	58.74	68.82	32.92	30.53
$3\frac{3}{8}$	$\frac{1}{4}$	26	6.814	4.727	26.71	13.01	5.30	3.096
		26.56	6.559	4.544	27.18	13.24	5.39	3.15
		36.78	7.978	5.54	35.98	17.53	7.24	4.17
		37.175	7.866	5.46	36.37	17.72	7.22	4.22
		53.25	9.643	6.69	49.13	23.93	9.75	5.69

TABLE III

1	2	3	4	5	6	7	8	9
$3\frac{3}{8}$	$\frac{1}{4}$	53.57	9.558	6.63	49.01	23.87	9.73	5.68
		64.83	9.96	6.91	57.55	28.04	11.42	6.67
		64.515	10.17	7.07	56.6	27.57	11.23	6.56
		77.18	10.63	7.37	65.52	31.92	13.0	7.59
		76.06	10.69	7.42	65.46	31.89	12.99	7.59
		88.04	10.92	7.57	73.04	35.58	14.5	8.47
		87.31	11.17	7.746	72.43	35.28	14.38	8.39
$3\frac{3}{8}$	$\frac{3}{8}$	24.83	8.825	6.57	25.53	17.91	7.296	3.918
		24.88	8.916	6.64	26.04	18.26	7.44	4.0
		38.85	10.03	7.46	37.35	26.2	10.67	5.73
		39.41	10.22	7.61	38.25	26.83	10.93	5.87
		53.46	11.59	8.63	49.53	34.75	14.16	7.60
		53.14	11.75	8.745	49.03	34.39	14.01	7.53
		67.6	12.51	9.31	59.07	41.44	16.88	9.07
		68.67	12.26	9.13	60.0	42.09	17.15	9.21
		84.71	12.85	9.57	70.27	49.3	20.08	10.79
		83.7	13.23	9.84	69.76	48.94	19.94	10.71
		94.85	13.69	10.2	75.52	52.98	21.58	11.59
		95.73	13.47	10.03	76.07	53.36	21.74	11.68
$3\frac{3}{8}$	$\frac{1}{2}$	25.94	10.49	8.41	26.35	24.83	10.12	5.33
		26.25	10.37	8.31	26.76	25.22	10.28	5.52
		37.28	11.52	9.23	36.14	34.05	13.88	7.45
		37.3	11.45	9.18	36.09	34.01	13.86	7.44
		48.91	12.69	10.17	45.50	42.89	17.47	9.38
		49.53	12.70	10.18	45.69	43.06	17.54	9.42
		63.05	13.44	10.77	54.41	51.28	20.89	11.21
		62.69	13.49	10.81	55.4	52.22	21.27	11.42
		77.7	14.14	11.33	64.75	61.03	24.86	13.35
		77.25	14.28	11.44	64.92	61.18	24.93	13.38
		90.2	14.51	11.63	71.82	67.69	27.58	14.8
		89.96	14.46	11.59	72.54	68.36	27.86	14.95

TABLE III

1	2	3	4	5	6	7	8	9
$3\frac{3}{8}$	$\frac{6}{8}$	31.05	9.84	8.84	30.69	41.36	16.94	10.0
		30.86	9.84	9.74	30.53	41.59	16.85	9.95
		45.03	10.84	9.74	42.41	56.64	23.41	13.82
		44.49	10.77	9.68	41.8	57.47	23.07	13.63
		63.98	12.02	10.8	56.3	76.28	31.08	18.35
		64.19	12.0	10.78	56.49	26.53	31.18	18.41
		76.98	12.75	11.46	64.46	87.34	35.58	21.01
		76.99	12.75	11.46	64.67	87.33	35.59	21.01
		87.75	13.15	11.81	72.12	103.2	39.81	23.5
		87.87	13.09	11.76	71.43	97.7	39.43	23.31
		95.84	13.18	11.84	76.15	101.8	42.04	24.82
		94.41	13.5	12.13	75.17	96.78	41.49	24.5
Square Finned Tube	$\frac{1}{4}$	39.81	8.22	6.381	27.83		5.52	5.45
		39.68	8.32	4.451	27.97		5.54	5.48
		52.77	8.93	6.93	34.83		6.90	6.88
		53.89	8.74	6.78	36.78		7.29	7.20
		65.26	9.40	7.29	42.37		8.398	8.3
		65.88	9.53	7.39	42.04		8.333	8.24
		74.28	10.73	8.32	45.25		8.988	8.88
		77.15	10.71	8.31	46.67		9.25	9.14
		89.48	11.57	8.97	53.63		10.63	10.5
		89.32	11.11	8.62	52.05		10.32	10.2
Square Finned Tube	$\frac{3}{8}$	18.66	7.37	6.116	14.18		4.07	3.655
		18.54	7.34	6.094	13.99		3.96	3.61
		29.58	9.29	7.714	21.34		6.05	5.5
		28.43	9.47	7.862	19.72		5.59	5.08
		43.07	9.63	7.998	28.44		8.06	7.23
		42.88	9.71	8.06	28.56		8.09	7.36
		57.8	10.22	8.48	36.25		10.27	9.34
		57.4	10.26	8.52	35.36		10.02	9.11

TABLE III

1	2	3	4	5	6	7	8	9
Square Finned Tube	3/8	80.04	11.36	9.43	45.75		12.96	11.79
		79.89	11.5	9.54	45.22		12.81	11.65
		103.05	12.16	10.1	54.33		15.39	14.0
		103.45	12.18	10.11	55.69		15.78	14.35
Square Finned Tube	1/2	21.48	8.342	7.39	15.85		5.85	5.29
		21.52	8.178	7.25	16.12		5.95	5.38
		32.07	10.05	8.91	22.60		8.34	2.55
		33.55	9.38	8.31	23.65		8.73	7.90
		46.48	11.17	9.89	30.96		11.43	10.34
		45.84	11.28	9.99	31.30		11.55	10.45
		61.92	12.23	10.83	39.52		14.59	13.19
		62.05	12.26	10.87	40.29		14.87	13.45
		81.36	12.76	11.31	47.86		17.67	15.98
		80.72	12.92	11.45	48.38		17.86	16.15
		96.25	14.22	12.60	55.02		20.31	18.37
		93.43	14.52	12.86	54.44		20.1	18.13
Square Finned Tube	6/8	27.76	8.97	9.07	20.03		11.27	11.34
		27.73	8.71	8.80	19.24		10.82	10.89
		42.26	10.31	10.43	28.14		15.83	15.94
		42.86	10.29	10.14	28.54		16.06	16.17
		61.14	11.03	11.15	38.34		21.57	21.71
		62.11	10.90	11.02	38.60		21.72	21.86
		83.7	11.79	11.92	49.24		27.7	27.89
		83.87	11.59	11.72	48.87		27.49	27.63
		107.04	12.20	12.33	57.63		32.41	32.63
		106.99	12.48	12.61	58.78		38.69	33.29
	6/8	23.45	9.888	10.0	17.56		9.88	9.95
		23.11	10.04	10.15	17.44		9.8	9.88
		39.91	11.36	11.48	27.24		15.33	15.43
		40.79	11.37	11.49	28.29		15.92	16.02

TABLE III

1	2	3	4	5	6	7	8	9
Sq. Finned Tube	6/8 (2.548 inches chimney)	58.66	12.29	12.43	36.78		20.69	20.83
		58.23	12.34	12.47	37.16		20.9	21.05
		79.93	13.05	13.2	47.46		26.7	26.88
		77.6	13.57	13.72	46.94		26.41	26.58
		96.28	15.05	15.21	55.03		30.96	31.17
		100.41	14.23	14.38	55.55		31.25	31.46
Square Finned Tube	6/8 (with 3.78 inches chimney)	21.87	10.62	10.74	16.39		9.22	9.35
		21.19	10.58	10.69	16.29		9.17	9.23
		38.61	12.13	12.27	26.57		14.95	15.05
		37.69	12.41	12.55	26.56		14.94	15.04
		55.85	13.87	14.02	36.27		20.4	20.54
		55.56	13.56	13.71	37.00		20.81	20.96
		71.31	14.68	14.84	43.93		24.71	24.88
		74.73	14.11	14.27	45.20		25.43	25.6
		93.78	14.83	14.99	54.65		30.74	30.95
		92.4	15.1	15.26	52.82		29.71	29.91

A₁ — FICTITIOUS SURFACE

A₂ — SURFACE OF THE BASE TUBE

A₃,A₄ — SURFACES OF THE FIN PLATES
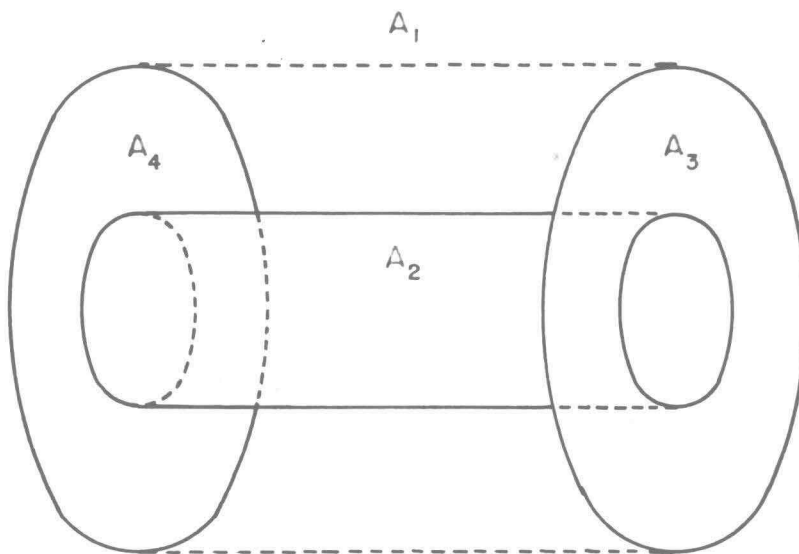
FIGURE 8   IMAGINARY CONFIGURATION OF FINNED TUBES
FOR RADIATION LOSS CALCULATION
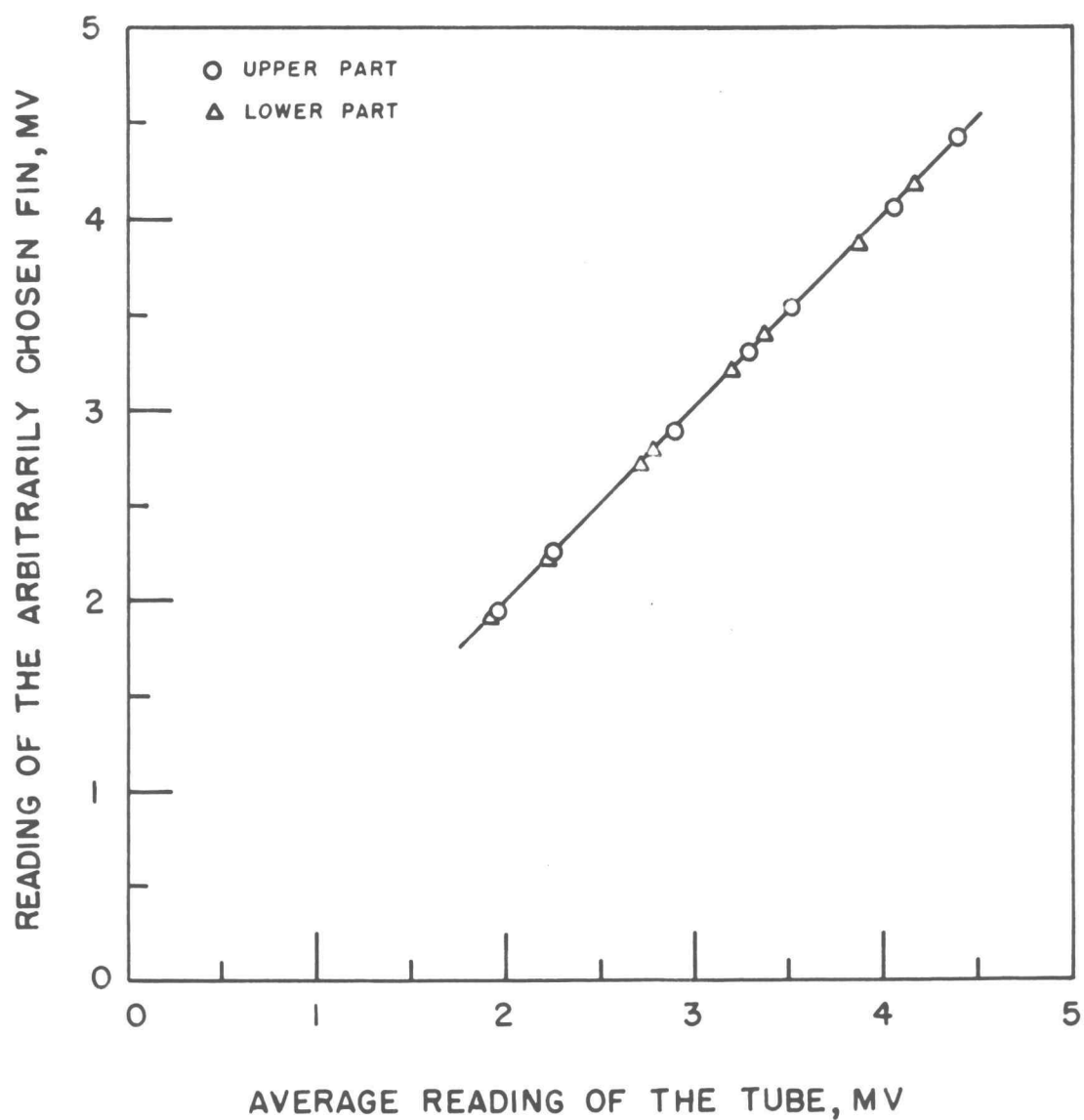
FIGURE 9   TEMPERATURE — AVERAGING CALIBRATION
— 2 3/8 INCH FIN DIAMETER AND   1/4
INCH FIN SPACING
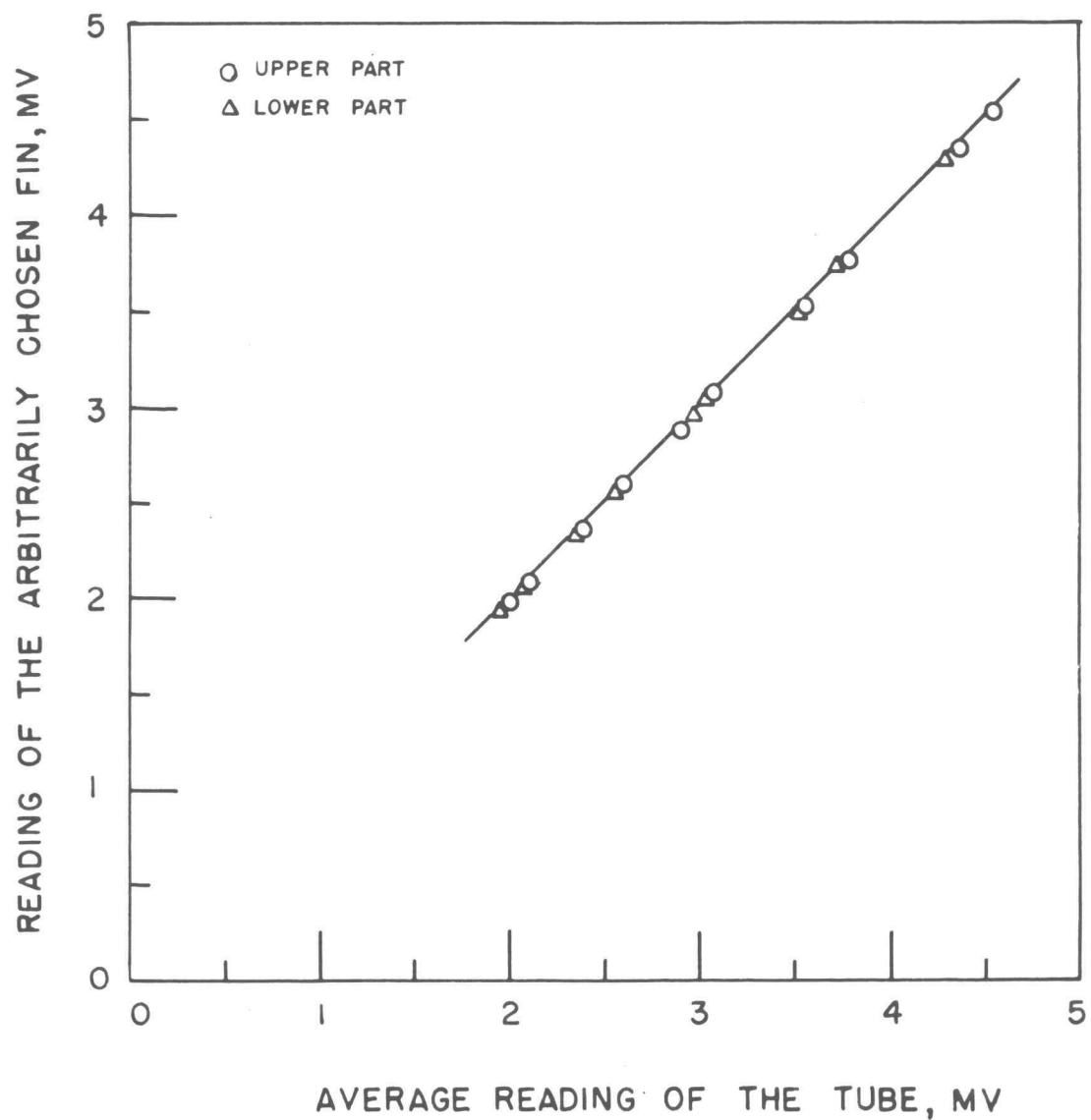
FIGURE 10   TEMPERATURE - AVERAGING CALIBRATION
— 2 3/8 INCH FIN DIAMETER AND 3/8
INCH FIN SPACING
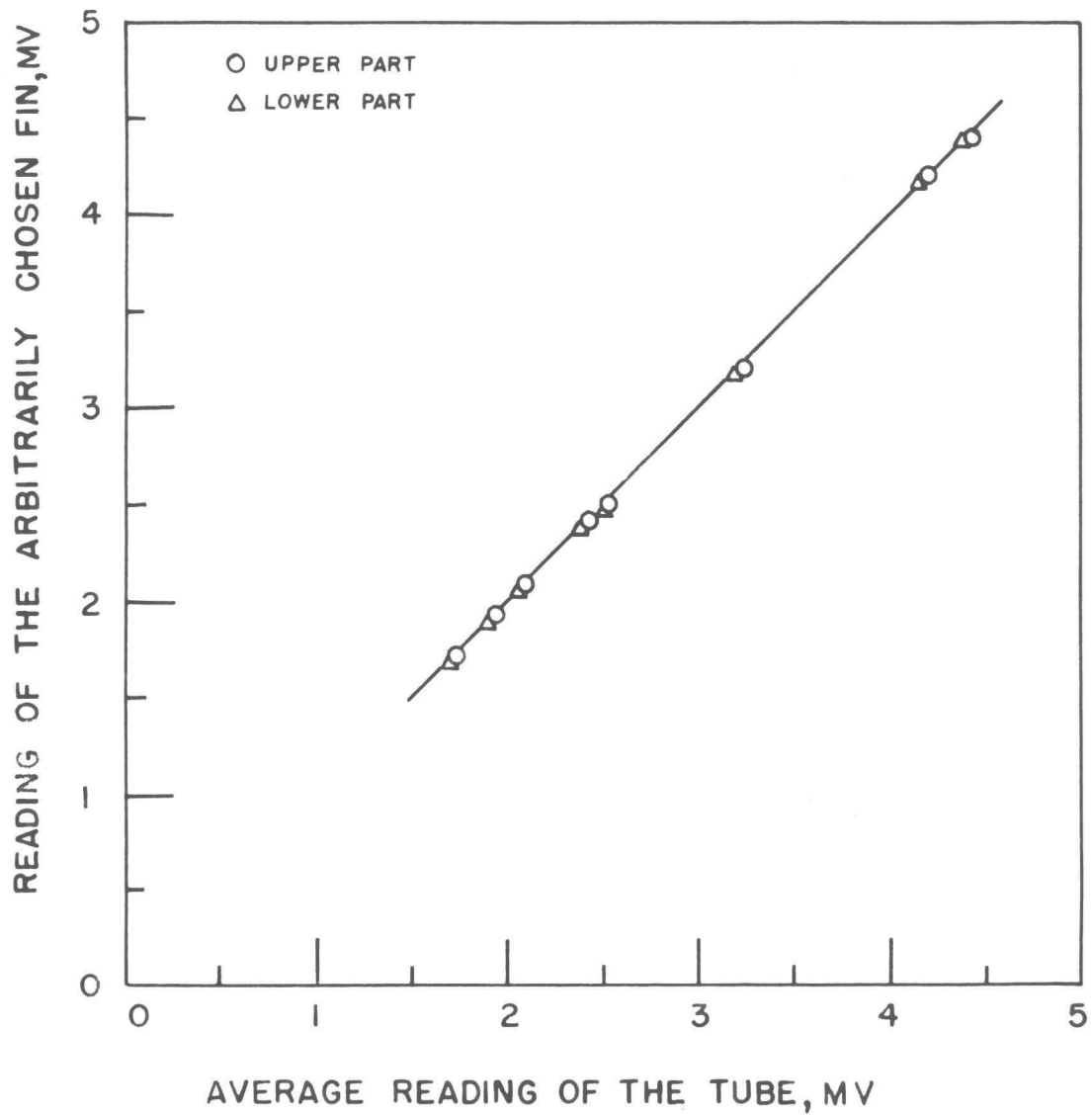
FIGURE 11   TEMPERATURE – AVERAGING   CALIBRATION
—2 3/8 INCH FIN DIAMETER AND   1/2
INCH FIN SPACING
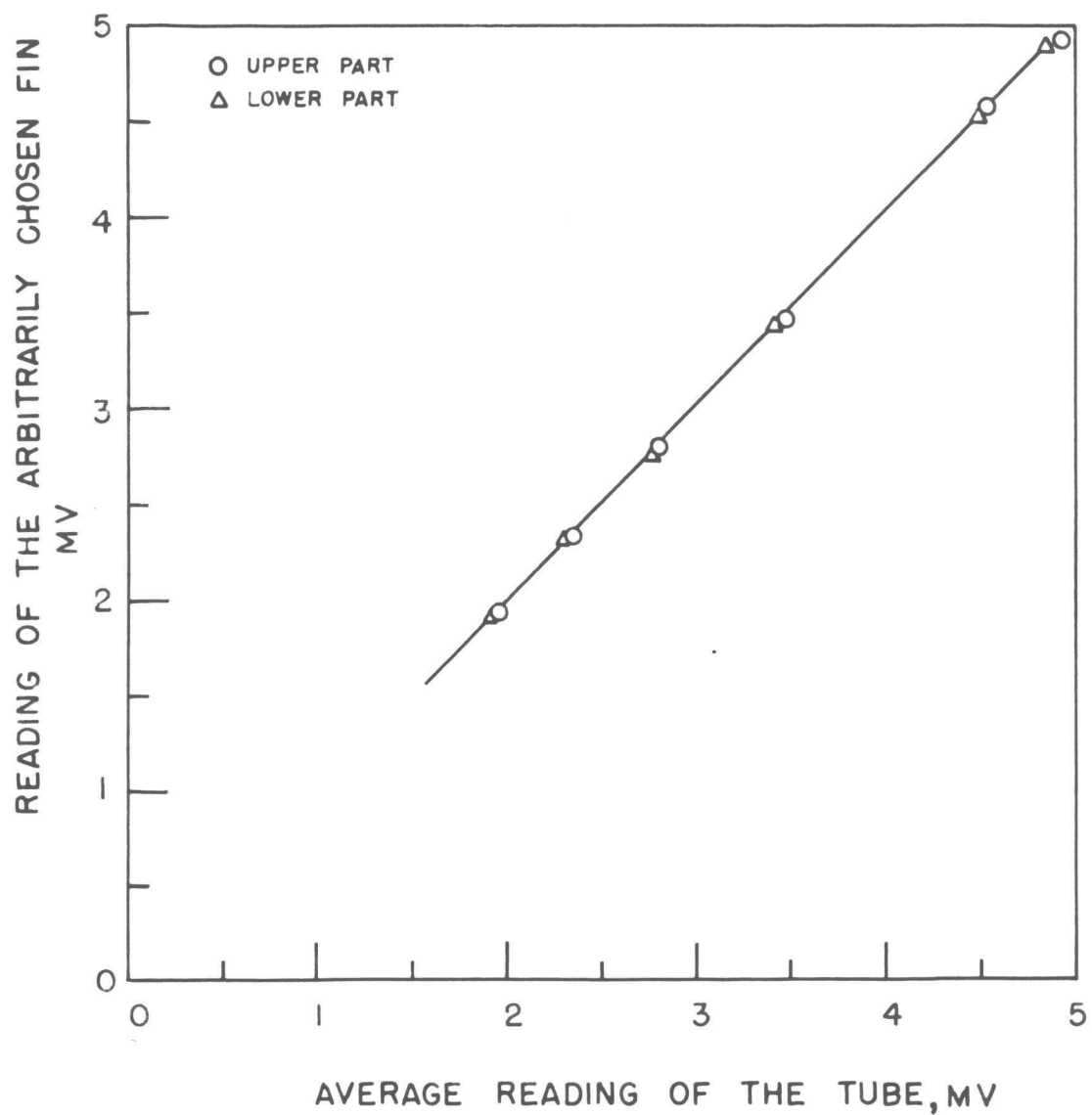
FIGURE 12   TEMPERATURE — AVERAGING   CALIBRATION
— 2³/8   INCH   FIN   DIAMETER   AND   6/8
INCH   FIN   SPACING
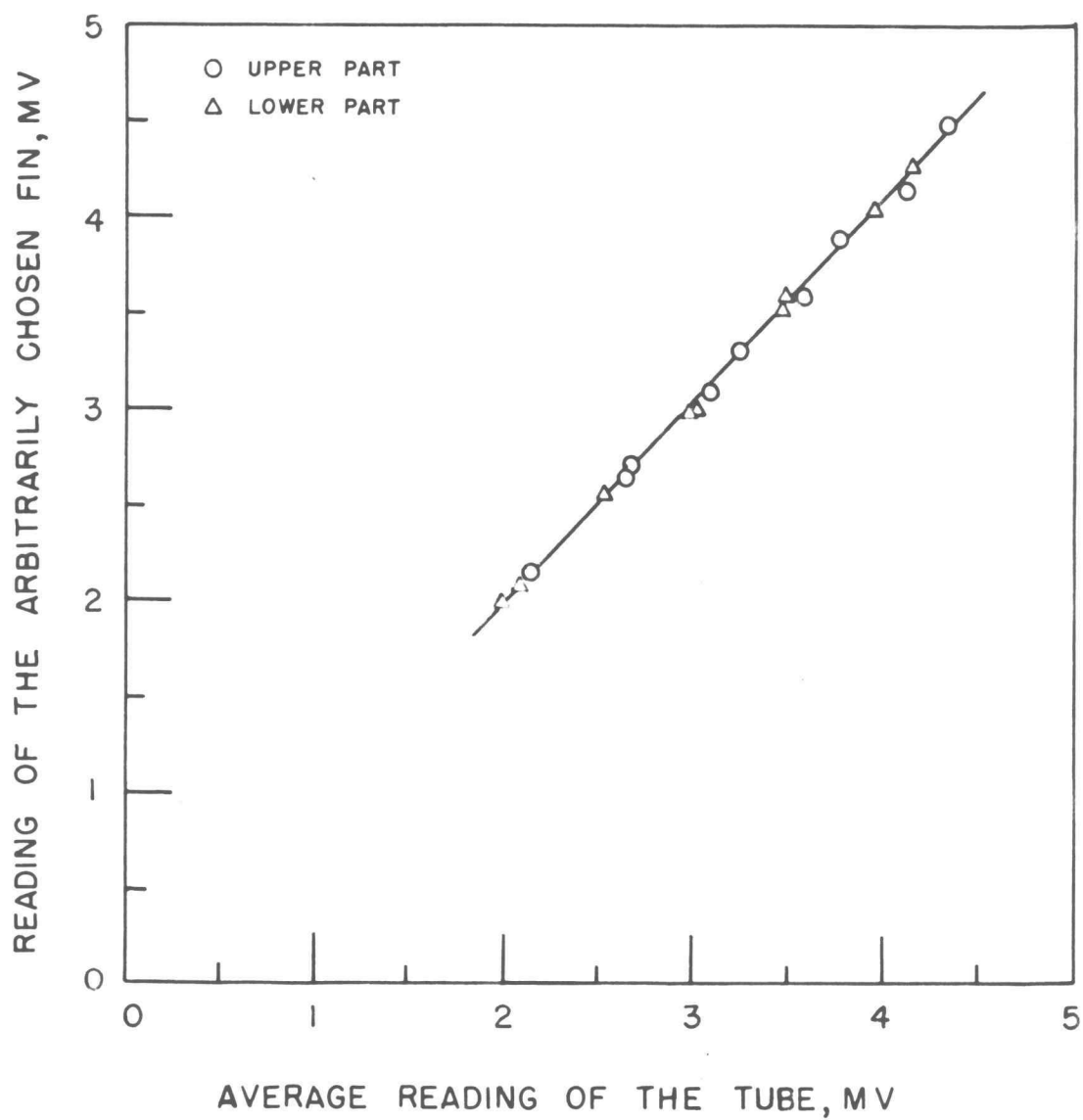
FIGURE 13   TEMPERATURE – AVERAGING   CALIBRATION
– 2 7/8 INCH FIN DIAMETER AND   1/4
INCH FIN SPACING
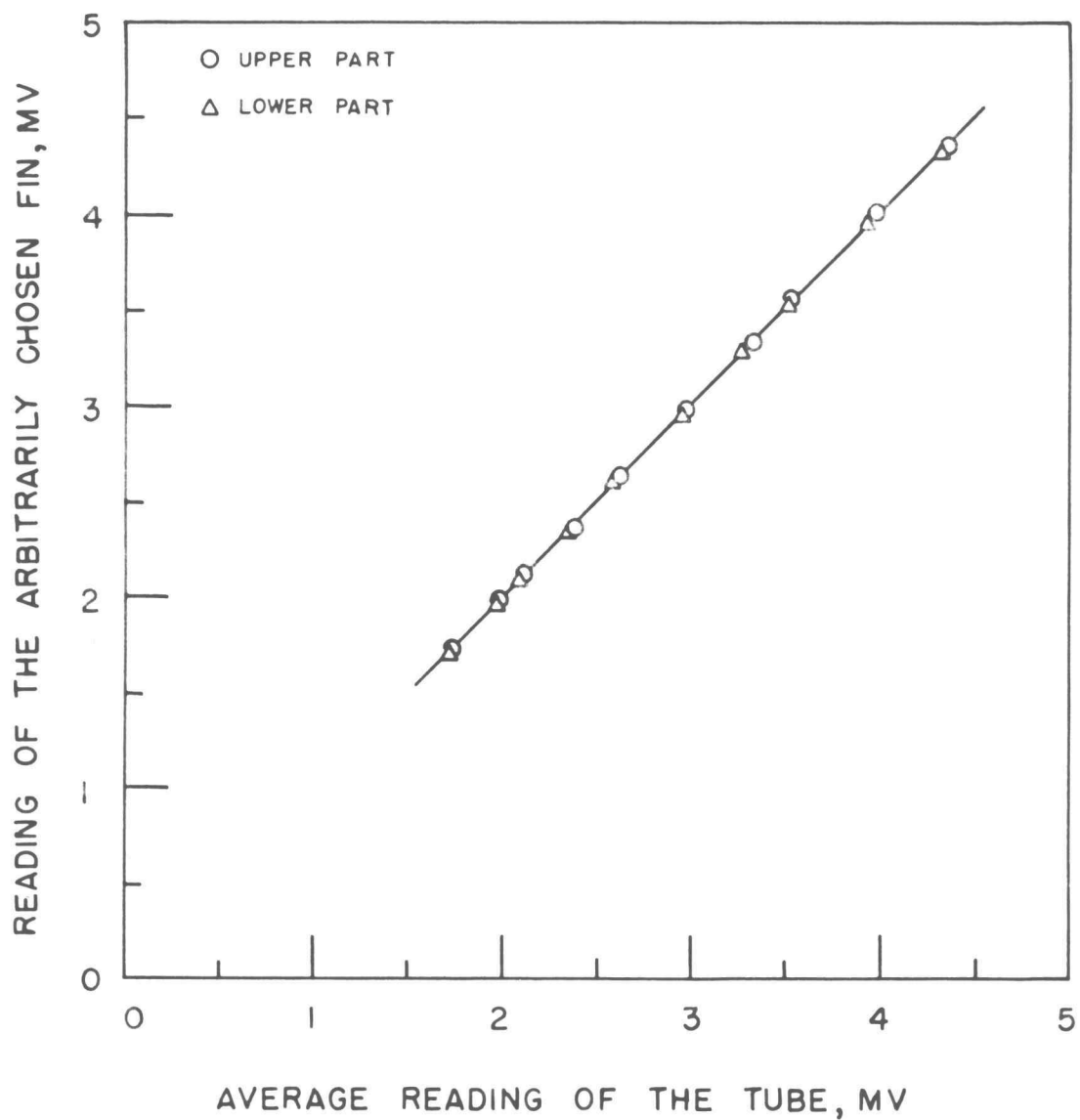
FIGURE 14   TEMPERATURE — AVERAGING CALIBRATION
— 2 7/8 INCH FIN DIAMETER AND   3/8
INCH FIN SPACING
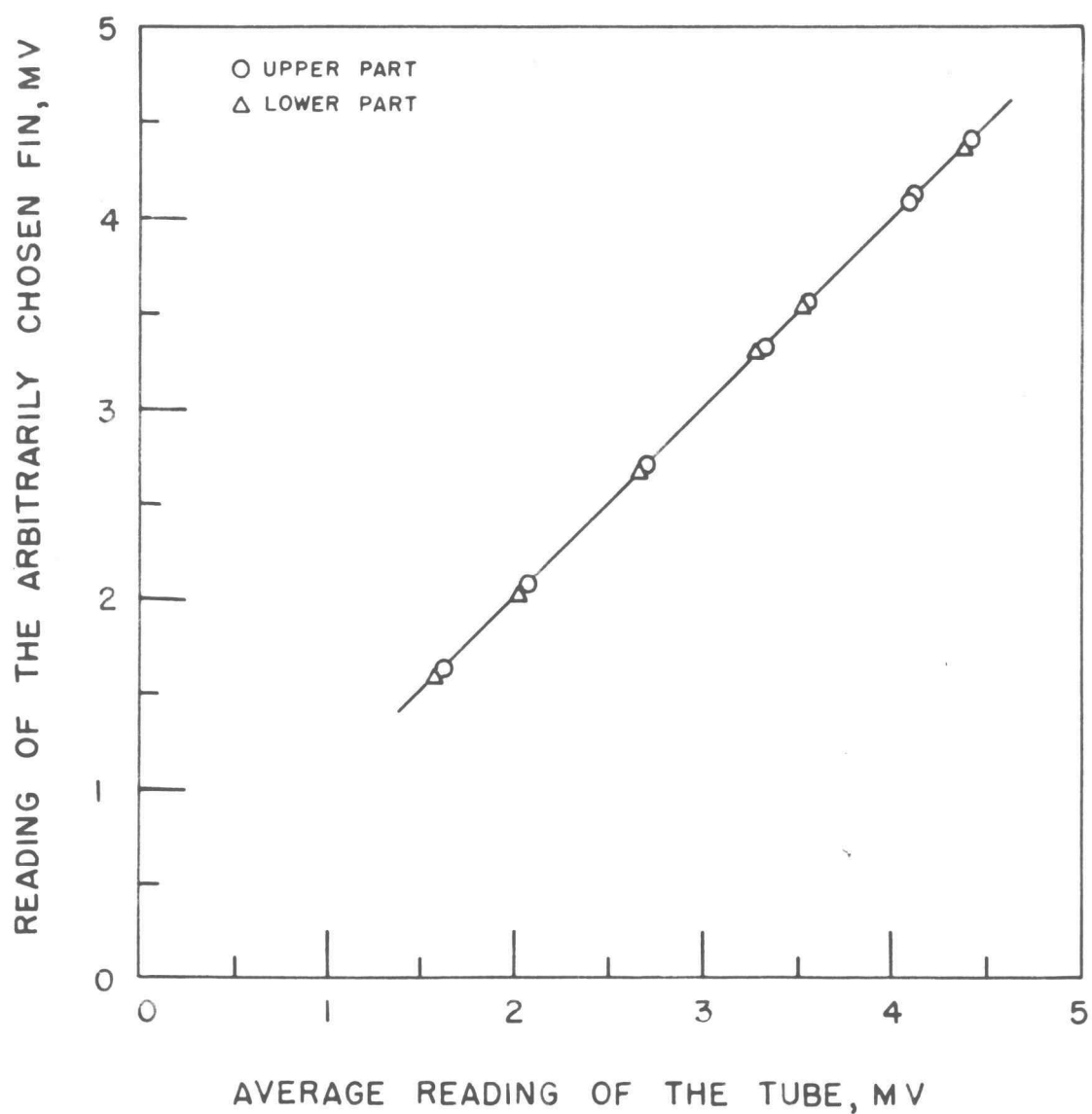
FIGURE 15   TEMPERATURE – AVERAGING CALIBRATION
           – 2⁷/8 INCH FIN DIAMETER AND 1/2
           INCH FIN SPACING
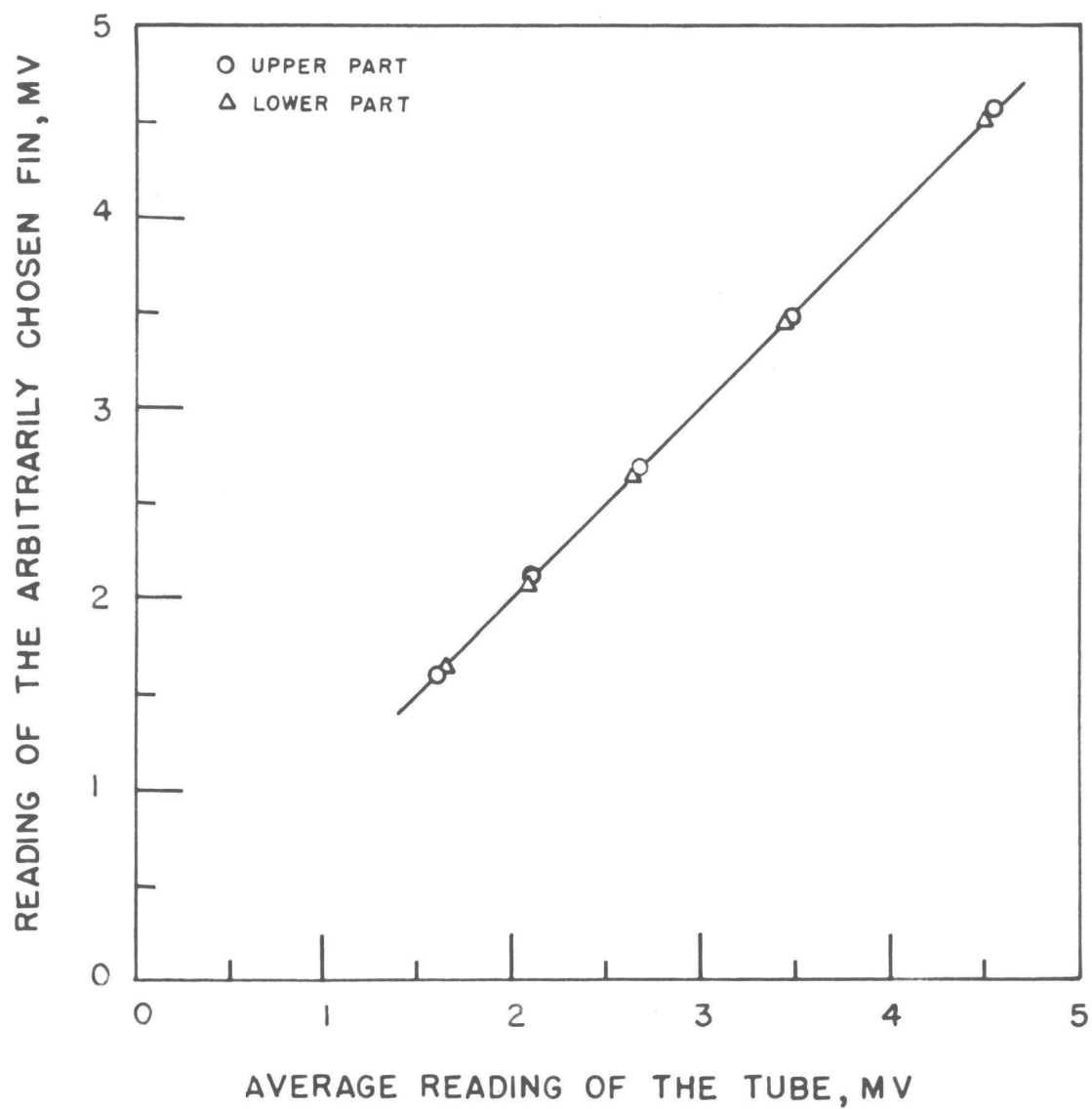
FIGURE 16   TEMPERATURE−AVERAGING CALIBRATION
−2⁷/8 INCH FIN DIAMETER AND 6/8
INCH FIN SPACING
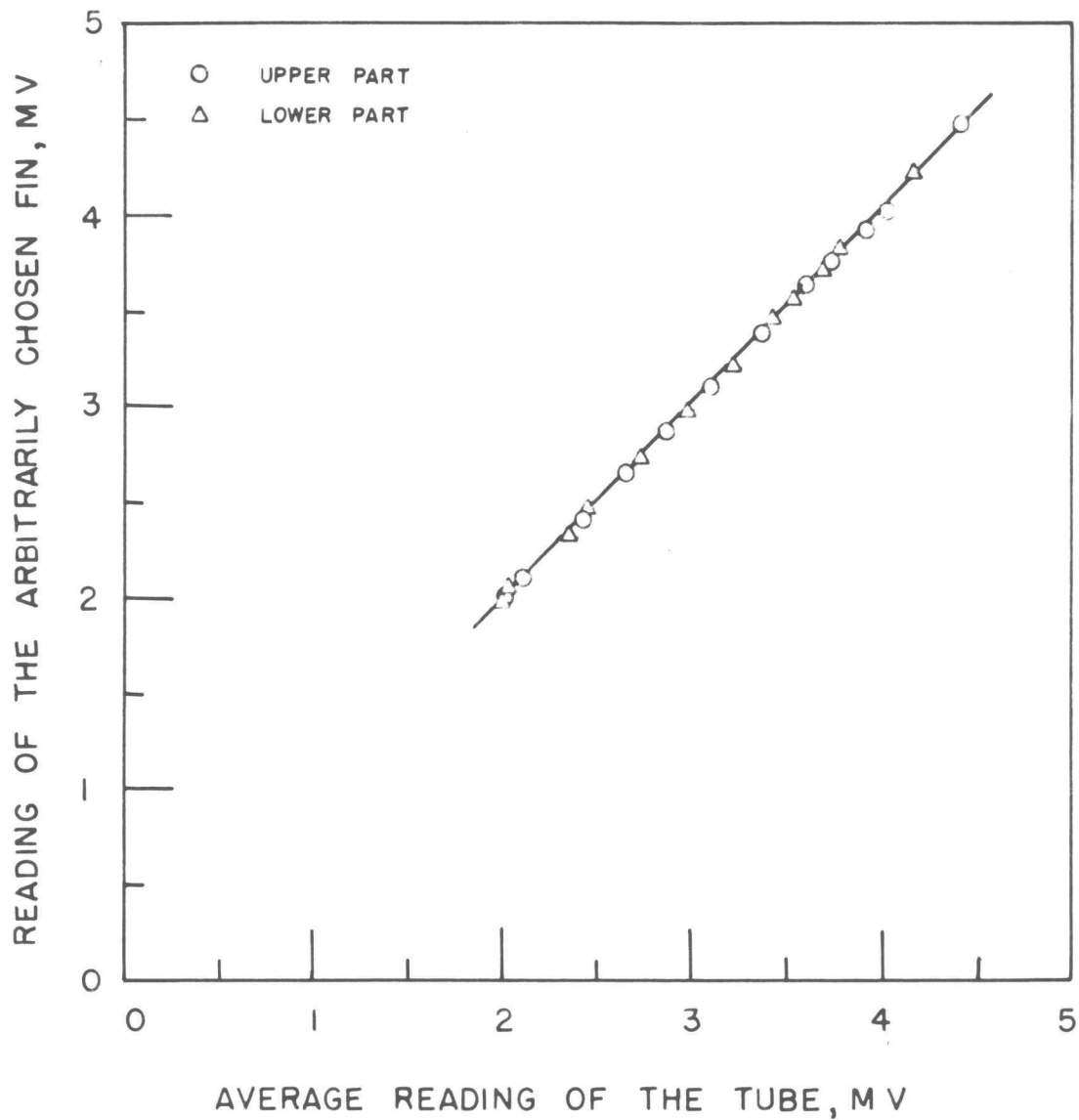
FIGURE 17   TEMPERATURE – AVERAGING   CALIBRATION
– 3⅜ INCH FIN DIAMETER AND 1/4
INCH FIN SPACING
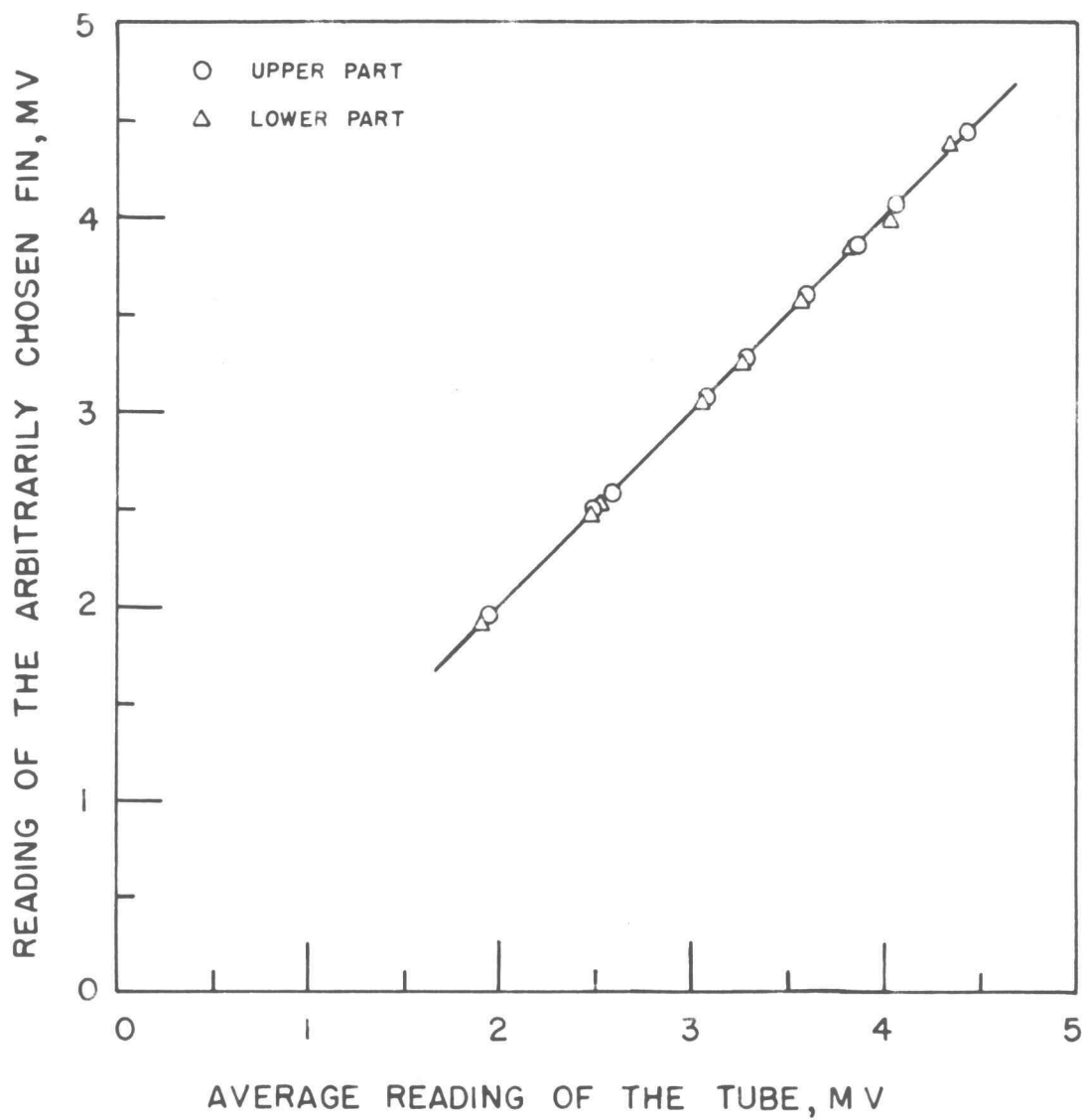
FIGURE 18 TEMPERATURE—AVERAGING CALIBRATION
— $3\frac{3}{8}$ INCH FIN DIAMETER AND 3/8
INCH FIN SPACING
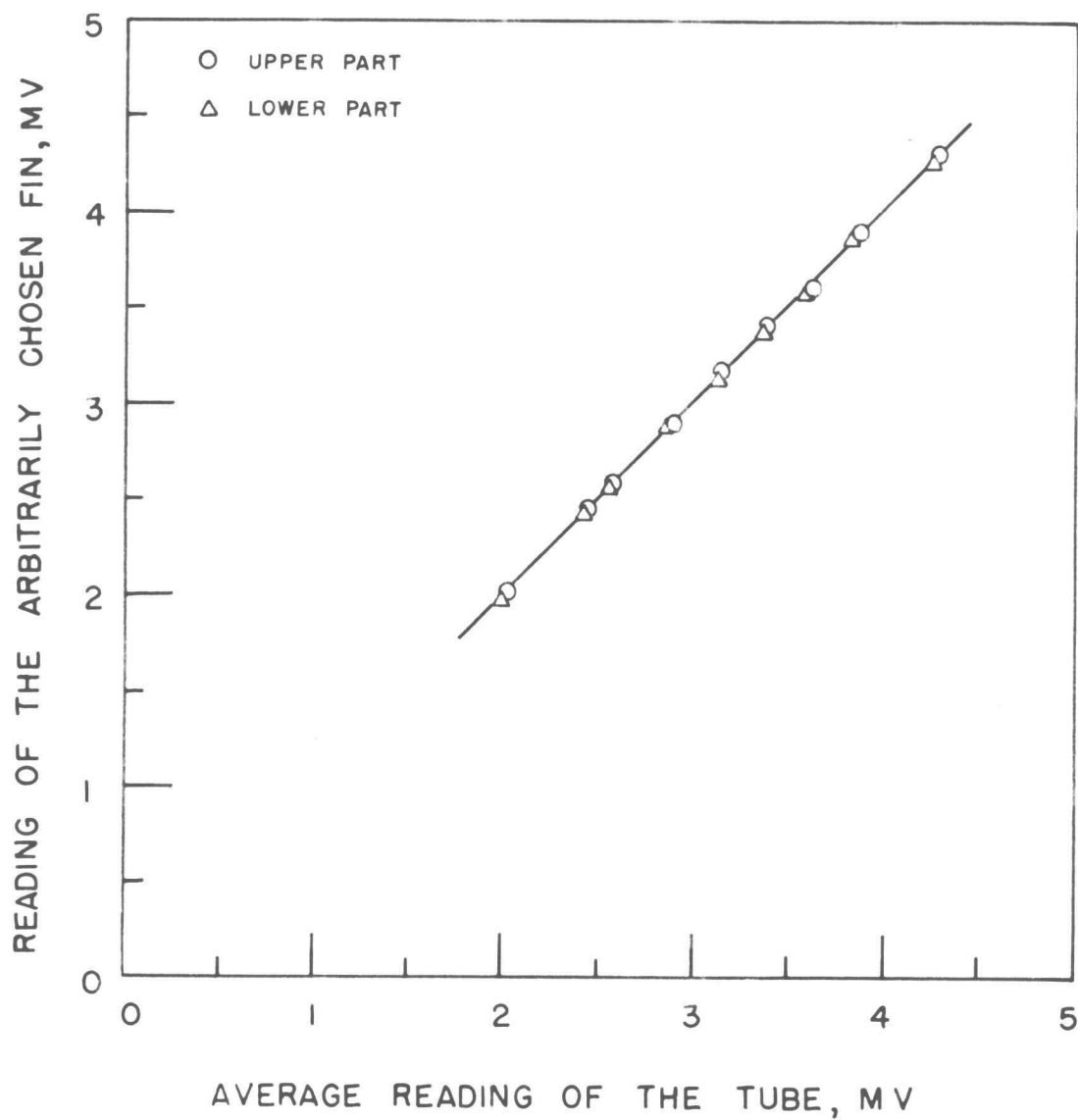
FIGURE 19   TEMPERATURE – AVERAGING   CALIBRATION
– 3³/8 INCH FIN DIAMETER AND 1/2
INCH FIN SPACING
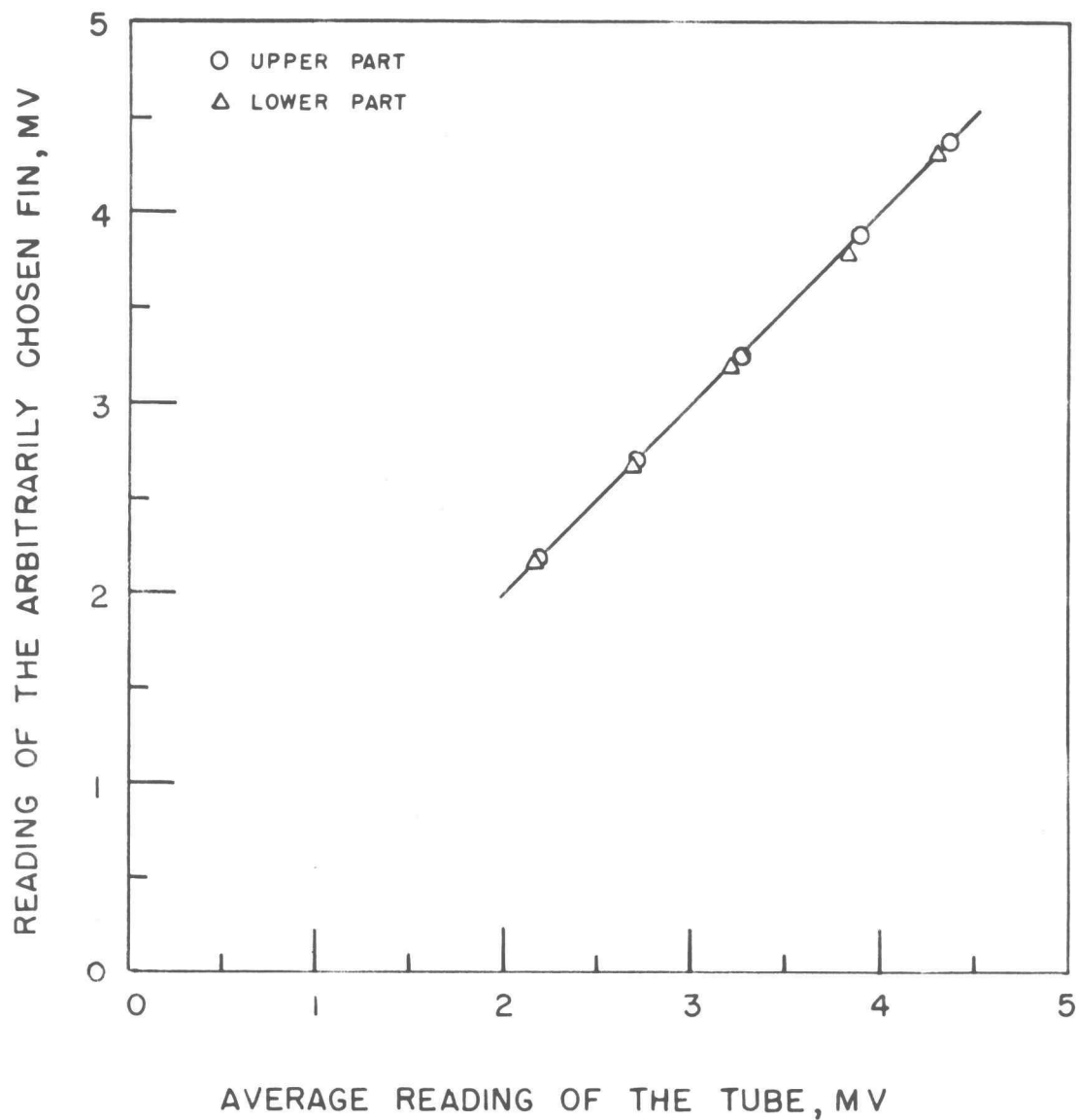
FIGURE 20   TEMPERATURE - AVERAGING   CALIBRATION
            - $3\frac{3}{8}$ INCH FIN DIAMETER AND   6/8
            INCH FIN SPACING
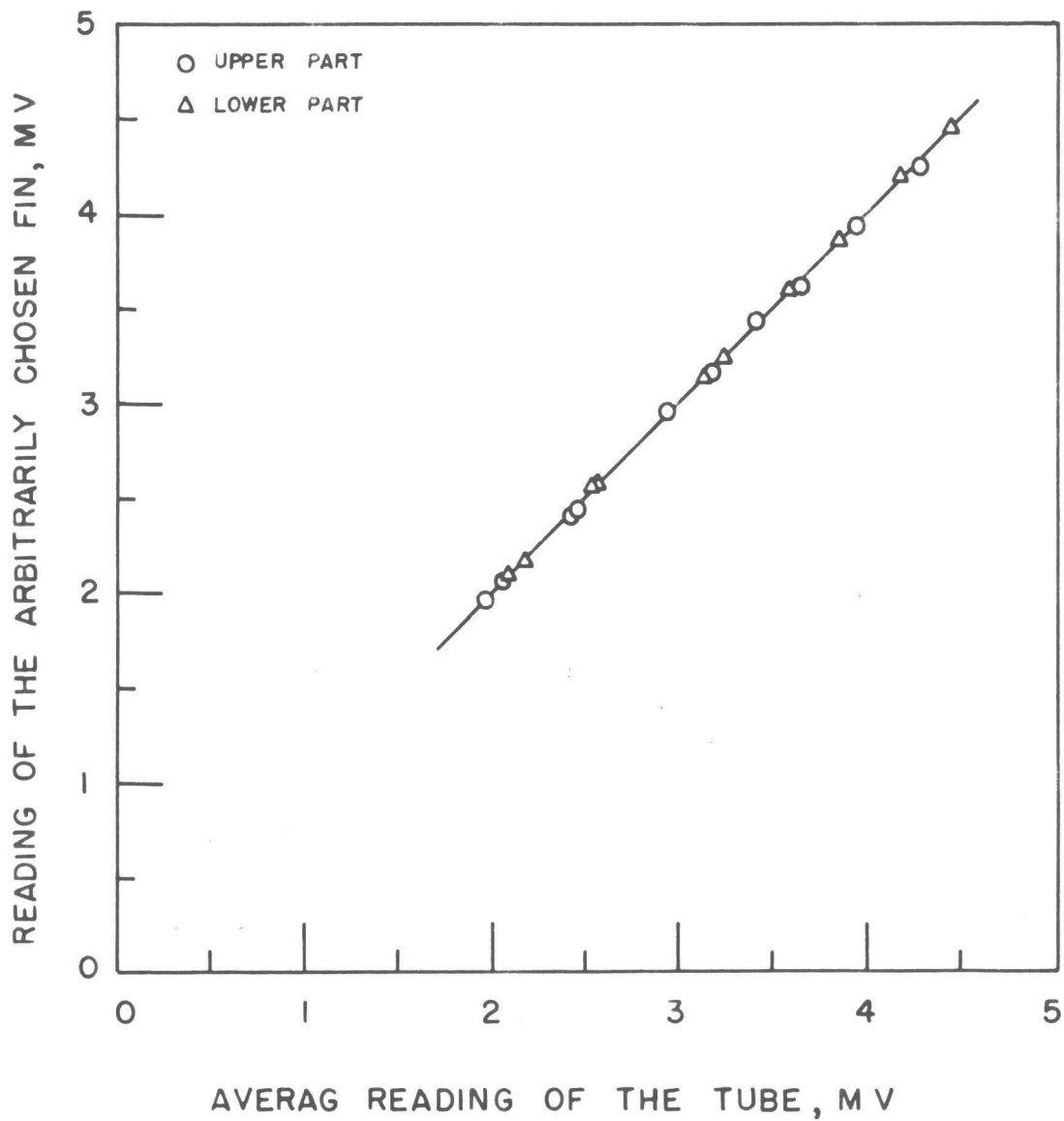
FIGURE 21   TEMPERATURE-AVERAGING   CALIBRATION
            -SQUARE   FINNED   TUBE   WITH   1/4
            INCH   FIN   SPACING
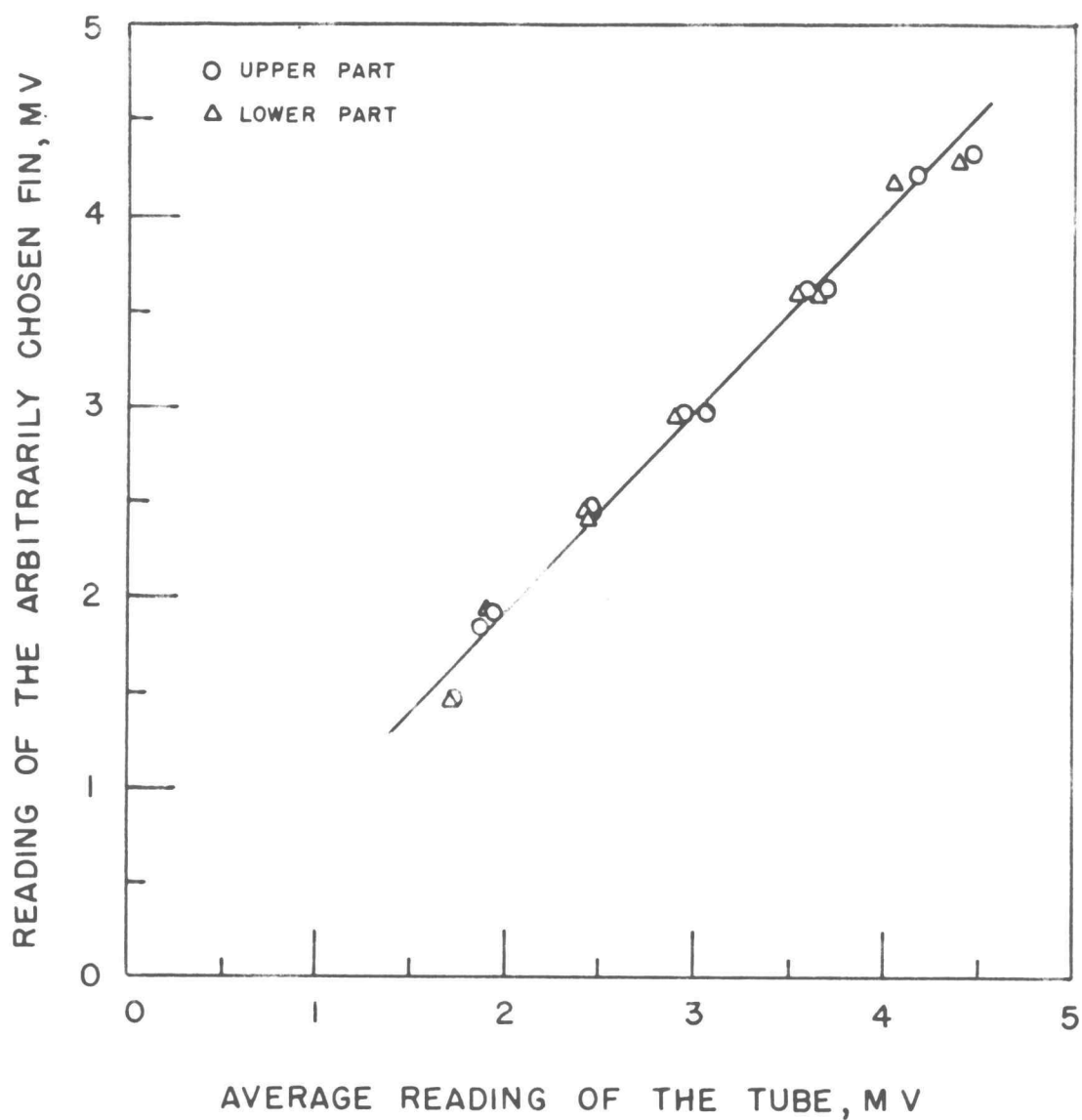
FIGURE 22   TEMPERATURE — AVERAGING   CALIBRATION
— SQUARE   FINNED   TUBE   WITH   3/8
INCH   FIN   SPACING
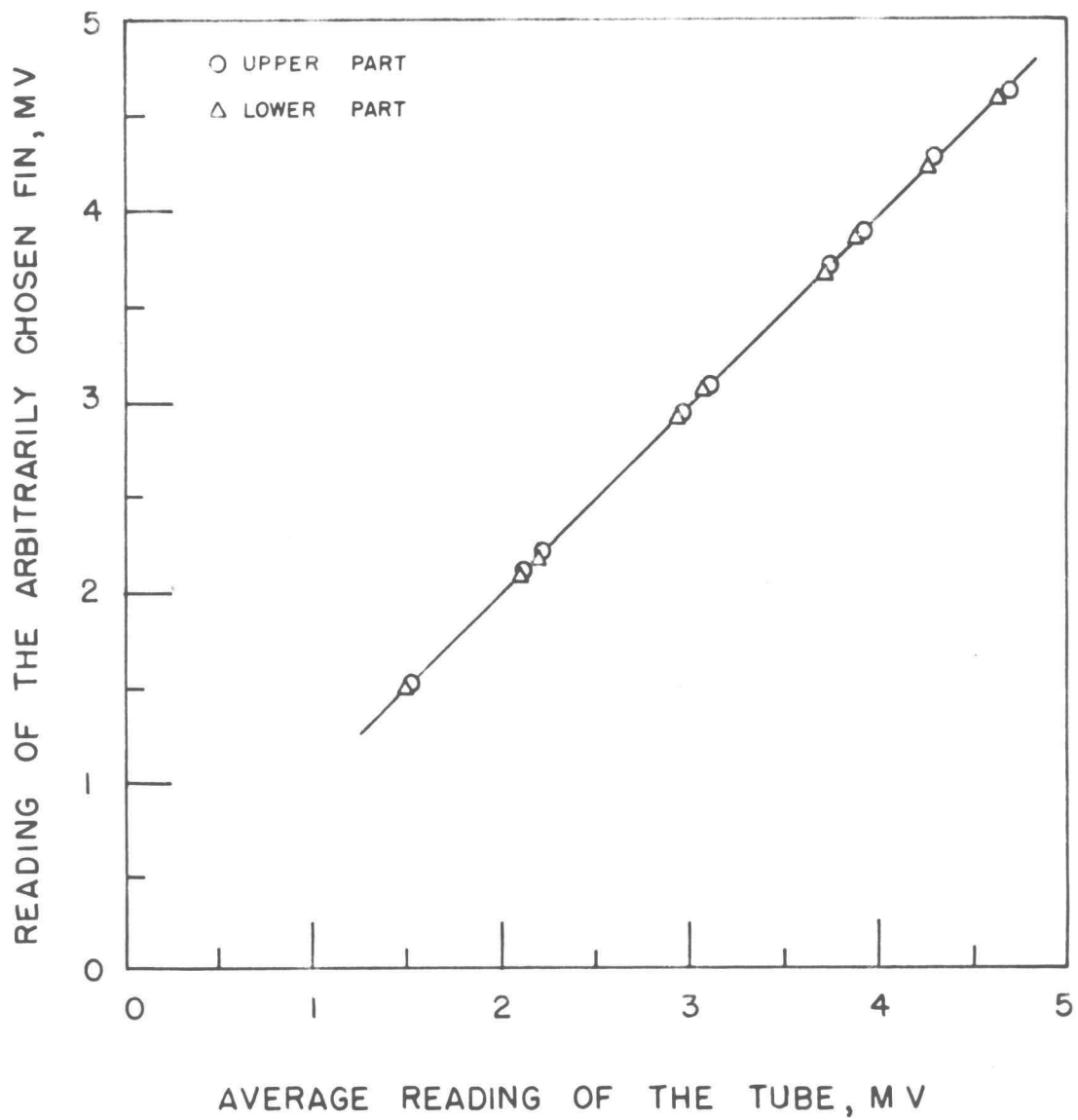
FIGURE 23   TEMPERATURE – AVERAGING   CALIBRATION
– SQUARE   FINNED   TUBE   WITH   1/2
INCH   FIN   SPACING
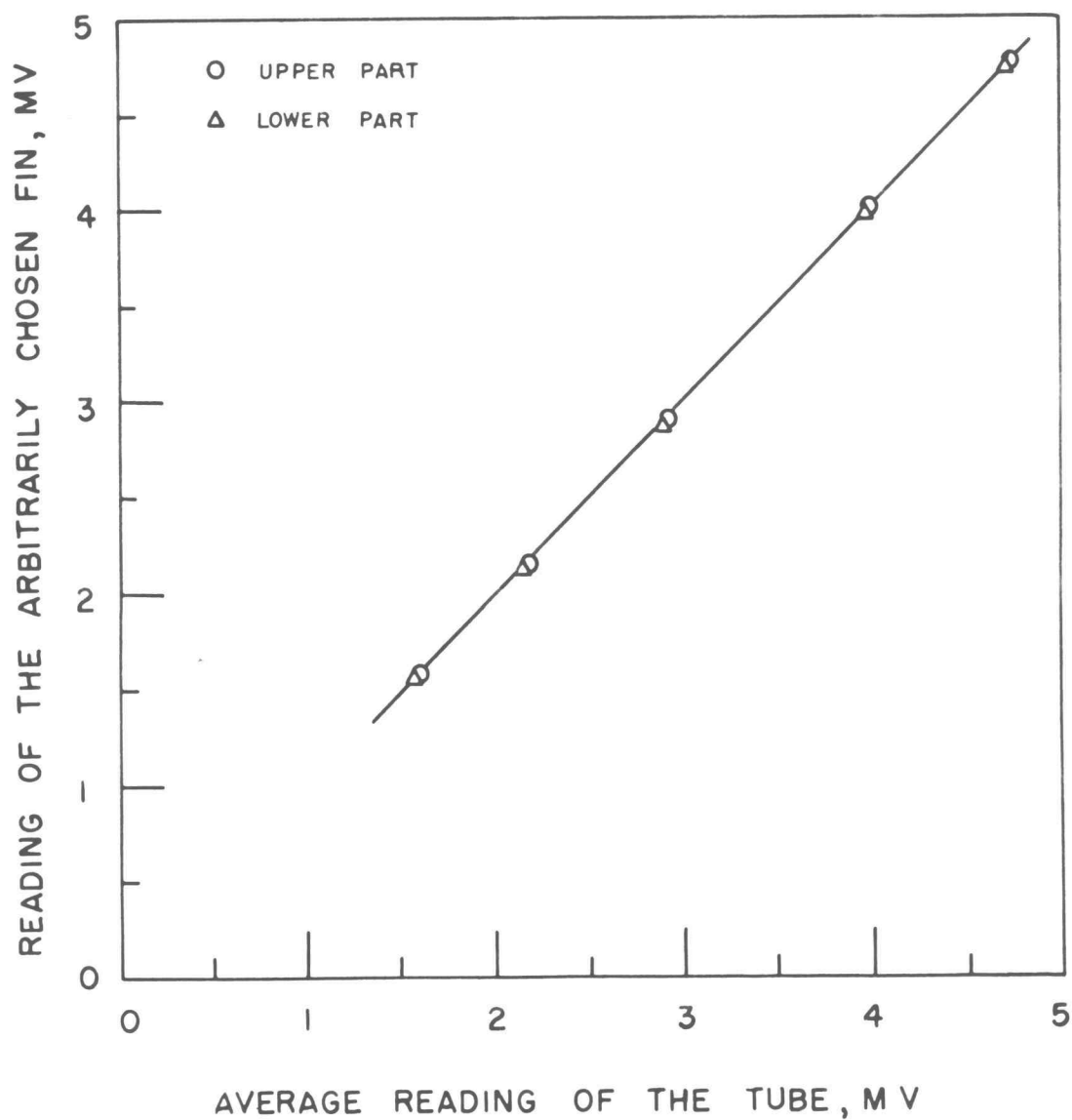
FIGURE 24   TEMPERATURE – AVERAGING   CALIBRATION
– SQUARE   FINNED   TUBE   WITH   6/8
INCH   FIN   SPACING
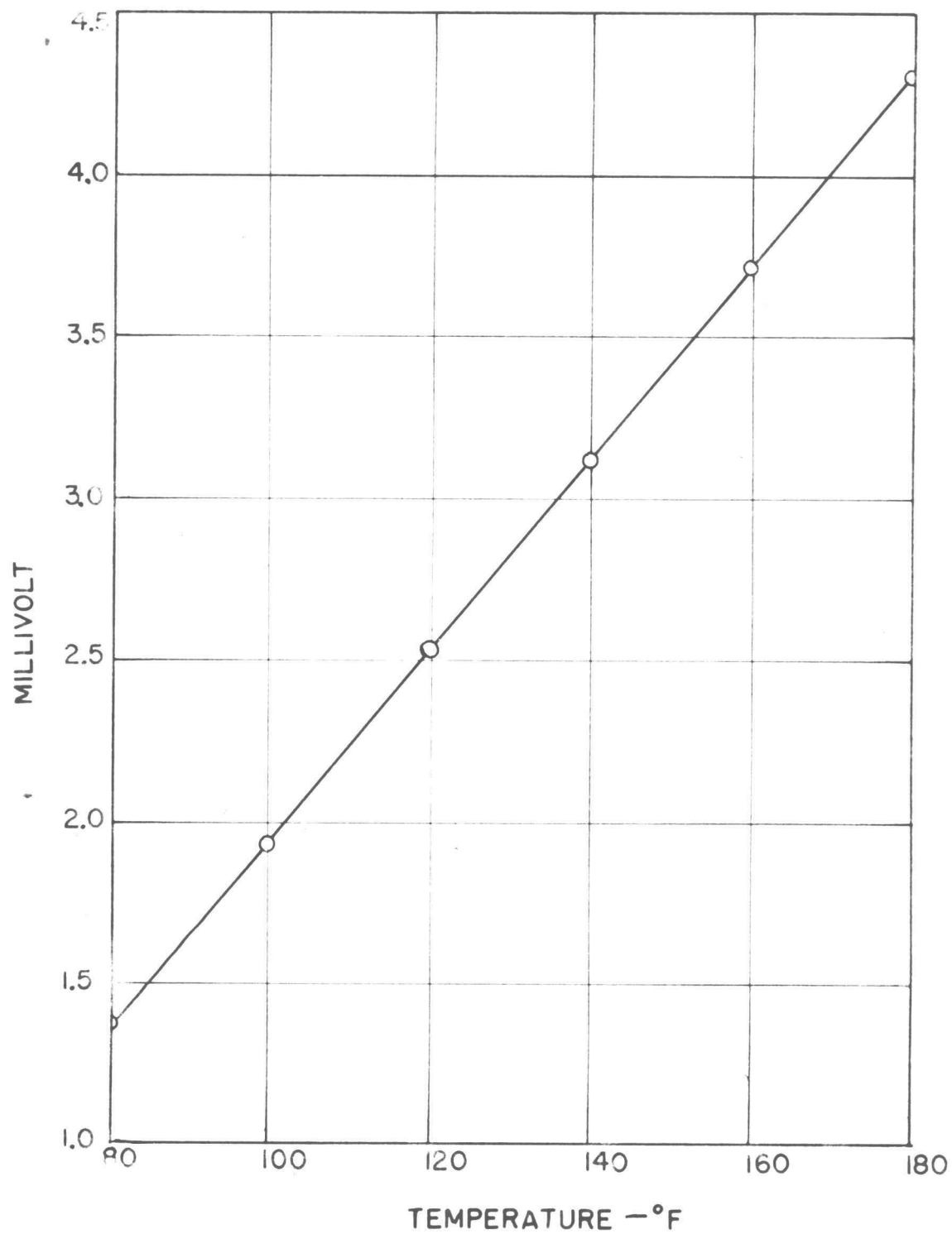
FIGURE 25 EMF – TEMPERATURE CONVERSION TABLE
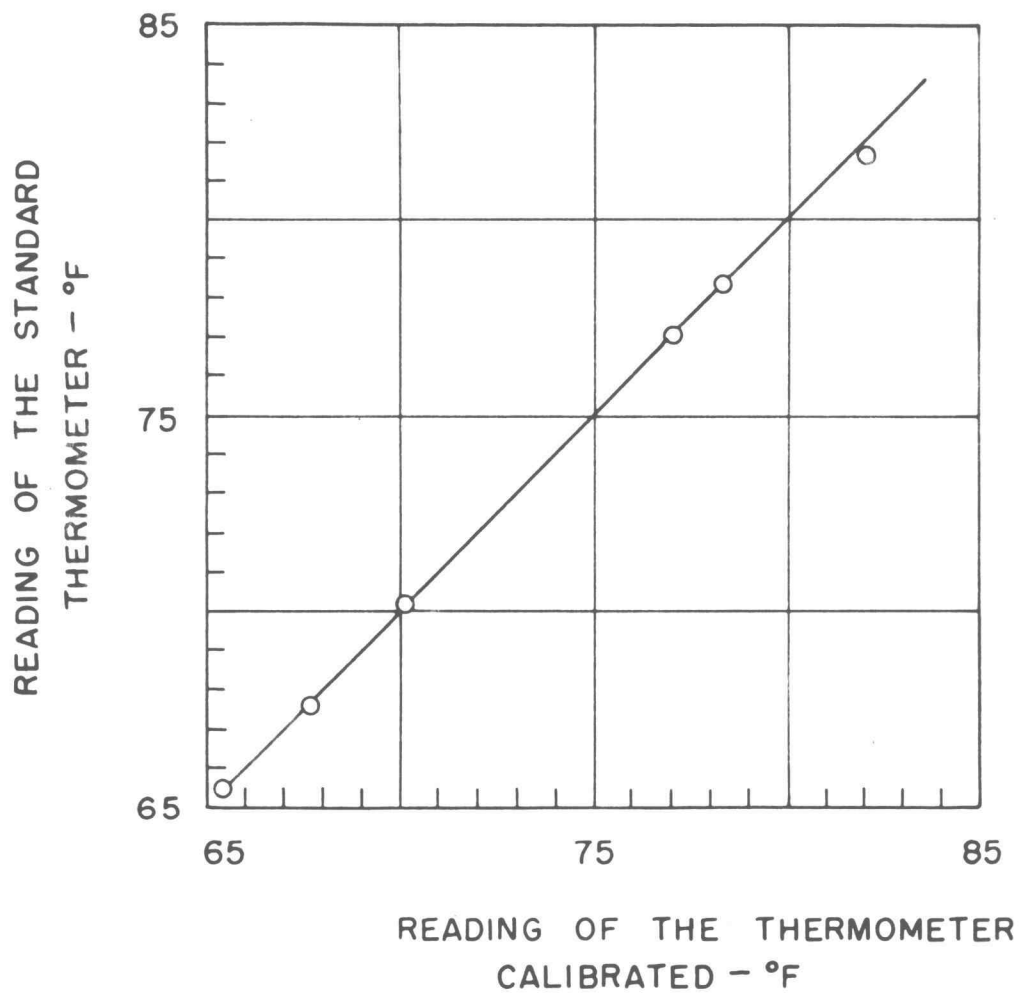
FIGURE 26   THERMOMETER   CALIBRATION   CURVE
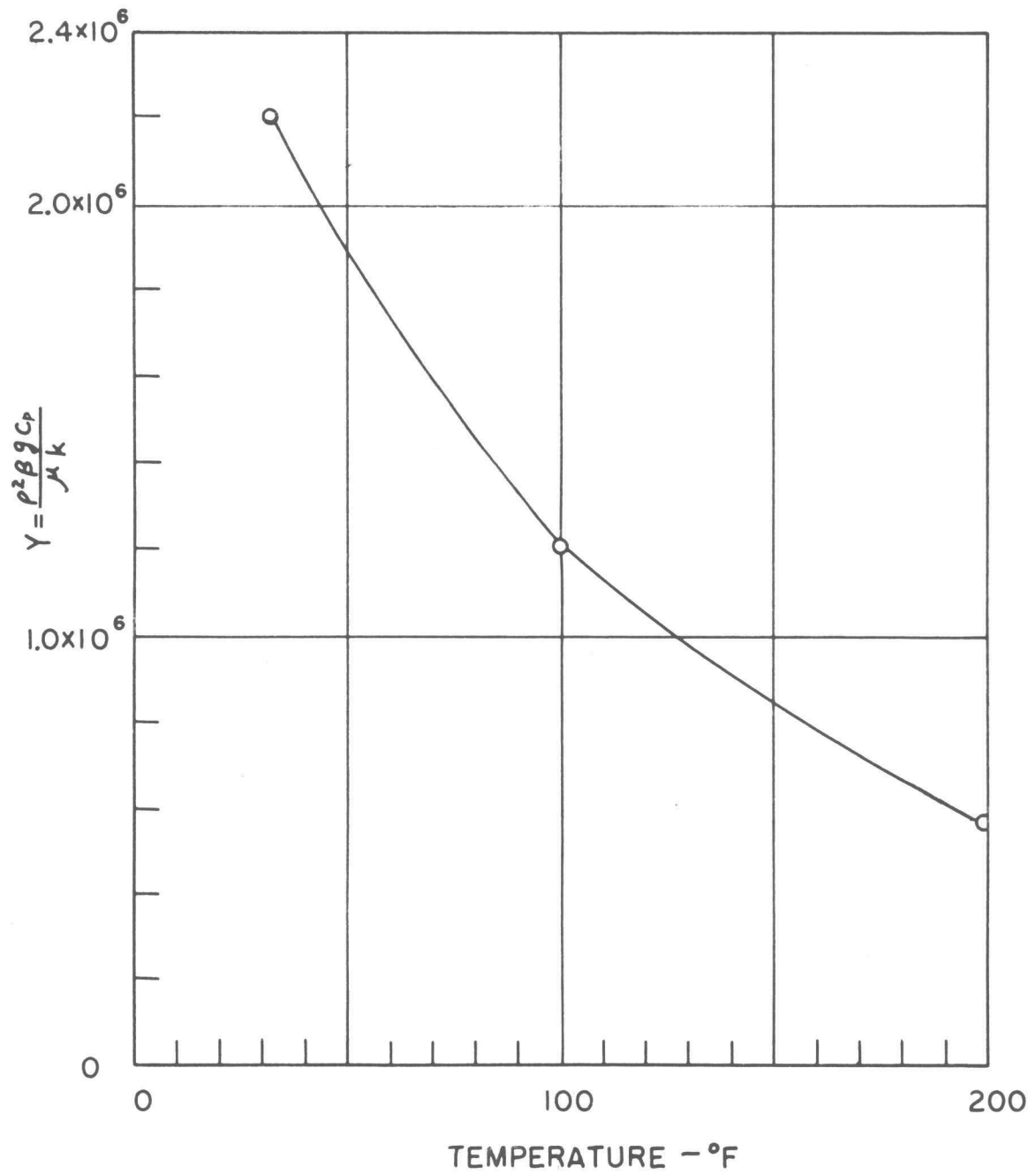
FIGURE 27 PHYSICAL PROPERTY OF AIR
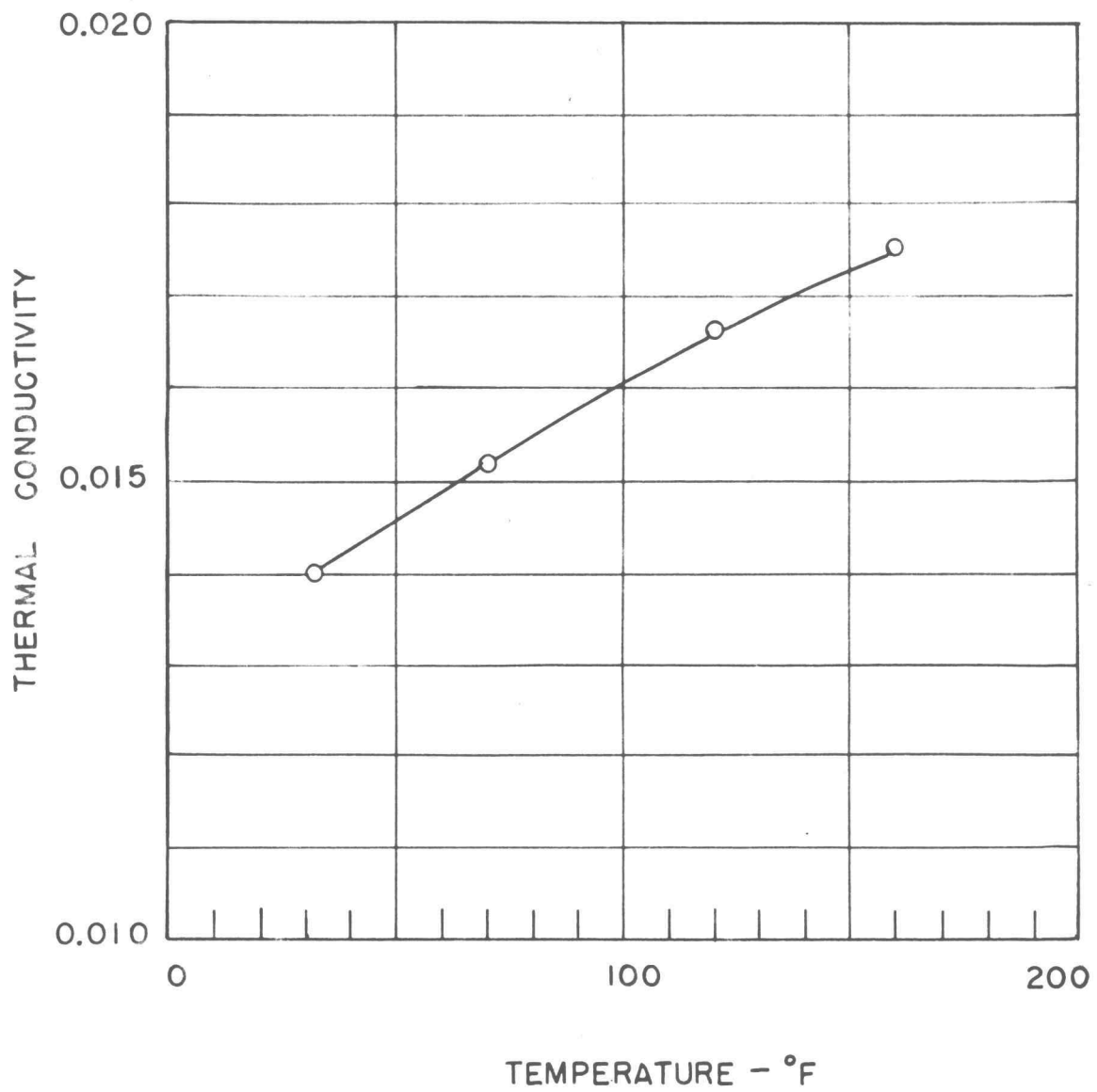
FIGURE 28   THERMOL CONDUCTIVITY
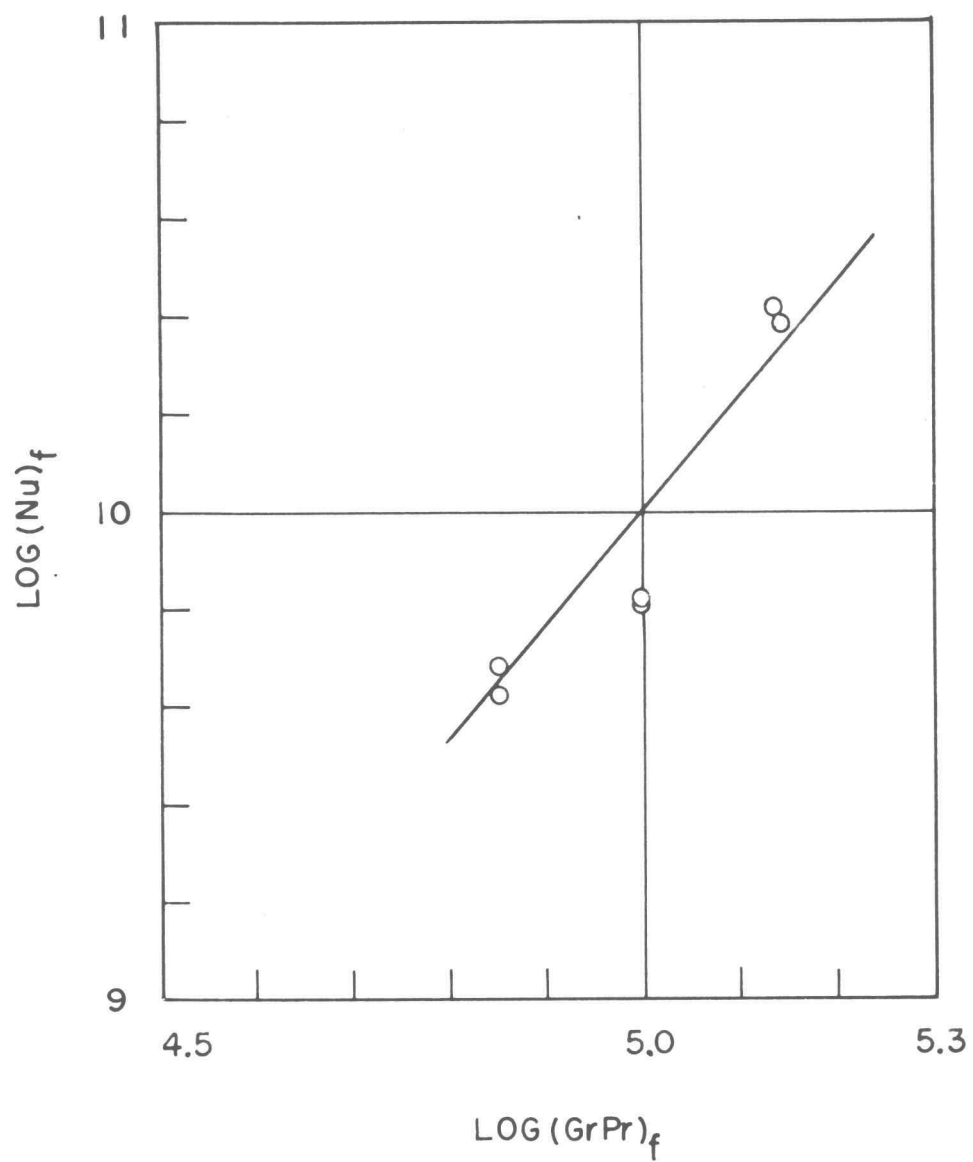
FIGURE 29   NUSSELT   NUMBER   AS   A   FUNCTION   OF
RAYLEIGH   NUMBER   FOR   HORIZONTAL   TUBE
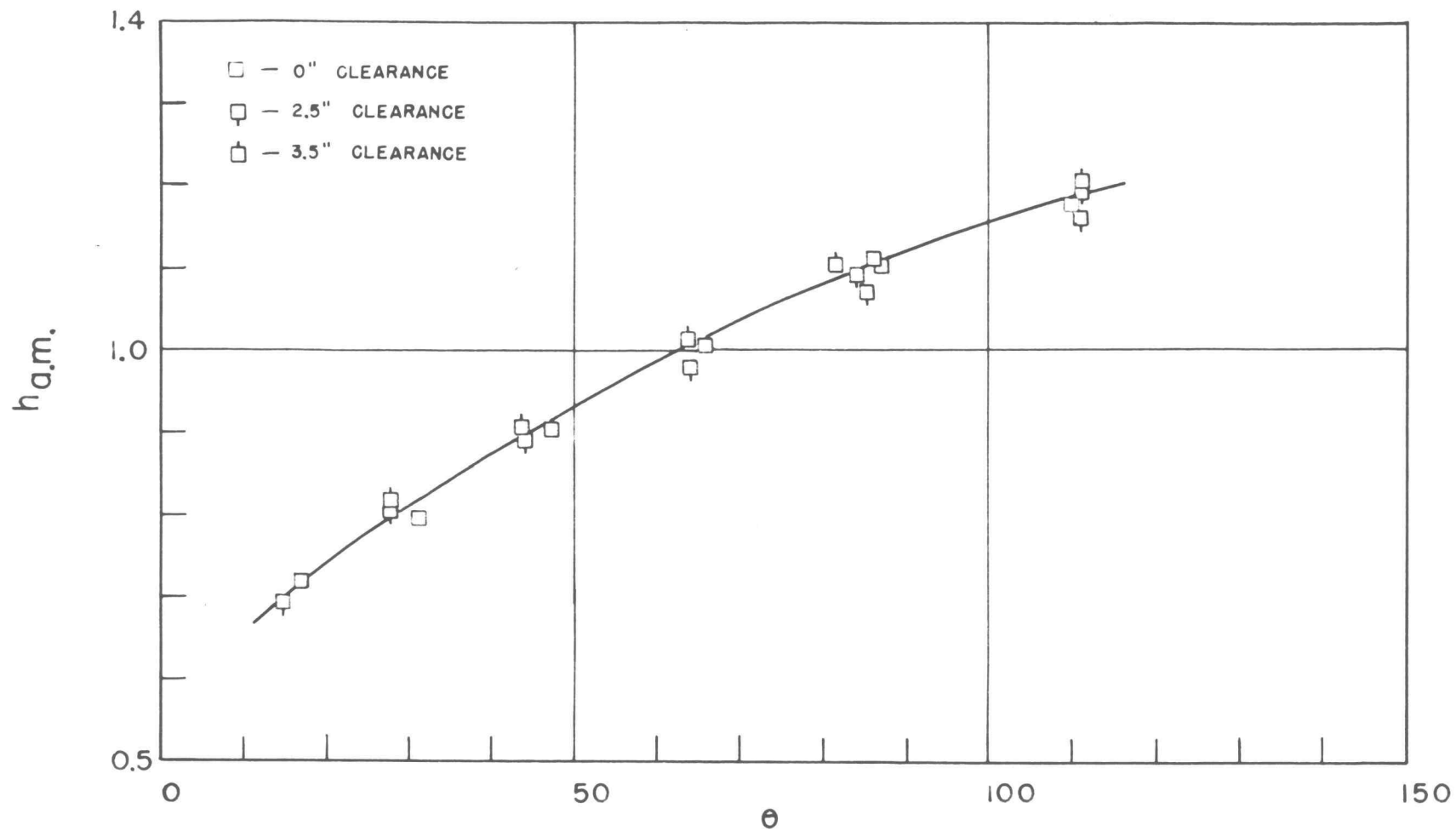
FIGURE 30 EFFECT OF CLEARANCE
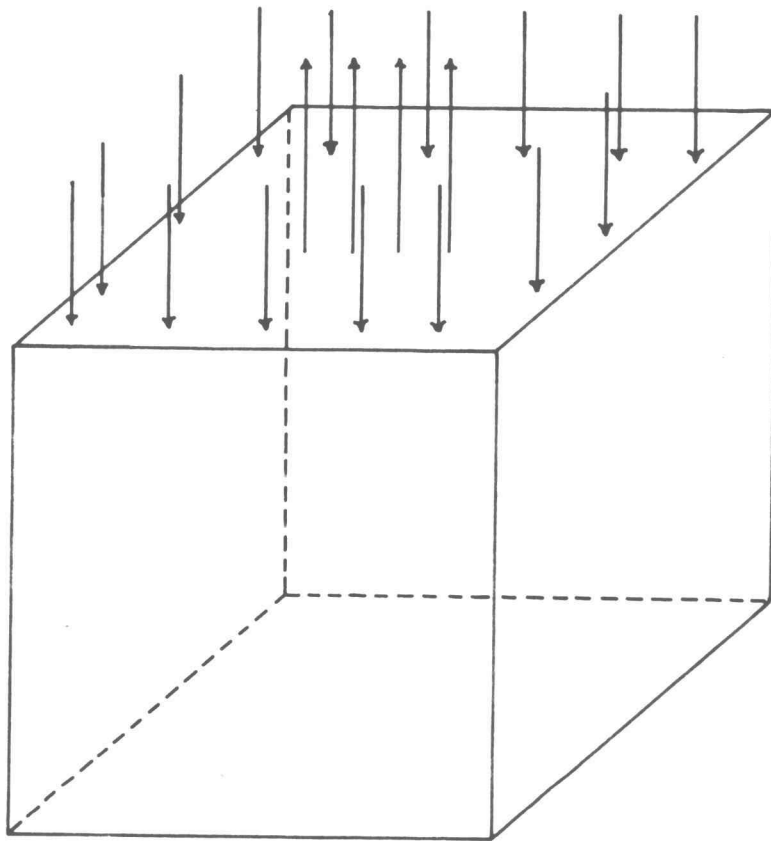
FIGURE 31   FLOW   PATTERN   OF   AIR   CIRCULATION
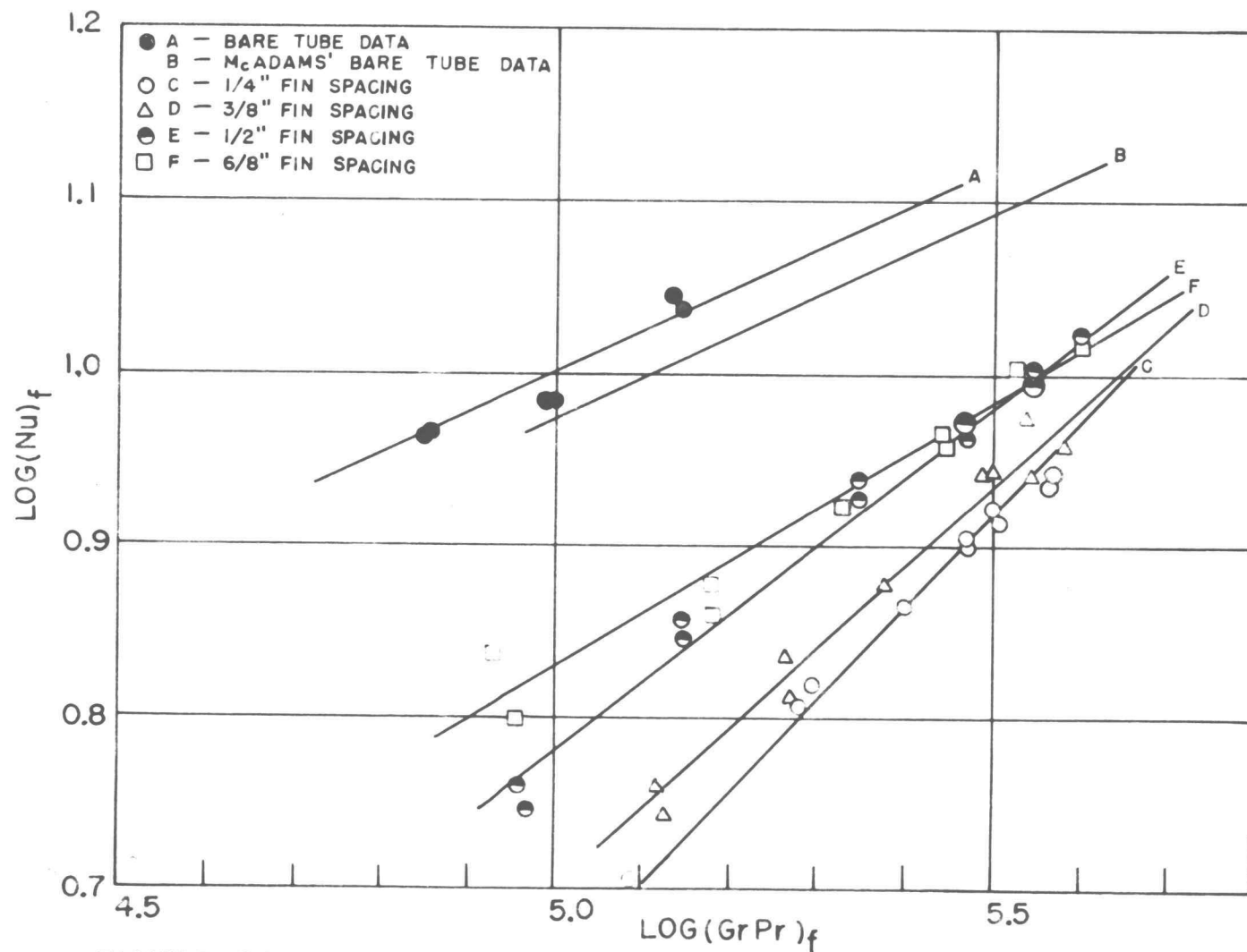
FIGURE 32 NUSSELT NUMBER AS A FUNCTION OF RAYLEIGH
NUMBER — 2 3/8 INCH FIN DIAMETER
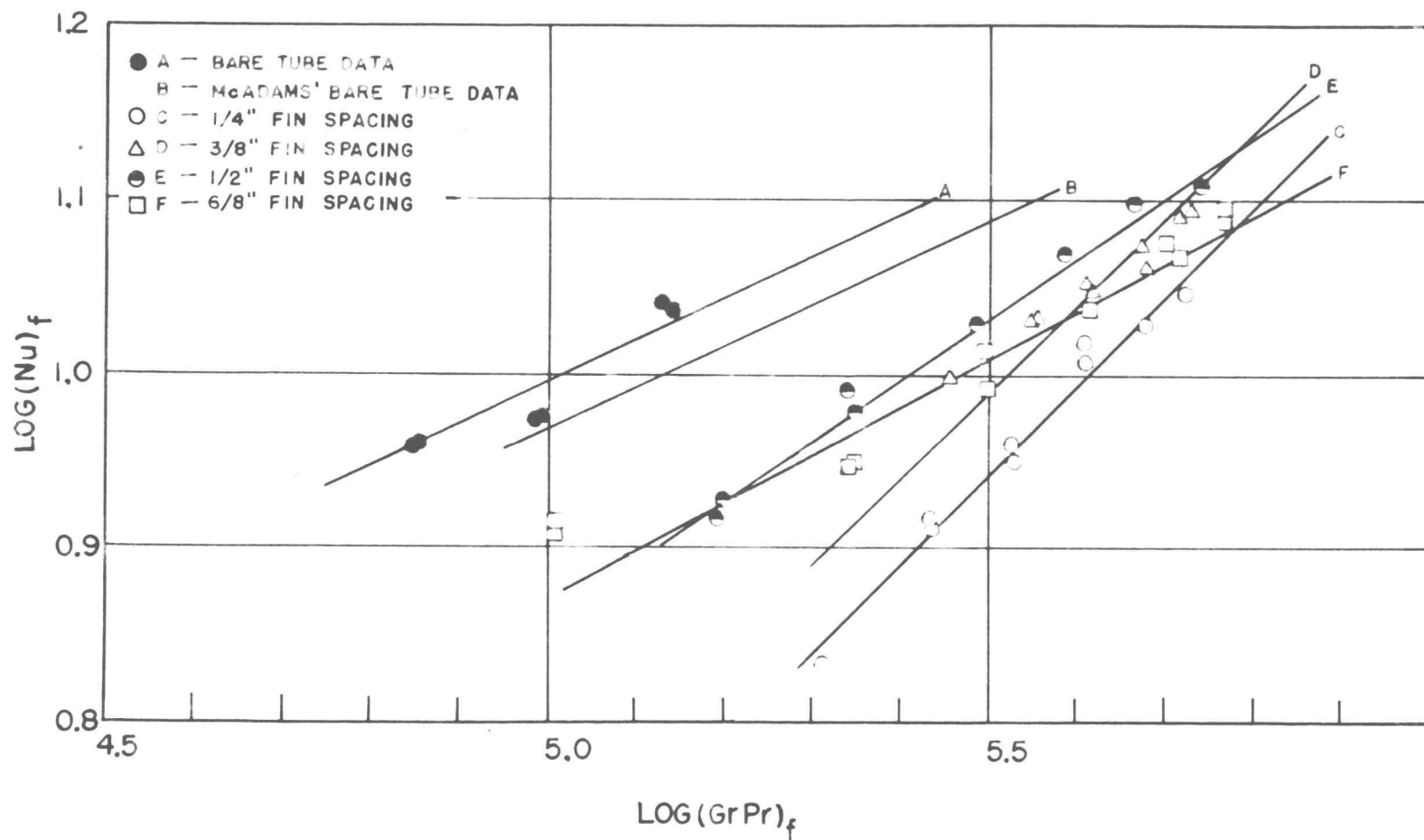
FIGURE 33   NUSSELT NUMBER AS A FUNCTION OF RAYLEIGH
NUMBER — $2\frac{7}{8}$ INCH FIN DIAMETER
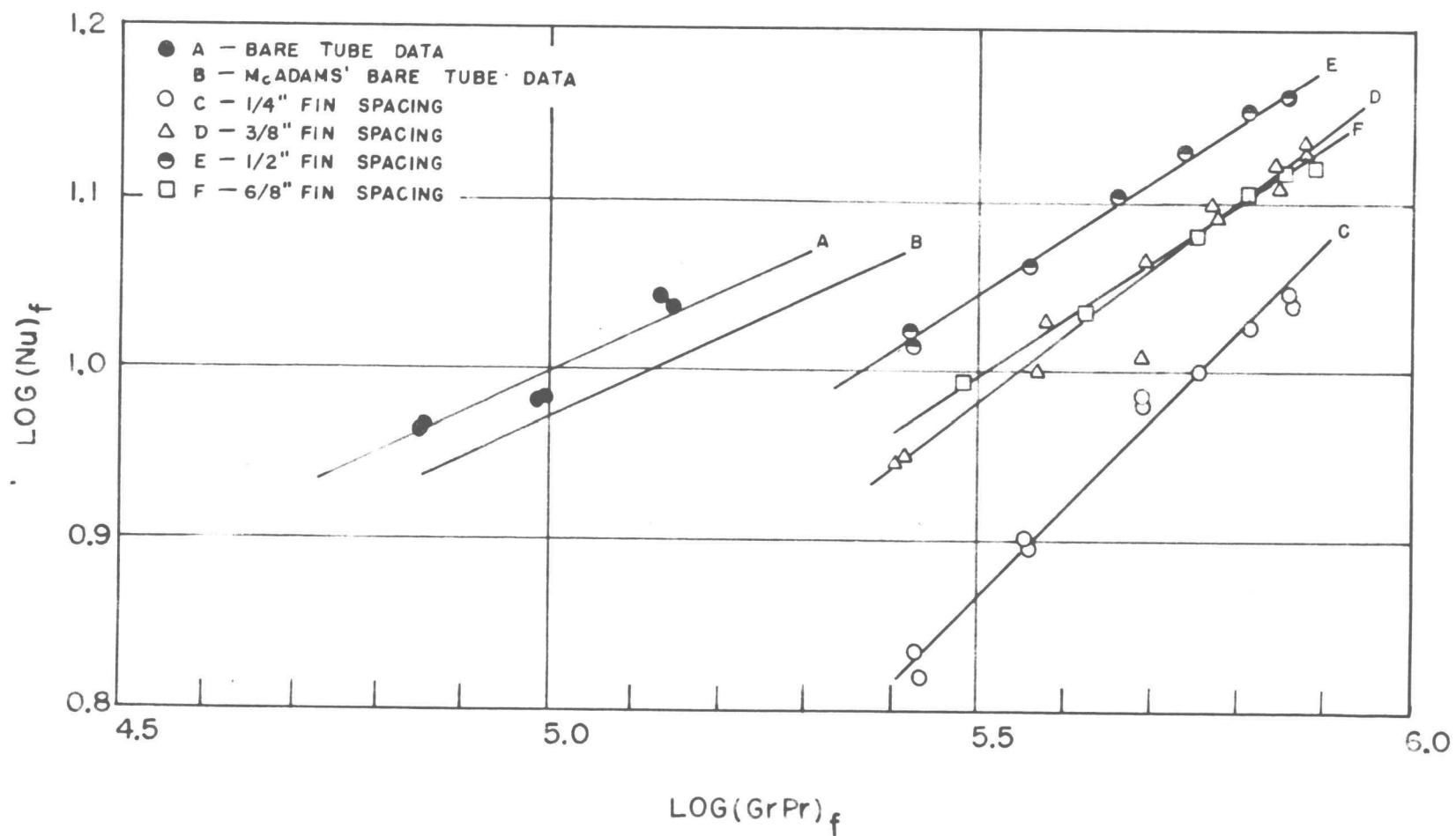
FIGURE 34   NUSSELT NUMBER AS A FUNCTION OF RAYLEIGH
NUMBER — 3 $\frac{3}{8}$ INCH FIN DIAMETER
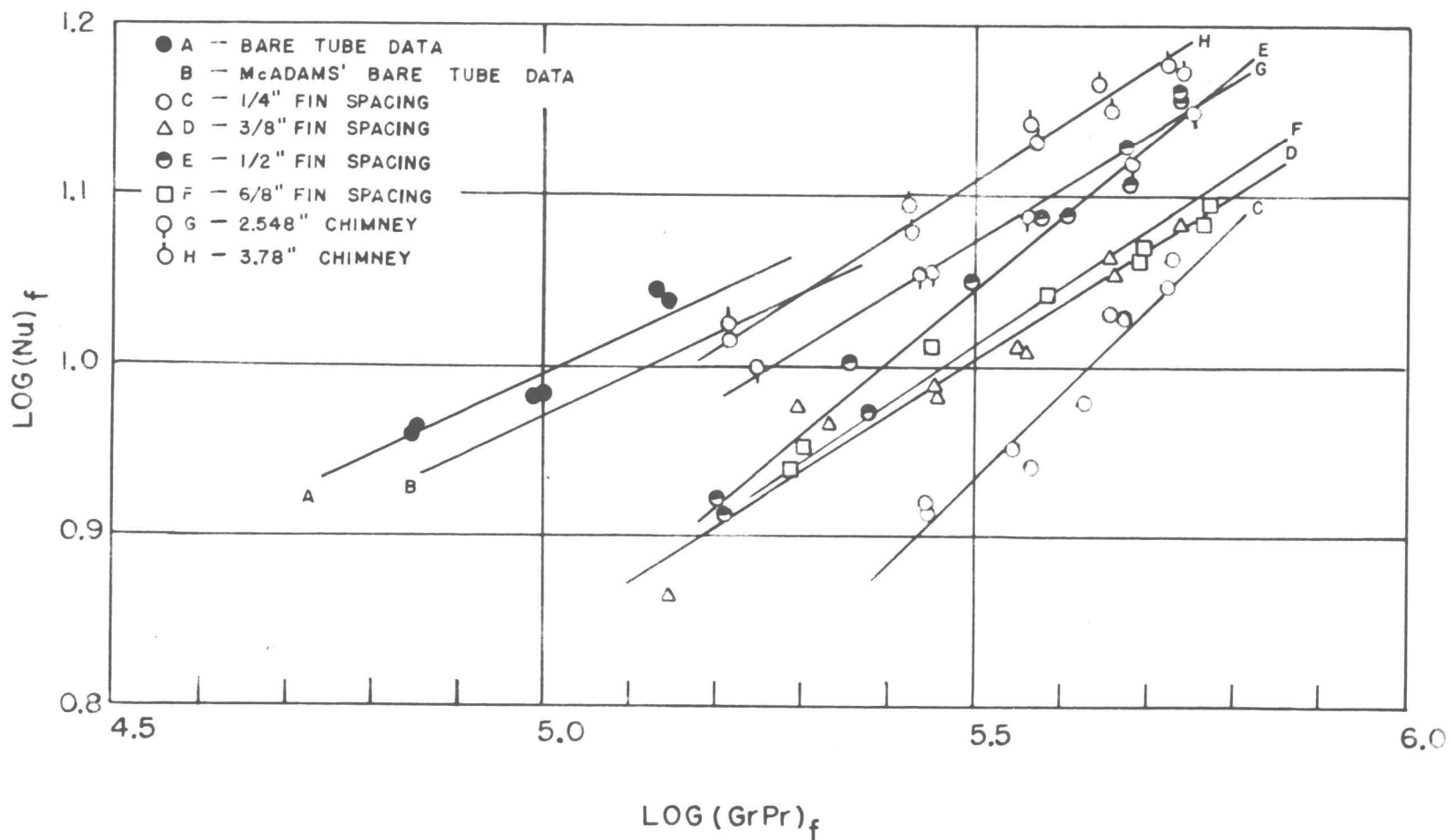
FIGURE 35 NUSSELT NUMBER AS A FUNCTION OF RAYLEIGH
NUMBER - SQUARE FINNED TUBES WITH AND
WITHOUT CHIMNEY
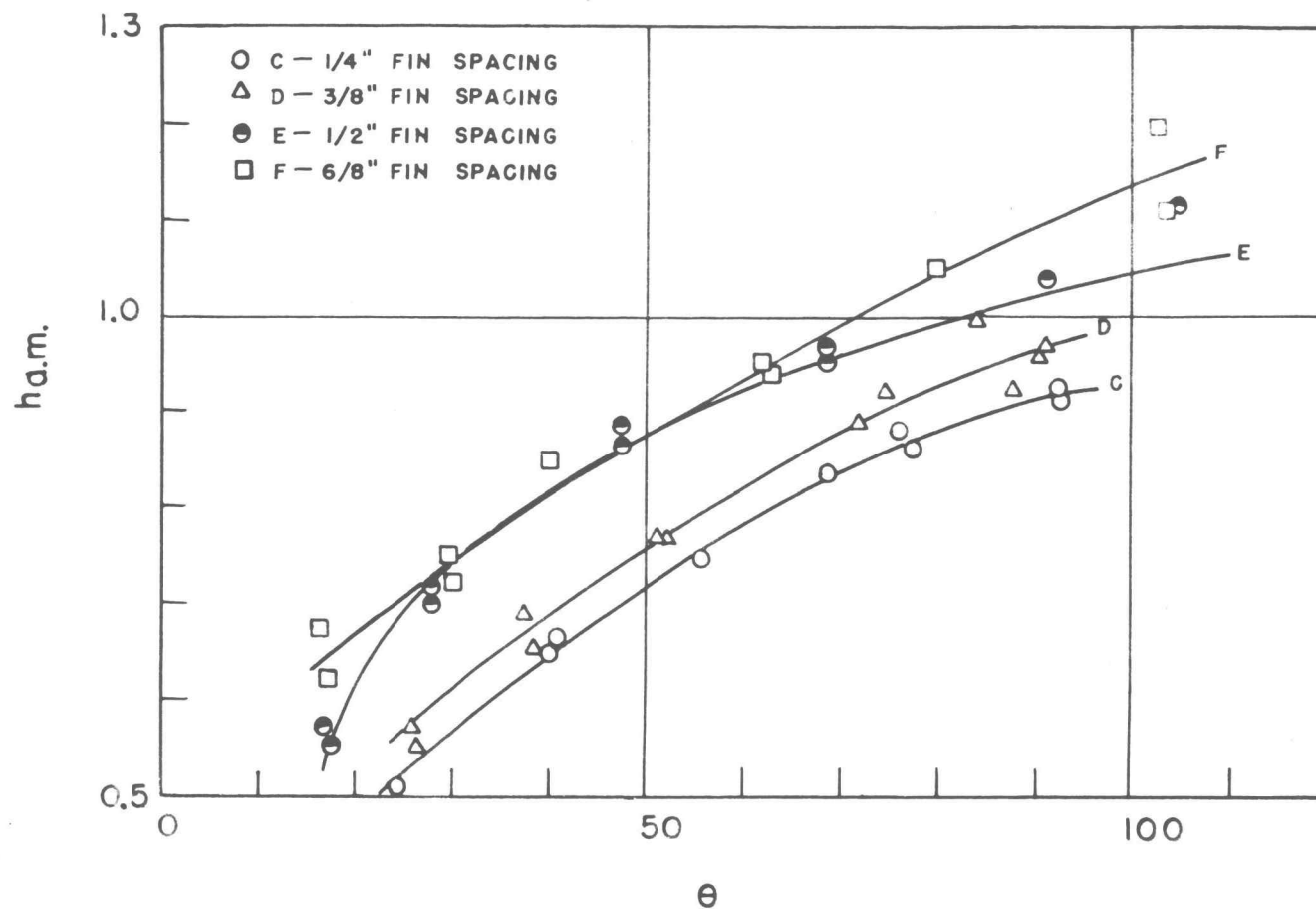
FIGURE 36   HEAT TRANSFER COEFFICIENT − 2 3/8 INCH
FIN DIAMETER
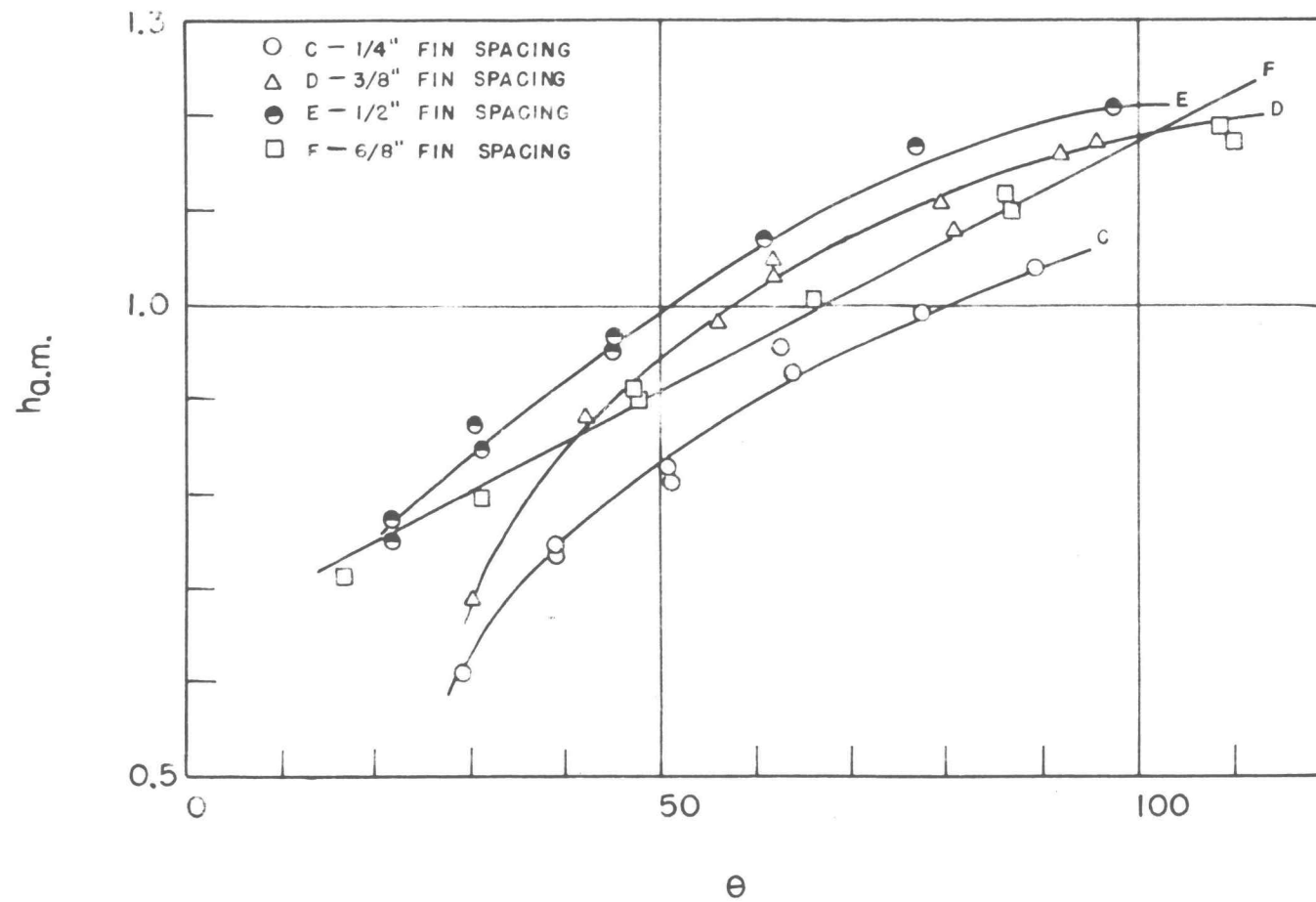
FIGURE 37   HEAT TRANSFER COEFFICIENT – 2⅞ INCH
FIN DIAMETER
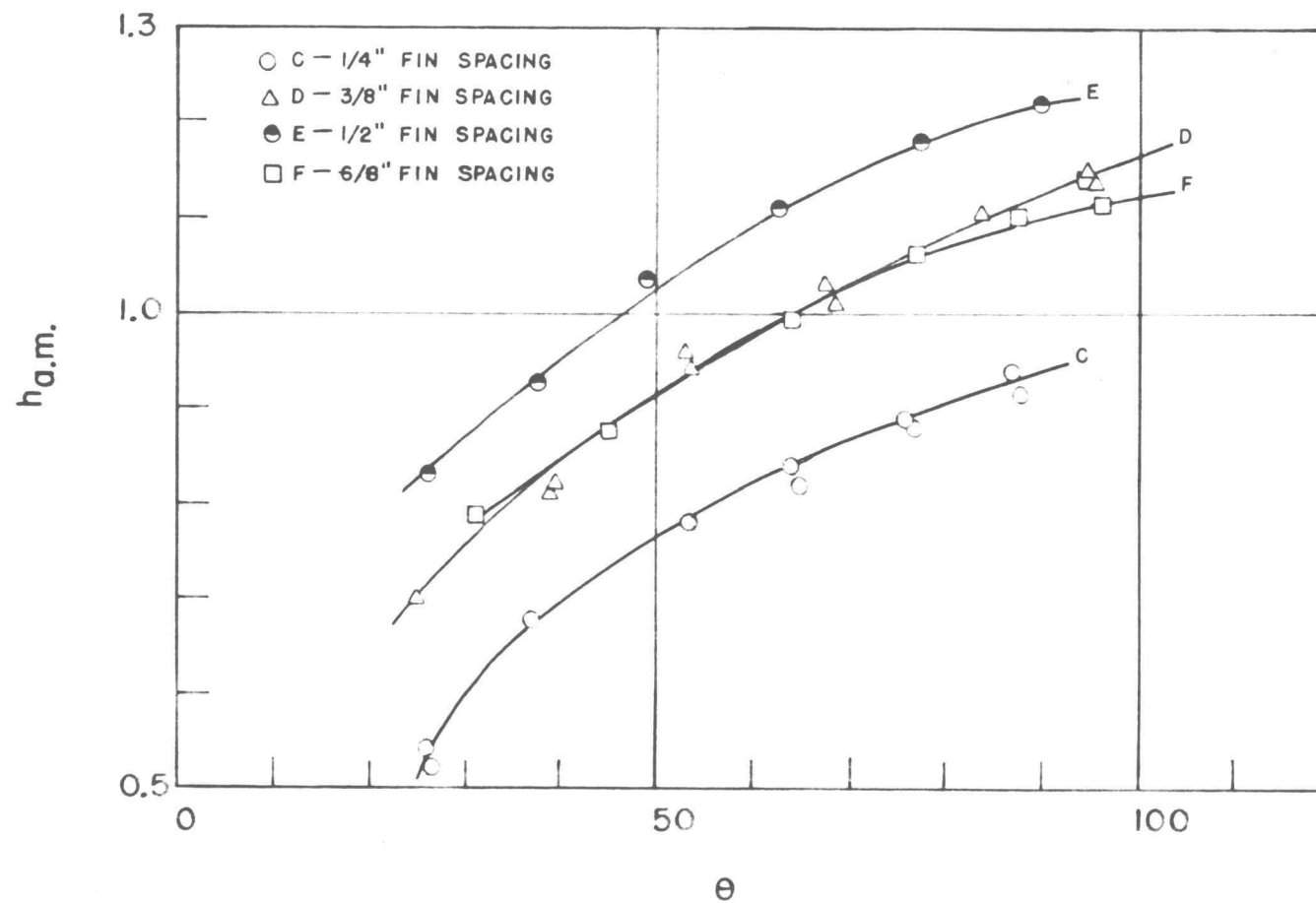
FIGURE 38   HEAT TRANSFER COEFFICIENT – $3\frac{3}{8}$ INCH
FIN   DIAMETER
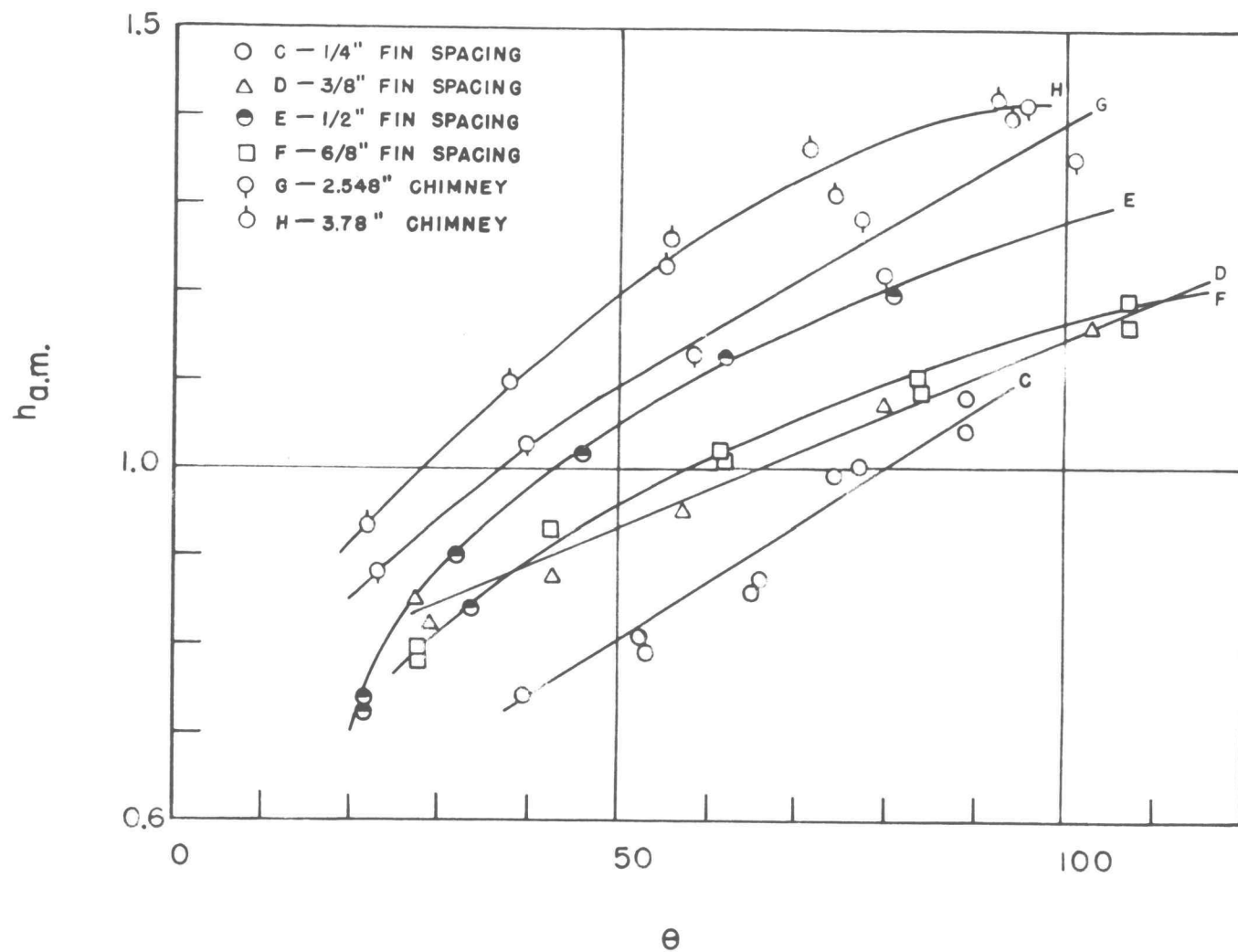
FIGURE 39 HEAT TRANSFER COEFFICIENT — SQUARE FINNED
TUBES WITH AND WITHOUT CHIMNEY
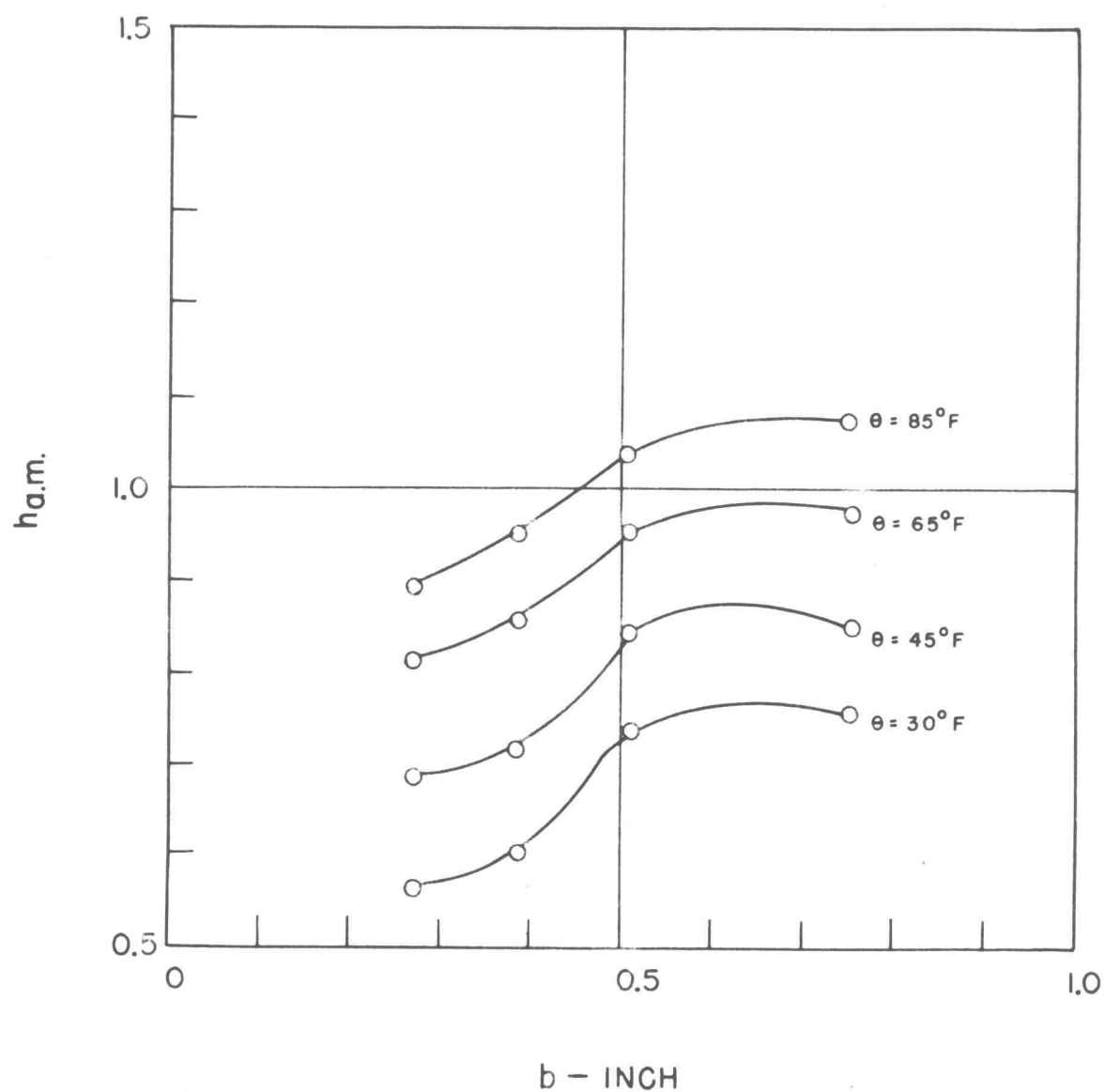
FIGURE 40   HEAT   TRANSFER   COEFFICIENT   AS   A
FUNCTION   OF   FIN   SPACING − 2 3/8
INCH   FIN   DIAMETER
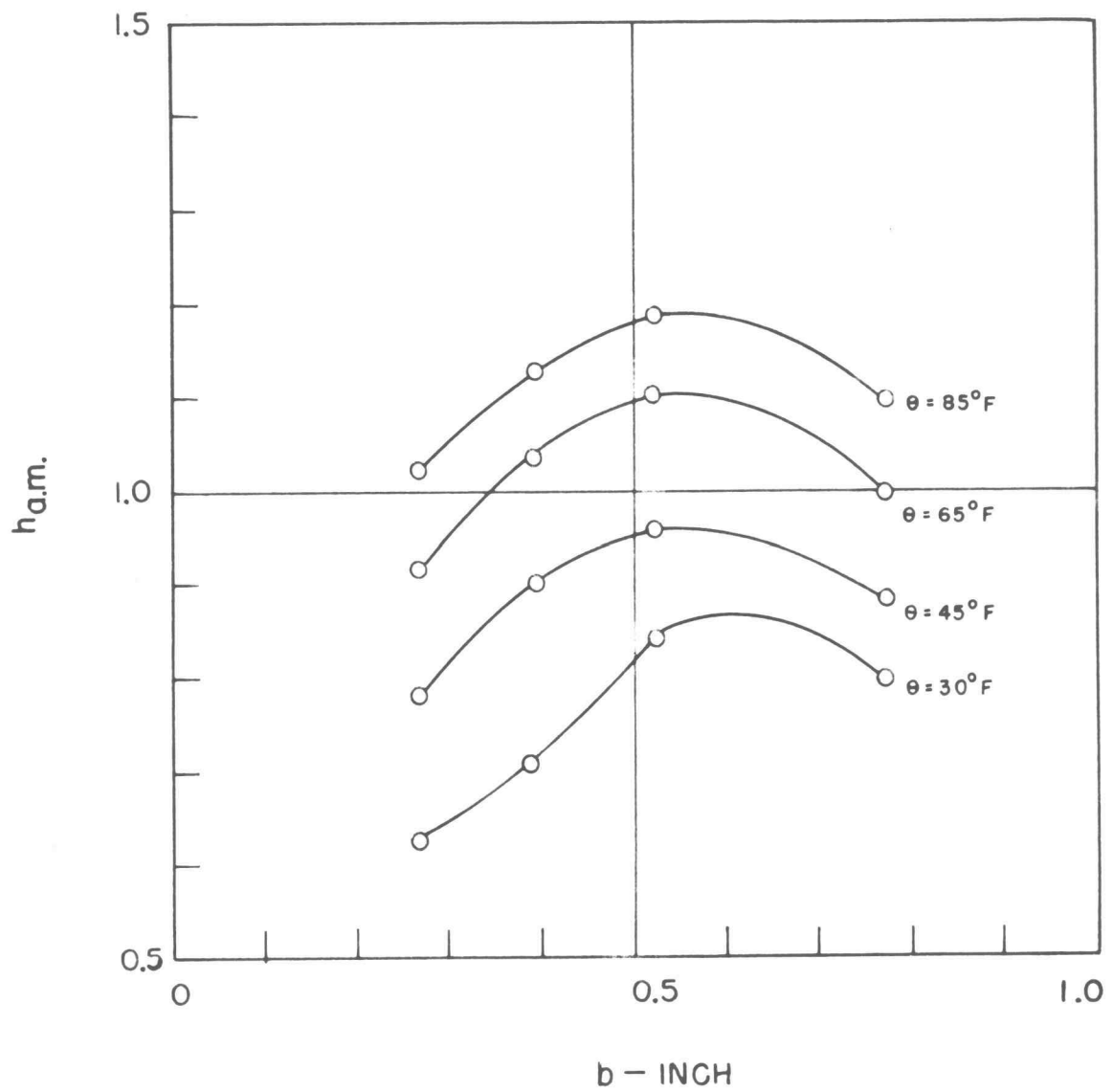
FIGURE 41   HEAT   TRANSFER   COEFFICIENT   AS   A
FUNCTION   OF   FIN   SPACING - $2\frac{7}{8}$
INCH   FIN   DIAMETER
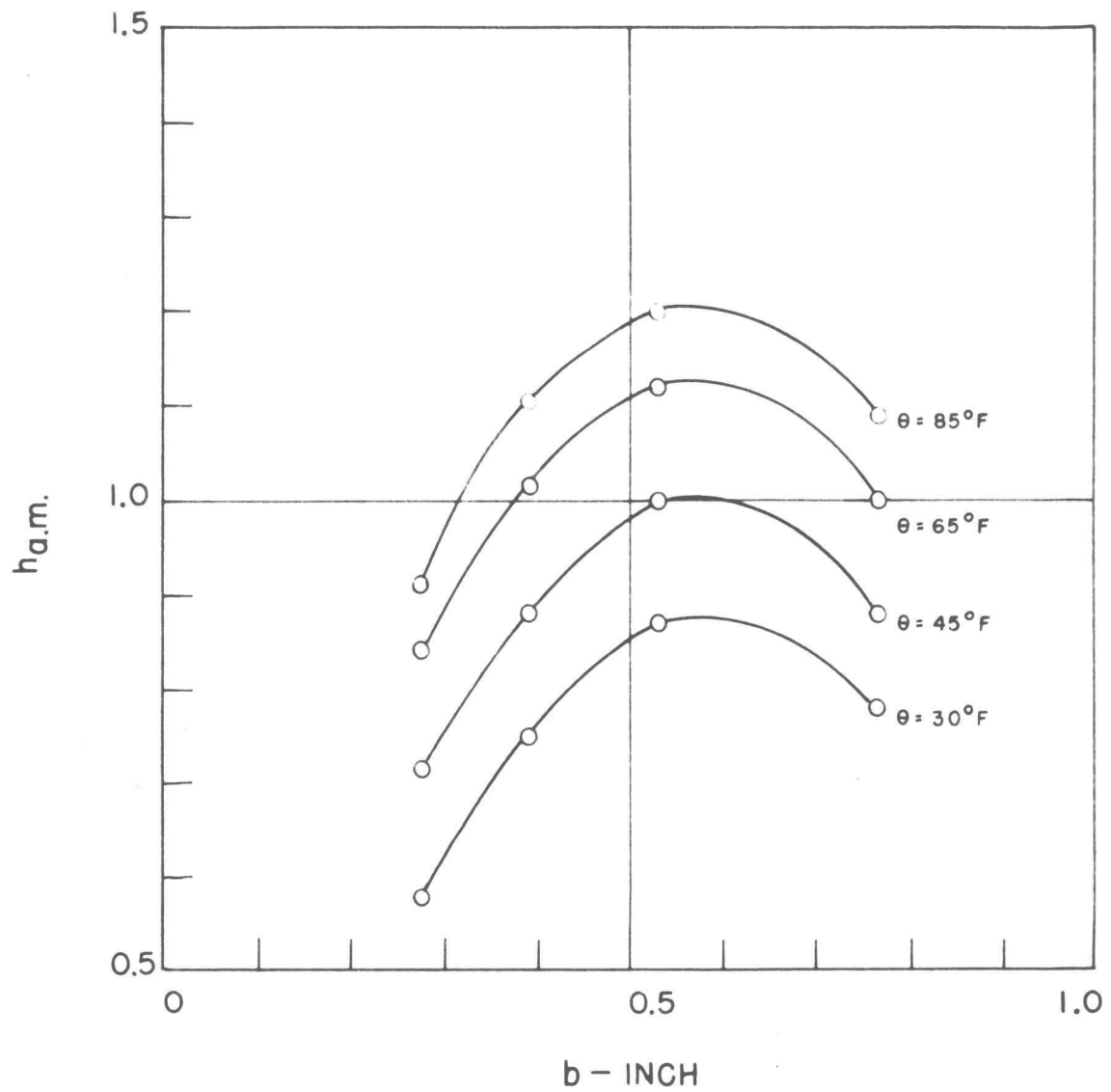
FIGURE 42   HEAT   TRANSFER   COEFFICIENT   AS   A
FUNCTION   OF   FIN   SPACING — $3\frac{3}{8}$
INCH   FIN   DIAMETER
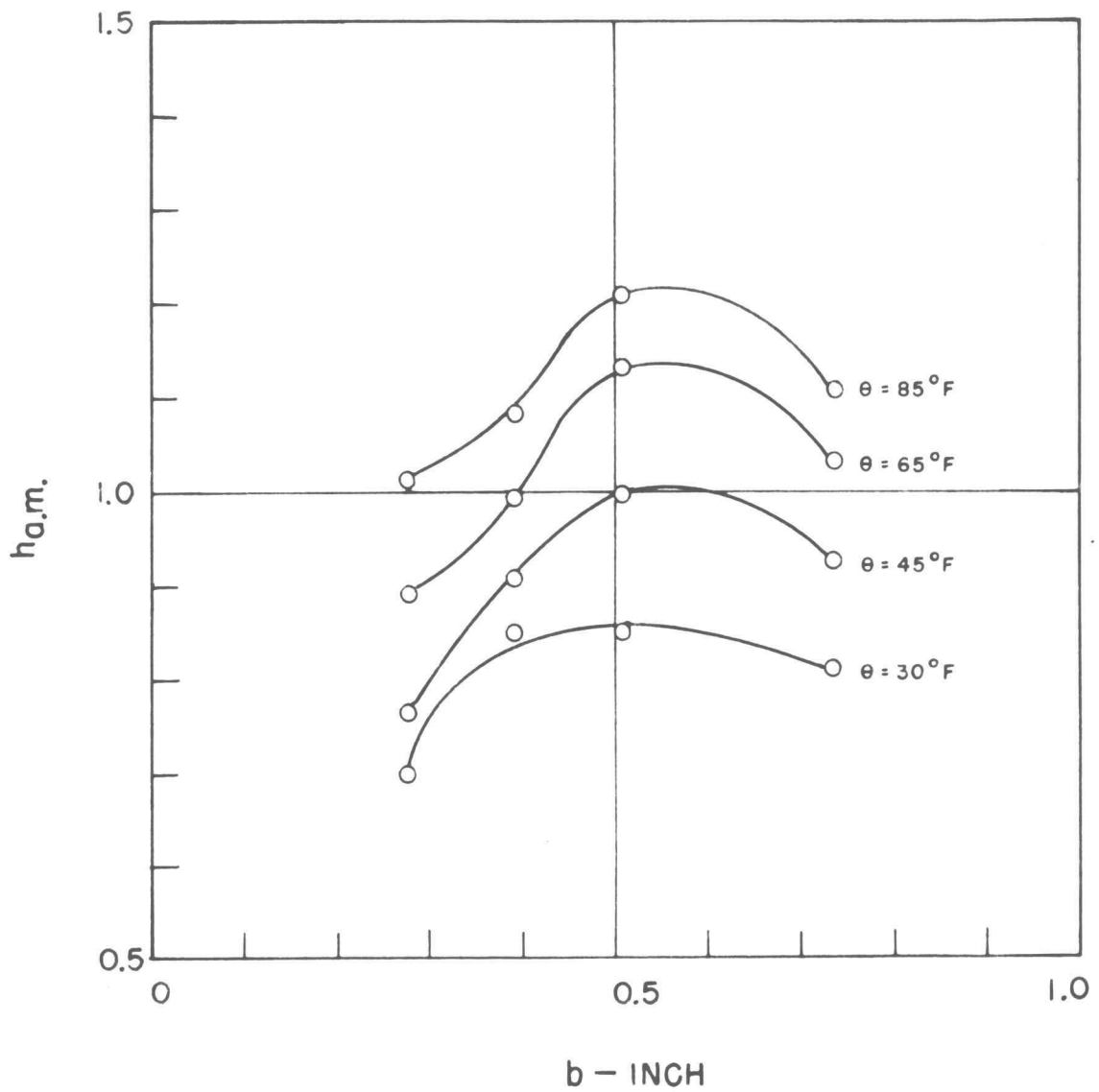
FIGURE 43   HEAT TRANSFER COEFFICIENT AS A
FUNCTION OF FIN SPACING – SQUARE
FIN TUBE
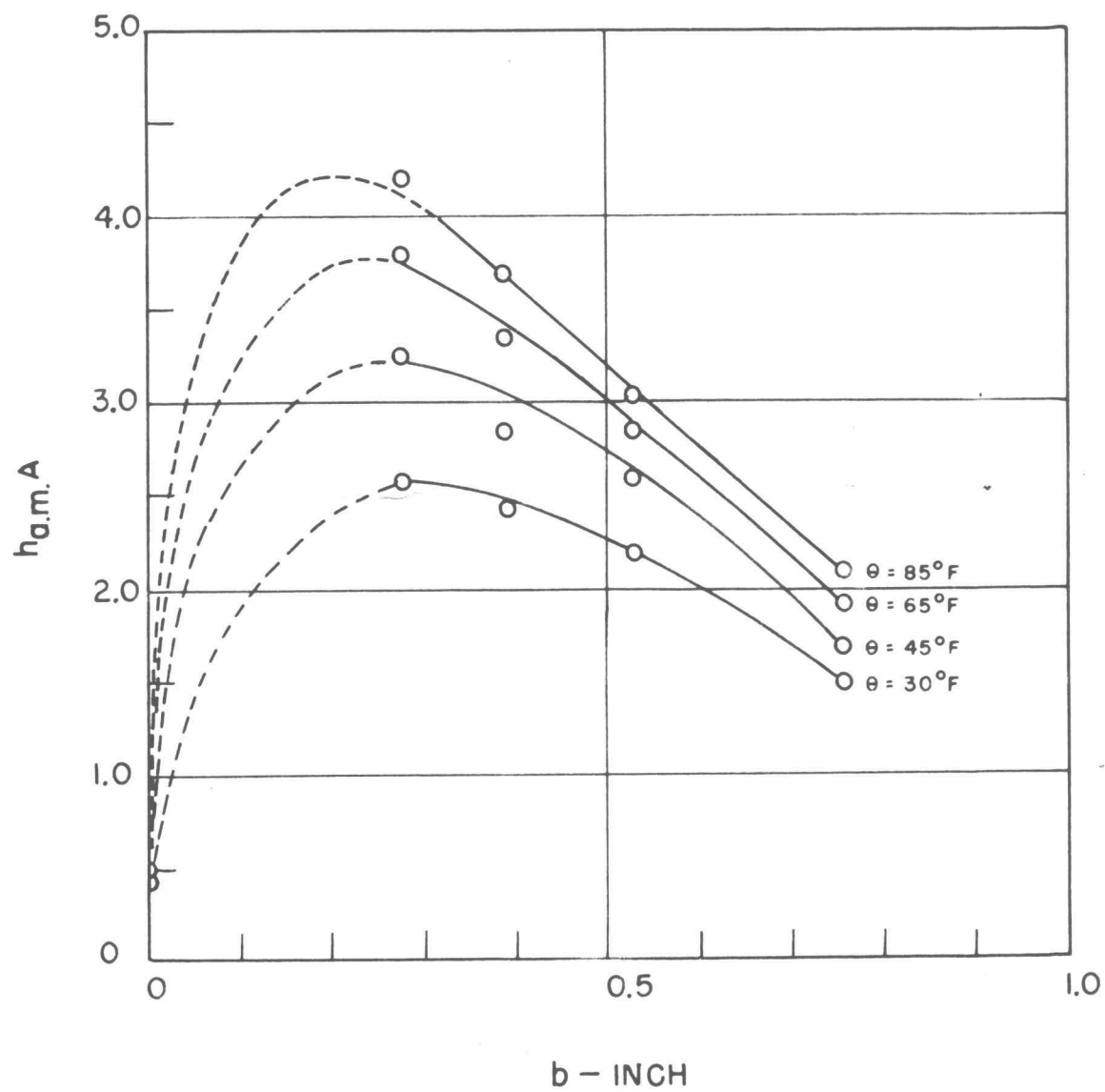
FIGURE 44 EFFECT OF FIN SPACING ON
HEAT TRANSFER COEFFICIENT
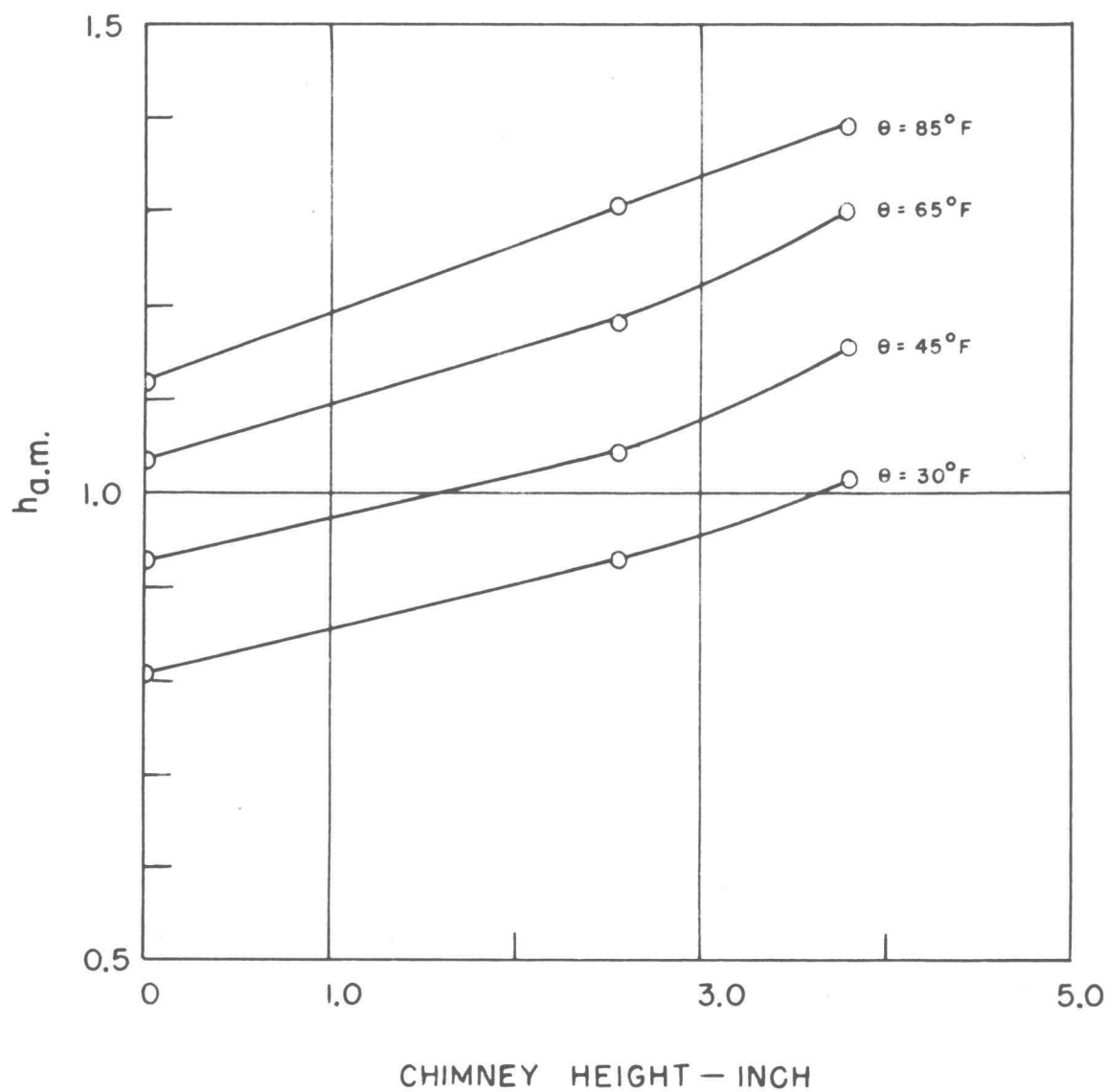
FIGURE 45   EFFECT OF CHIMNEY HEIGHT ON
HEAT TRANSFER COEFFICIENT
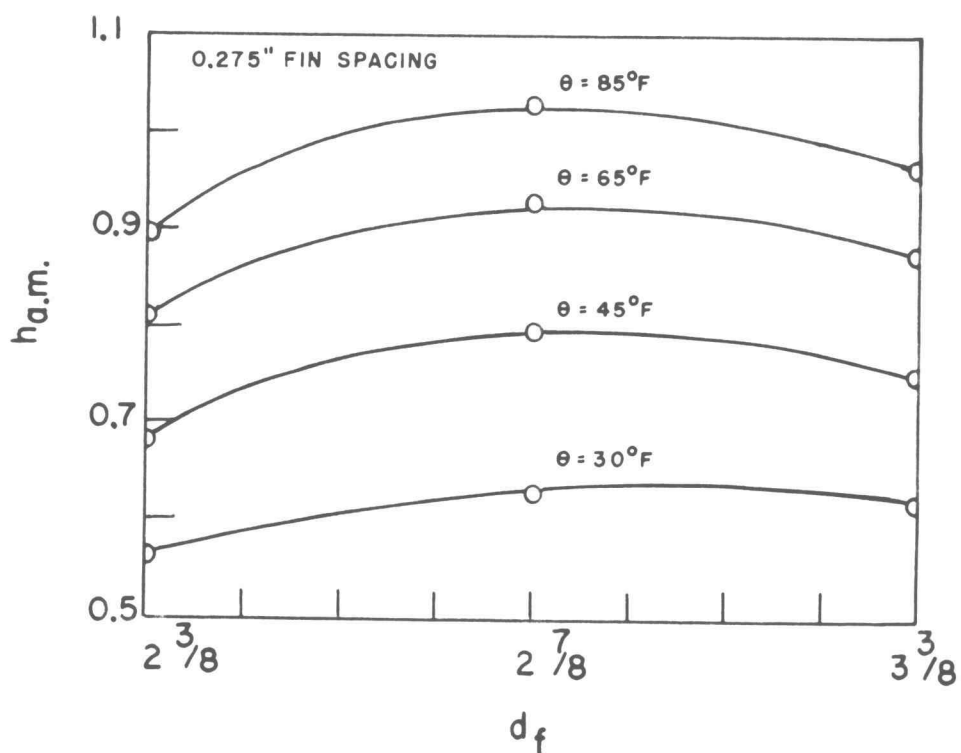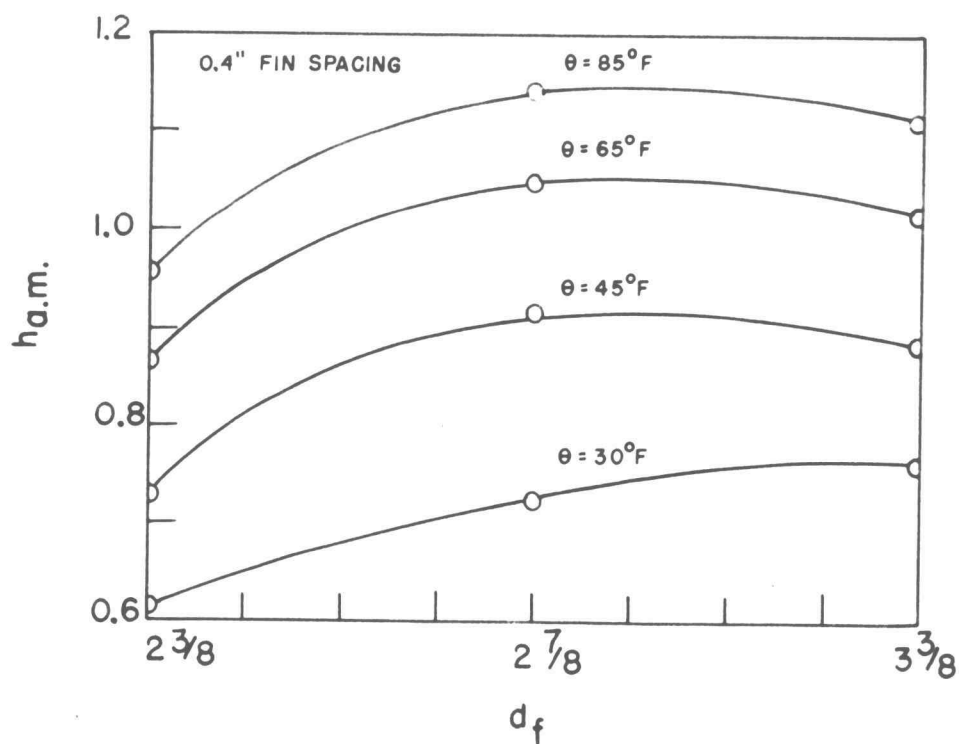
FIGURE 46   HEAT TRANSFER COEFFICIENT AS A FUNCTION
OF   FIN DIAMETER — 0.4 AND 0.275 INCH
FIN   SPACINGS
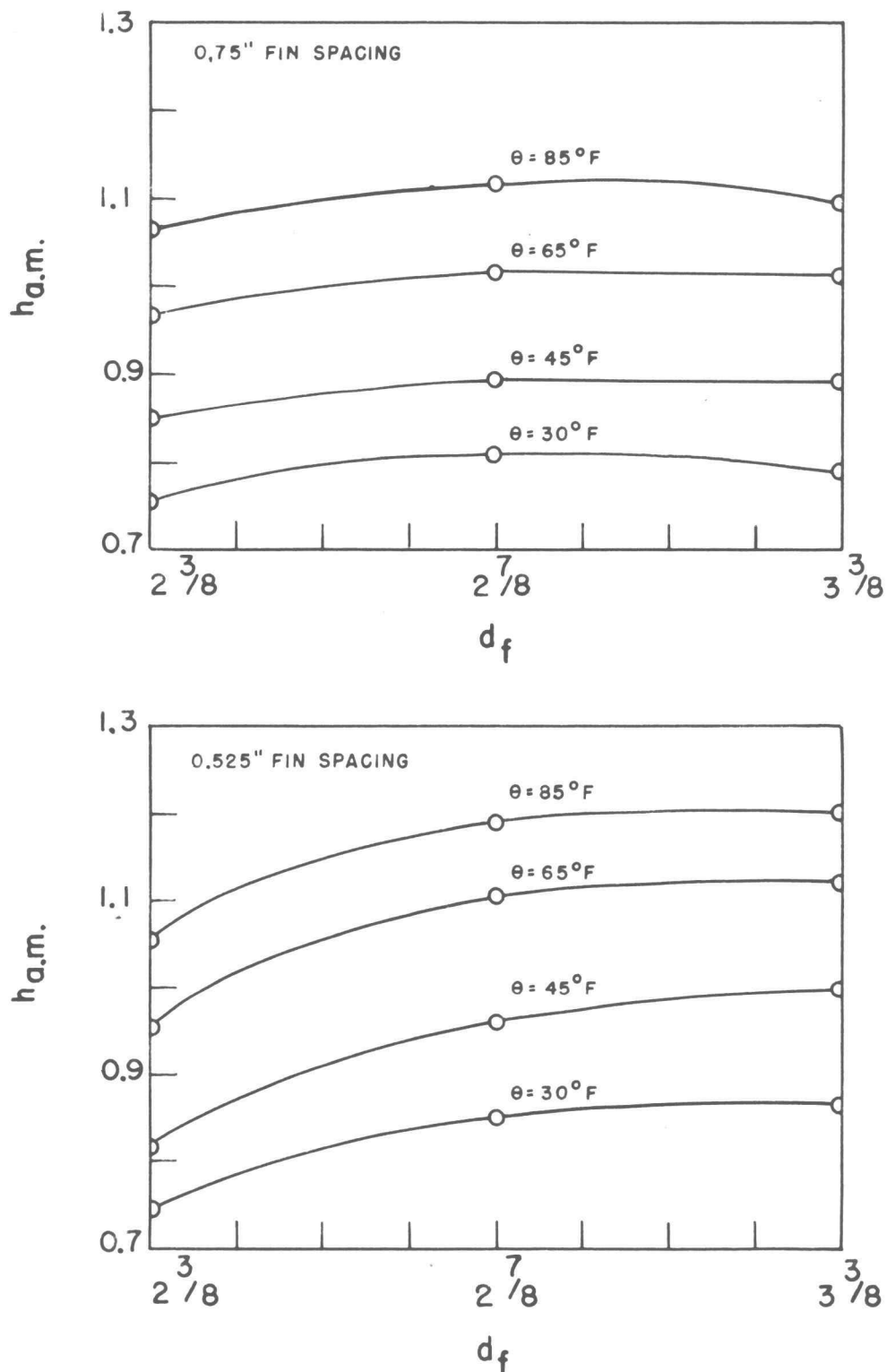
FIGURE 47   HEAT TRANSFER COEFFICIENT AS A FUNCTION
OF FIN DIAMETER - 0.75 AND 0.525 INCH
FIN SPACINGS
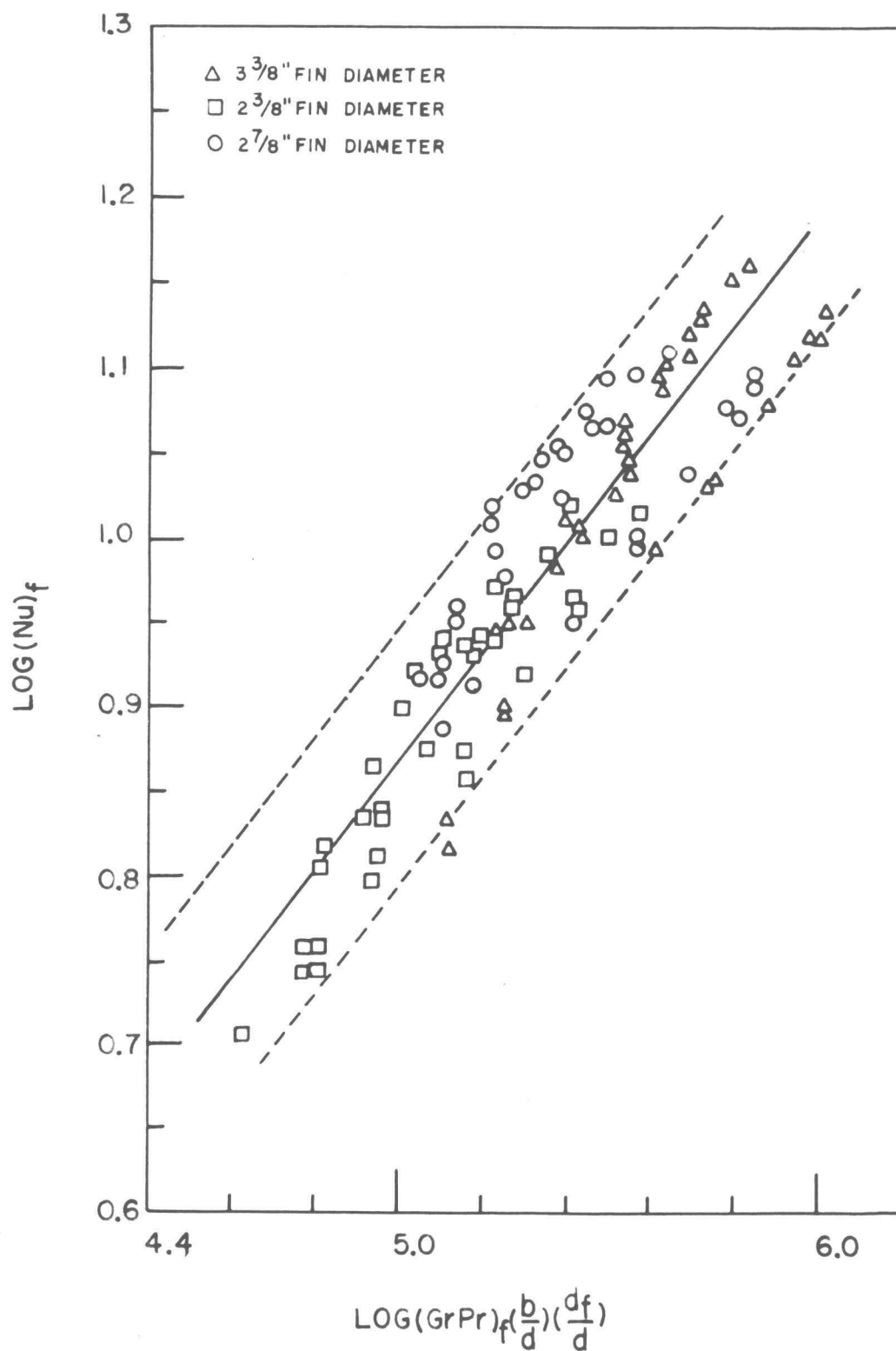
FIGURE 48 CORRELATION OF EXPERIMENTAL DATA
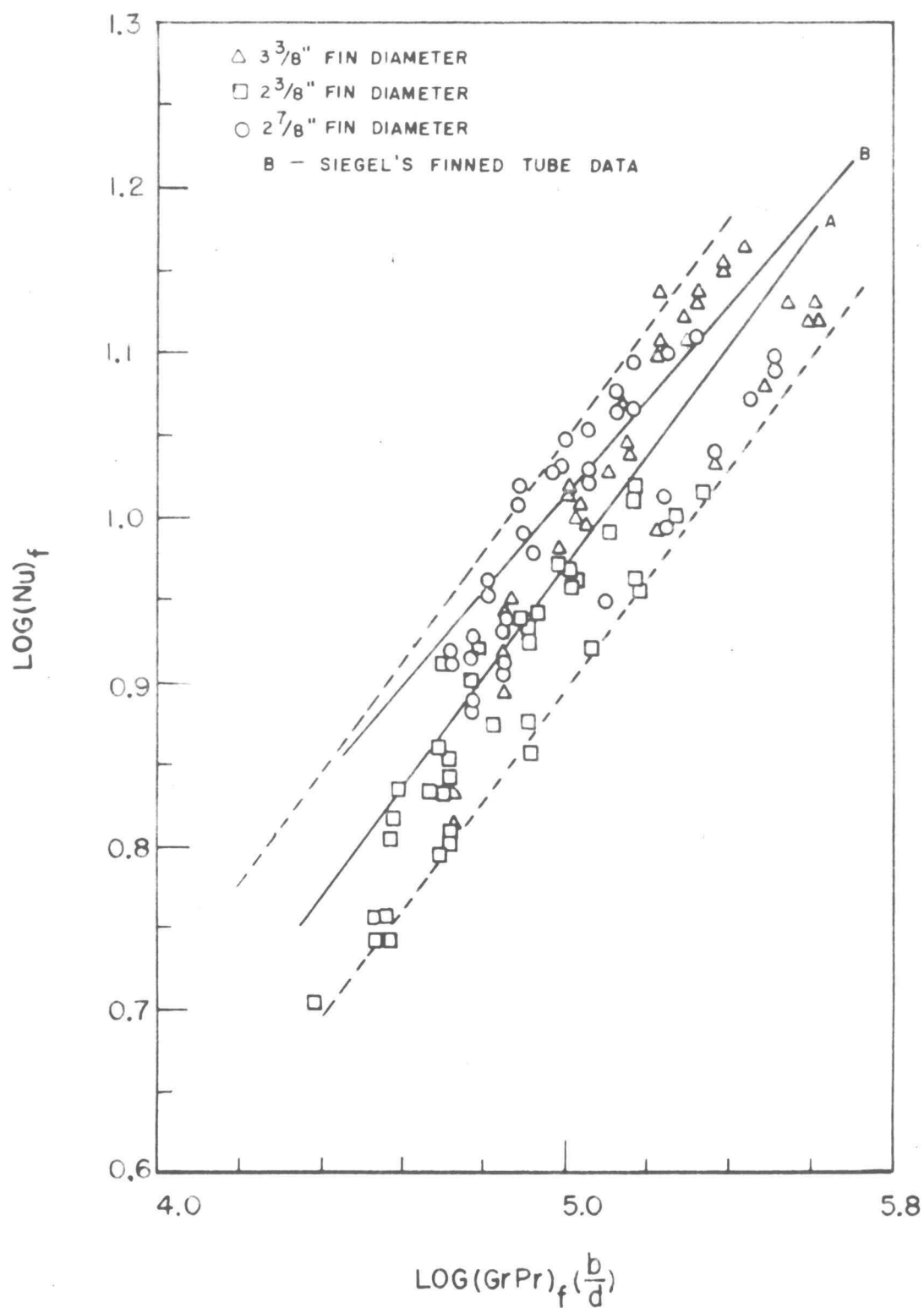
FIGURE 49   RECOMMENDED CORRELATION FOR ROUND
             FINNED TUBES
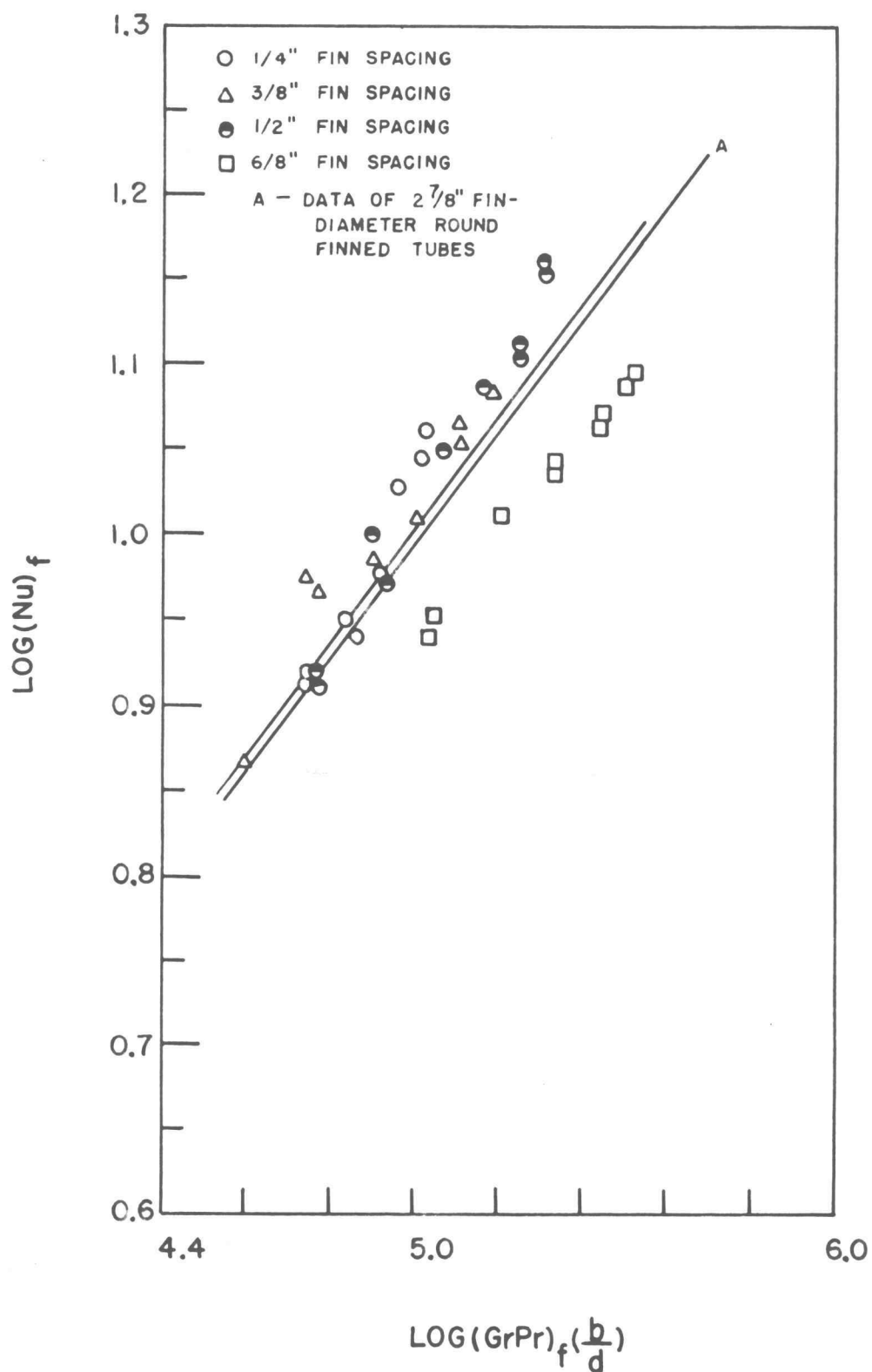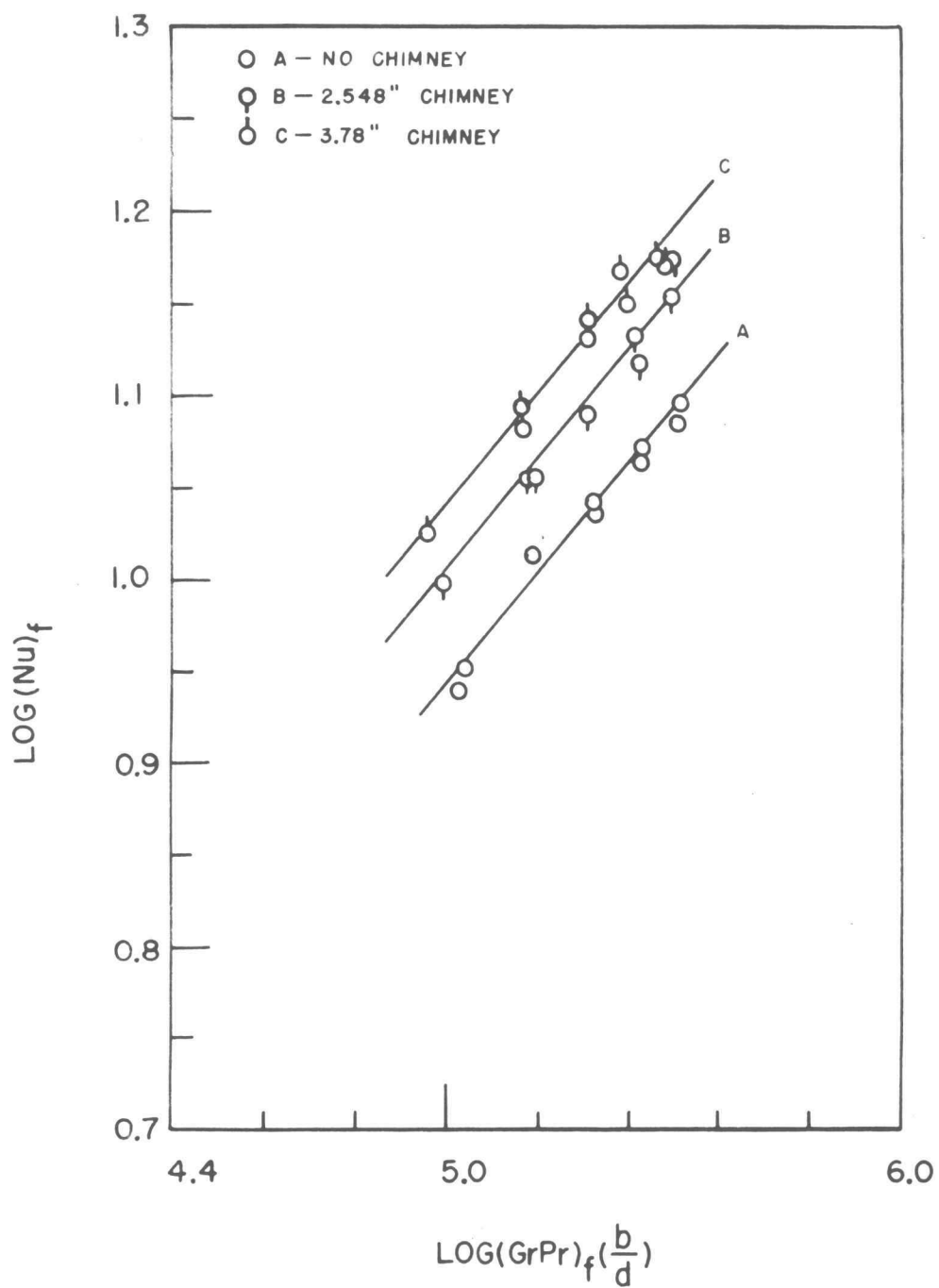
FIGURE 50 RECOMMENDED CORRELATION FOR SQUARE
FINNED TUBES

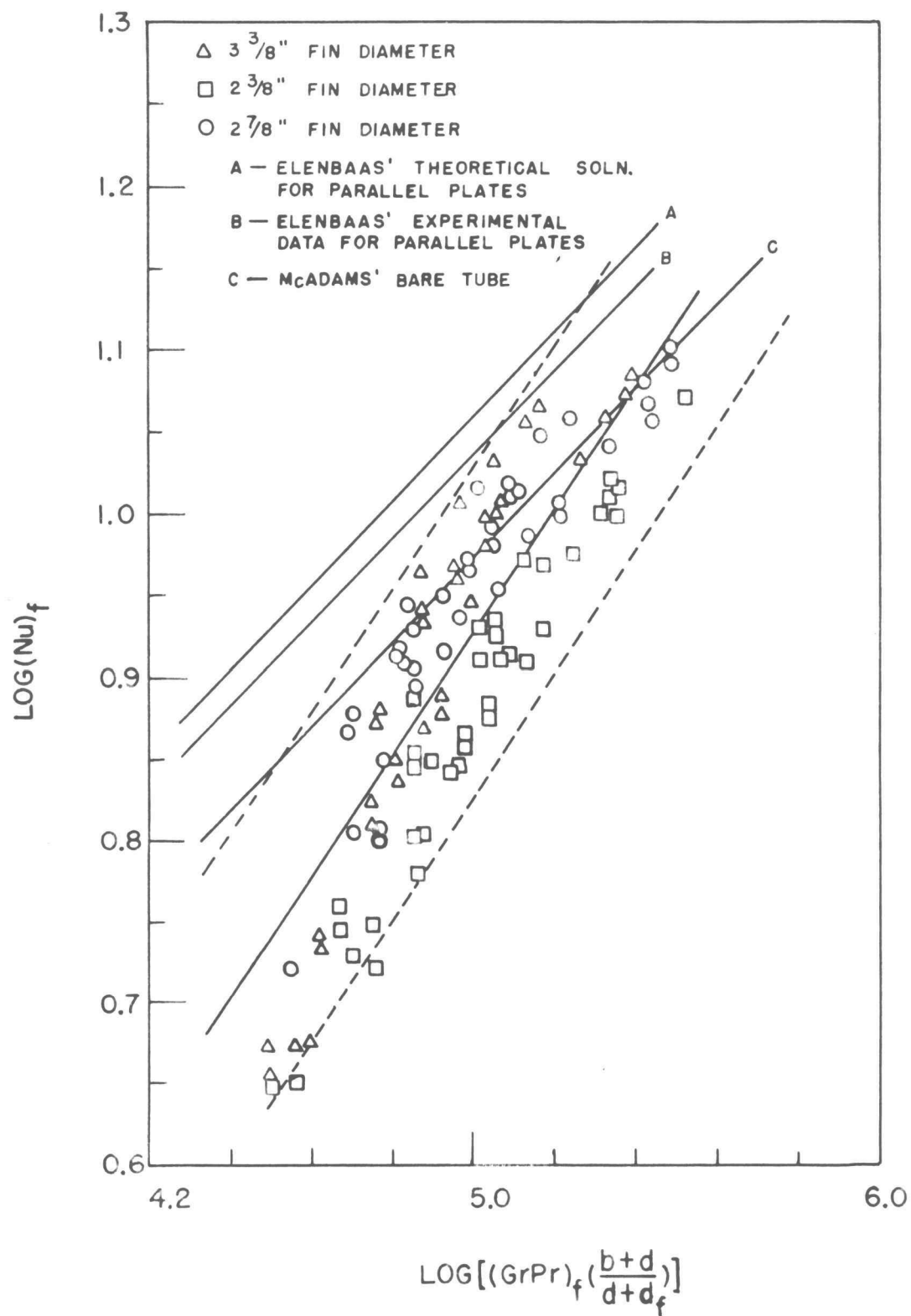FIGURE 51   EFFECT OF CHIMNEY HEIGHT

FIGURE 52   CORRELATION (ROUND FINNED TUBES) FOR
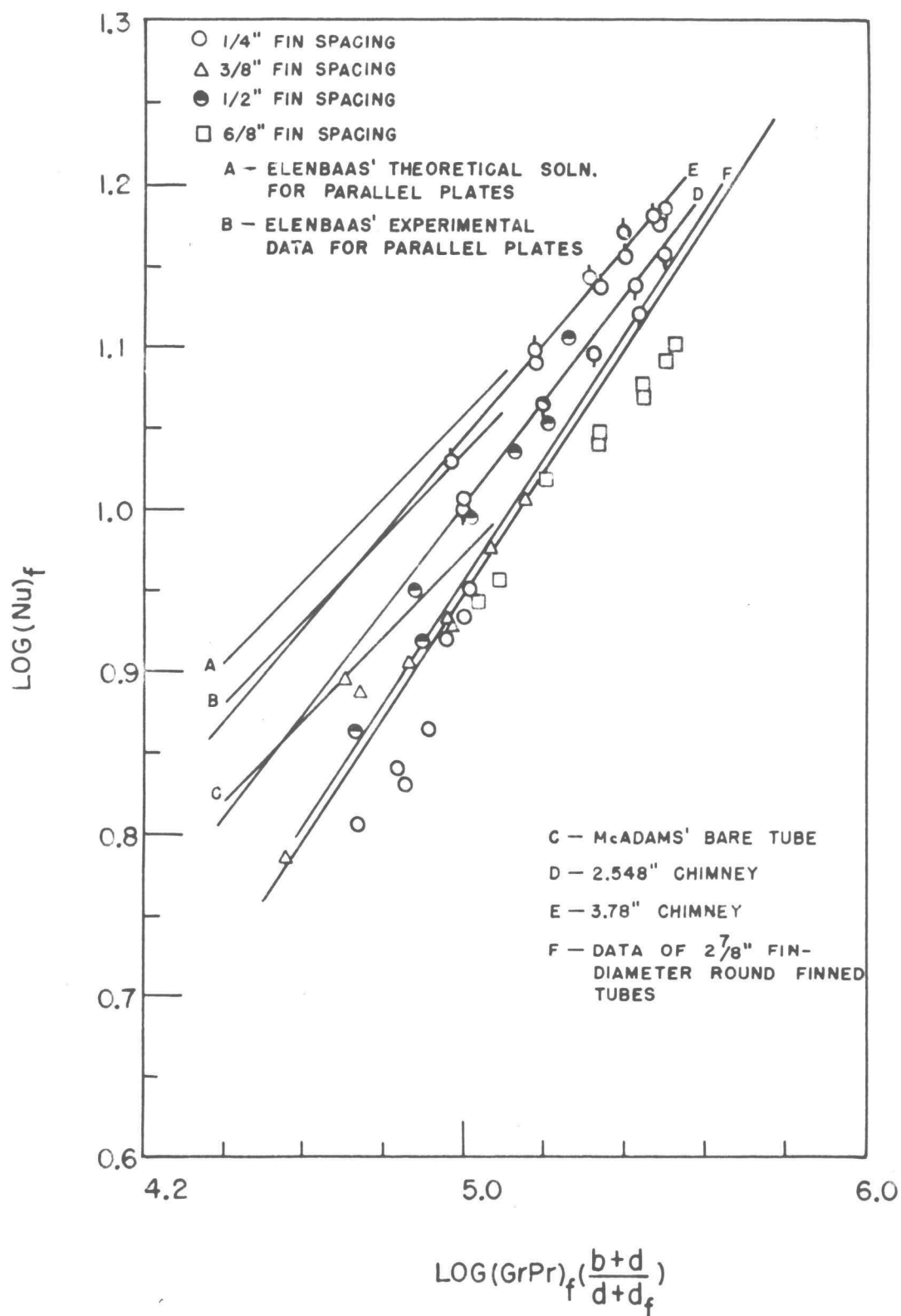COMPARISON WITH OTHER GEOMETRIC CONFIGURATION

FIGURE 53 CORRELATION (SQUARE FINNED TUBES) FOR COMPARISON WITH OTHER GEOMETRIC CONFIGURATION